

**282746
IMPACT2C**

Quantifying projected impacts under 2°C warming

Instrument Large-scale Integrating Project
Thematic Priority FP7-ENV.2011.1.1.6-1

D8.1 Design and production of an ensemble of air quality simulations and evaluation of health impacts

Due date of deliverable 31.03.2015
Actual submission date

Start date of the project 01.10.2011
Duration 48 months

Organisation name of lead contractor for this deliverable CNRS – IPSL

Revision: V1.0

Project co-funded by the European Commission within the Seventh Framework Programme		
Dissemination Level		
PU	Public	X
PP	Restricted to other programme participants (including the Commission Services)	
RE	Restricted to a group specified by the consortium (including the Commission Services)	
CO	Confidential, only for members of the consortium (including the Commission Services)	

Authors

Gwendoline Lacressonnière (CNRS-IPSL), Robert Vautard (CNRS-IPSL), Guillaume Siour (CNRS-IPSL), Audrey Cheiney (CNRS-IPSL), Gilles Forêt (CNRS-IPSL), Matthias Beekmann (CNRS-IPSL), Laura Watson (Météo-France), Virginie Marécal (Météo-France), Béatrice Josse (Météo-France), Michael Gauss (MET.NO), Agnes Nyiri (MET.NO), Magnuz Engardt (SMHI), Camilla Andersson (SMHI), Paul Watkiss (PWA), Alistair Hunt (PWA), Vladimir Kendrowski (WHO), Bettina Menne (WHO), Tanja Wolf (WHO), Gerardo Sanchez Martinez (WHO ECEH), Michela Baccini (University of Florence, Italy), Katrina Lyne (WHO intern).

Objectives

The objective of WP8 is to estimate the pan-European impacts of a global +2°C temperature change on health, including change in air pollution. The work has essentially been divided into

- Impact of climate change on air pollution and subsequent consequences upon health
- Impacts of climate change on health not due to air pollution

1. Key findings of WP8

Air pollution and health consequences

Using four suites of global, regional climate, air quality and health impact assessment models we have found that a +2°C global climate change modifies the near-surface atmospheric composition of air pollutants in Europe. This is due to several reasons such as changes in weather variables (temperature, precipitation, water vapour, atmospheric flow, boundary layer turbulence) and to biogenic emissions (dust, sea salt, biogenic volatile organic compounds). We have identified areas where changes are robust, where 3 of the 4 models give a change with the same sign. Changes are calculated relative to a reference period of 1971-2000.

- **In many areas the sign of concentrations change is robust, but its amplitude remains small as compared to the variability of concentrations.** For ozone, models predict an average increase across Southern and Central Europe due to climate change which does not exceed 1 ppb. An average decrease of similar amplitude is predicted over Scandinavia. In summer, all models predict an increase in ozone in most of Europe, but in winter the uncertainty on the sign of change is high. For particulate matter, changes due to a +2°C global warming are uncertain, as models do not agree on sign. In addition, a conclusion on the sign of change is made more difficult as models do not simulate the same composition of PM components composition. However, an agreement is found on an increase of desert dust concentration over the Iberian Peninsula and Southern France in a 2°C warmer climate.
- **The changes due to a 2°C warming are small compared to changes expected from air pollutant emission reductions for 2050.** Assuming European countries manage to adhere to the current legislation (CLE), all air pollution models agree on a decrease in both ozone and PM concentrations, with a typical reduction of 2-5 ppb for ozone and 2-5 $\mu\text{g}/\text{m}^3$ for PM_{2.5}, largest over Benelux for PM and Southern Europe for ozone. A “maximum feasible reduction” (MFR) scenario induces an effect that is approximately doubled as compared to the CLE scenario.

- **A 3°C warming leads to concentration changes remaining marginal compared to the effects of air pollutant emission policies.** For two models (EMEP and CHIMERE), a decrease of ozone is found in Northern Europe and an increase in South Western Europe. For PM, a similar increase due to dust is found over the Iberian Peninsula for 2°C and 3°C.
- **City-scale air pollution changes examined for two cities (Stockholm and Paris) are consistently small as compared to the effects of the changes in air pollutant emissions.**
- **The health impacts of changes in air pollution under 2°C warming follow the patterns reported above, and lead to small changes in health impacts related to baseline levels.** For particulates, there is a wide range reported by the models, which varies even in sign. For ozone, there is a more robust increase in health impacts, but the level of additional health impacts is low.

Health impacts beyond air pollution

The impact of heat was studied quantitatively using the regional climate model simulations while the impact of other changes was determined in a more qualitative manner based on an extensive literature review.

- **Heat:** climate-change induced heat under a 2°C warming will lead to between 13000 and 26000 additional deaths per year, while a 3°C climate change would lead to additional deaths between 37000 and 96000 per year in EU28. The fraction of deaths attributable to heat is found increasing, with large differences between a 2°C warming and a 3°C warming.
- **Vector-borne diseases:** Climate change-induced ecosystem changes will affect disease vectors (as well as intermediate hosts and hosts) that can transmit serious infectious diseases. Climate modelling suggests that the geographic range of *Ixodes ricinus* ticks will increase during the 21st century. The *Anopheles atroparvus* mosquito is a potential vector for malaria in many parts of Europe, with re-establishment of transmission a possibility. However, numerous factors make the re-emergence of malaria in Europe unlikely, including health system functionality, building and development regulations, and patterns of land use. An overall increase in dengue risk is predicted, with the greatest increase expected in southern Europe, particularly coastal areas. Central parts of Europe, including France, Germany and Hungary, may also see an increase in dengue fever incidence, while the British Isles and northern Europe are predicted to remain at near-zero risk.
- **Food-borne diseases:** The cases of salmonellosis and campylobacteriosis (only climate change-attributable ones) are projected to increase from 28438 per year in 2010-2040, to 32501 in 2041-2070 for EU total. Resource costs are calculated for both additional hospital admissions and additional cases of salmonellosis and campylobacteriosis are calculated to be around 700 M Euros in 2041-2170 period in A1B scenario and around 650 M Euros in the E1 scenario.
- **Allergies:** Climate change is likely to trigger further changes in pollen concentration, volume and distribution, with an associated increase in the prevalence and severity of allergic diseases in many parts of Europe. While increasing temperatures may prompt earlier flowering and hence prolongation of the pollen season, rising atmospheric carbon dioxide concentrations will result in increased plant growth and pollen production. Furthermore, changing weather patterns may prompt an increase in the geographic range of many allergenic plants, with increasing population risk of allergic disease.

Policy-relevant key messages

- **Air pollutant emission reductions will continue to largely improve air quality and reduce associated health issues in Europe**, and there is a large room for improvement beyond current legislation. The abatement measures will have a larger effect than changes due to climate warming only.
- **Links between health and climate policy should be improved**. It is important that actions in protecting health and the environment are coherent and mutually reinforcing, from individual, to community, national and international levels.
- **Strengthening of health programmes to address climate risks is necessary**. Even in 2°C world we will require a comprehensive approach to strengthen the core health system functions, and to identify and prioritize the specific interventions that are most protective against climate risks.

2. Impact of climate change on air pollution

Since the Gothenburg Protocol in 1999, methodologies have been set up at the EU level in order to control air pollutant emissions. However, as yet, none of them takes into account the effect of climate change, which affects atmospheric dispersion, biogenic and fire emissions, chemistry, and the frequency of extreme weather situations such as heat waves. These changes will have an impact on air quality with subsequent health consequences that must be evaluated.

One first step is to provide projections of air quality in a changing climate, to evaluate how climate change potentially affects the efficiency of emission abatement policies at European scale, and eventually how this affects health. In order to achieve this, chemistry-transport models (CTMs) are applied downstream of climate models (offline experiments), and several simulations are conducted. One of the strengths of the consortium is the opportunity to use 4 different CTMs (CHIMERE [IPSL], EMEP MSC-W [MET.NO], MATCH [SMHI], and MOCAGE [Météo-France]), in coordinated experiments, in order to provide, in addition to a mean projection of the effects of climate change, an estimate of the uncertainty in projections, as provided by the spread between models and driving meteorological data.

2.1 Model evaluation in current climate

To compare with future climate, air quality simulations have first been performed for the current climate: HINDCAST (CTMs forced by regional climate models [RCM] simulations with a common reanalysis boundary forcing) and HISTORICAL (global climate model boundary forcing of RCMs) simulations in order to evaluate the models. Several scientific objectives are considered in this project and concerning the current climate:

- The first objective is to evaluate the HINDCAST simulation against observations over Europe (AirBase and EMEP databases). This task has been largely accomplished in different studies.
- The second objective, more original, is to compare the HINDCAST and HISTORICAL simulations and evaluate how global climate models modify climate hindcasts by boundary conditions inputs. This is ground work needed for the analyses of future scenarios.

Participating models

Below we briefly describe the 4 CTMs involved in this study.

CHIMERE is a regional CTM (Bessagnet et al., 2004; Menut et al., 2013) and has been used in many air quality studies (Vautard et al., 2001; Colette et al., 2012) and model intercomparison exercises (Vautard et al., 2007; Solazzo et al., 2012a; Solazzo et al., 2012b). The LMDz-INCA concentrations are taken as boundary conditions (Szopa et al., 2012). In the present study, eight vertical hybrid σ -p levels represent the atmospheric column from the surface to 500 hPa. The chemical mechanism used is MELCHIOR2 (Lattuati et al., 1997; Derognat et al., 2003) for the gas-phase which includes 44 species and 120 reactions. CHIMERE simulates the evolution of 14 aerosol species: primary particulate matter (PPM), dust, black carbon (BC), organic carbon (OC), sea salt, 5 types of Secondary organic aerosols (SOA), sulphates, nitrates, ammonia and water droplets. They are compartmented in 9 size bins. More details of the model can be found on: <http://www.lmd.polytechnique.fr/chimere>.

The **EMEP MSC-W** model (hereafter referred to as 'EMEP model') is a CTM developed at the EMEP Meteorological Synthesizing Centre-West at the Norwegian Meteorological Institute. The model is a further development of the 3-D model of Berge and Jakobsen (1998), extended with photo-oxidant and aerosol chemistry (Andersson-Sköld and Simpson, 1999; Simpson et al., 2012). The model has been used with resolutions ranging from 5×5 km² over the UK (Vieno et al., 2010) to $1^\circ \times 1^\circ$ globally (Jonson et al., 2010). The vertical domain spans from the surface to 100 hPa. The methodology for biogenic emissions used in the EMEP model builds upon maps of 115 forest species generated by Köble and Seufert (2001). Emission factors for each forest species and for other land-classes are based upon Simpson et al. (1999), updated with recent literature (see Simpson et al. (2012) and references therein), and driven by hourly temperature and light using algorithms from Guenther et al. (1995). Other natural emissions include marine emissions of dimethyl sulfide, and SO₂ from volcanoes. Dry deposition is calculated using a resistance analogy combined with stomatal and non-stomatal conductance algorithms (e.g. Simpson et al., 2003; Tuovinen et al., 2004), whereas wet deposition uses scavenging coefficients applied to the 3-D rainfall. Full details and an evaluation of the EMEP model are given in Simpson et al. (2012).

MATCH is an off-line CTM applicable to scales from urban to hemispheric (Robertson et al., 1999). It is used operational at SMHI as a warning system for emergency preparedness and air quality forecasts as well as a research tool. MATCH has been used extensively to study the connection between climate change and air quality in Europe (e.g. Engardt et al., 2009; Andersson and Engardt, 2010; Langner et al., 2012a; 2012b). The model is typically applied to a European domain but can also be set up over other regions (e.g. Engardt, 2008). The chemical scheme (Langner et al. 1998; Andersson et al., 2007) considers ~60 species and is based on Simpson et al. (2012). The vertical resolution is copied from the driving RCM, i.e. the lowest 5 km is divided into 20 layers.

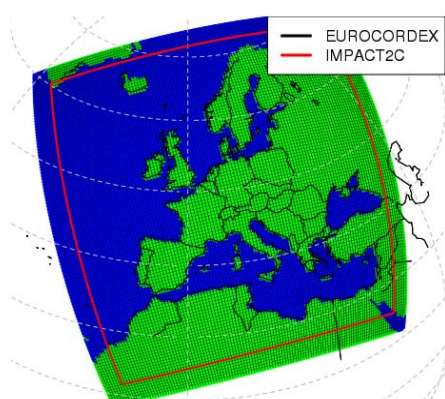
MOCAGE is a three-dimensional multi-scale CTM that simulates the interactions between the dynamical, physical and chemical processes in the troposphere and the stratosphere (Peuch et al., 1999; and Josse et al., 2004). MOCAGE is used for operational air quality forecasting in France (<http://www.prevoir.org>, Honoré et al., 2008) and has been evaluated during several campaigns (Dufour et al., 2004; and Bousseret et al., 2007). Global simulations of MOCAGE using anthropogenic emissions from IPCC-AR5 provide the boundary conditions for the present study, and the regional simulations are coupled to a global domain with 2-way nesting. MOCAGE has 47 hybrid levels from the surface up to 5 hPa with a resolution of about 150 m in the lower troposphere increasing to 800 m in the higher troposphere. The chemical scheme used is RACMOBUS, which is a combination of the stratospheric scheme REPROBUS (Lefèvre et al., 1994) and the

tropospheric scheme RACM (Stockwell et al., 1997). Overall, this chemical scheme includes 108 chemical species and four types of aerosols: BC, sea salt, desert dust, OC, and particulate matter.

The ensemble of model chains used is described in Table 1. Except for MOCAGE, which uses climate projections directly from the ARPEGE GCM in a stretched grid, all GCMs are first downscaled using a regional climate model (RCM). GCM simulations are issued in the new CMIP5 context.

Institute	CTM	Driving GCM	RCM used for downscaling	Chemical boundary conditions
CNRS-IPSL	CHIMERE	IPSL-CM5A-MR	WRF	LMDz-INCA
MET. NO	EMEP	NorESM	WRF	LMDz-INCA
SMHI	MATCH	EC-EARTH	RCA4	LMDz-INCA
Météo-France	MOCAGE	ARPEGE	ARPEGE	MOCAGE

Table.1 : description of the model chains used, from GCM simulations to regional CTMs.



It was decided to make the current climate experiment fully consistent with the new EUROCORDEX regional climate simulations, since these simulations will be used in other work packages of IMPACT2C and as meteorological drivers for the chemistry in WP8. The domain is represented in Figure 1. A medium resolution has been used (50 km, the EUROCORDEX grid) which allows a large number of simulations to be carried out to answer the main questions of the work package.

Figure.1: the domain used for the air pollution and climate simulations, which corresponds to the EUROCORDEX grid. The domain is a “rotated latitude-longitude grid” with the South Pole at 18.00°E, 39.25°S, with 106 × 103 cells in the east-west and north-south direction.

Boundary conditions

Concerning the chemical boundary conditions, each model uses its own boundary concentration set. For CHIMERE, MATCH, and EMEP, constant (i.e. same for each year) boundary concentrations are used, taken from global chemistry climatologies with a monthly variation, corresponding to the climate periods considered. For MOCAGE, boundary concentrations are taken from a corresponding global version of the MOCAGE global version and are nested into the domain of study.

Design of the experiments

Two evaluation simulations have been performed for the current climate, hereafter referred to as HINDCAST (forced by the CORDEX evaluation runs (reanalysis boundary forcing)) and HISTORICAL (forced by climate model) in Table 2. The HINDCAST period (1989-2008) is covered by the ERA-interim period. The HISTORICAL period (1971-2000) corresponds to simulations coming from the CMIP5 project.

In order to calculate the effect of climate change on emission reduction scenarios, the “climate penalty”, a simulation (S1) using the emissions reduction scenario for the future +2°C period was carried out and will be compared with a simulation (S2) using the same emissions but for the current climate. The future +2°C

period is different for each model. For instance, the IPSL GCM reaches this threshold during 2027-2056 in the RCP4.5 scenario.

Name	Climate	Boundary conditions	Emissions
HINDCAST	1989-2008	2005	ECLIPSE v4a 2005
HISTORICAL	1971-2000	2005	ECLIPSE v4a 2005
S1	+2°C period for RCP4.5	2050	ECLIPSE v4a 2050 CLE
S2	1971-2000	2050	ECLIPSE v4a 2050 CLE
S3	+2°C period for RCP4.5	2050	ECLIPSE v4a 2050 MFR

Table 2: descriptions of the simulations performed for the current (HINDCAST, HISTORICAL) and future periods (scenarios S1, S2, S3).

Pollutant emissions

It was decided to use ECLIPSE emissions of 2050 for future simulations in IMPACT2C (<http://eclipse.nilu.no/>). ECLIPSE was a EU FP7 collaborative project, where IIASA developed future emission data sets using the GAINS model (Amann et al., 2011). ECLIPSE developed and assessed effective emission abatement strategies for short-lived climate forcers such as ozone and aerosols to provide advice on measures that mitigate climate change and improve air quality. In order to compare present and future climates, we chose to use ECLIPSE Current Legislation (CLE) emissions of 2005 for HINDCAST and HISTORICAL simulations, and the corresponding 2050 CLE emissions for the future simulation. In addition a scenario using the 2050 maximum feasible reductions of emissions (MFR) was also tested (S3). The interpolation of the ECLIPSE data into the CORDEX grid (involving also the inclusion of country specific information and mapping into SNAP sectors) was done at MET.NO.

Even though air pollutant emissions vary across decades, fixed emissions of 2005 were used for HISTORICAL and HINDCAST simulations, and this will simplify the identification of biases due to climate simulations only.

Figure 2 displays comparisons between 2005 and 2050 ECLIPSE emissions for NO_x and SO_x. For both species, a decrease of the emissions is predicted for 2050 in the CLE scenario over all Europe. NO_x and SO_x decrease to 38 % and 9 % of 2005 levels, respectively, over the domain (international shipping included).

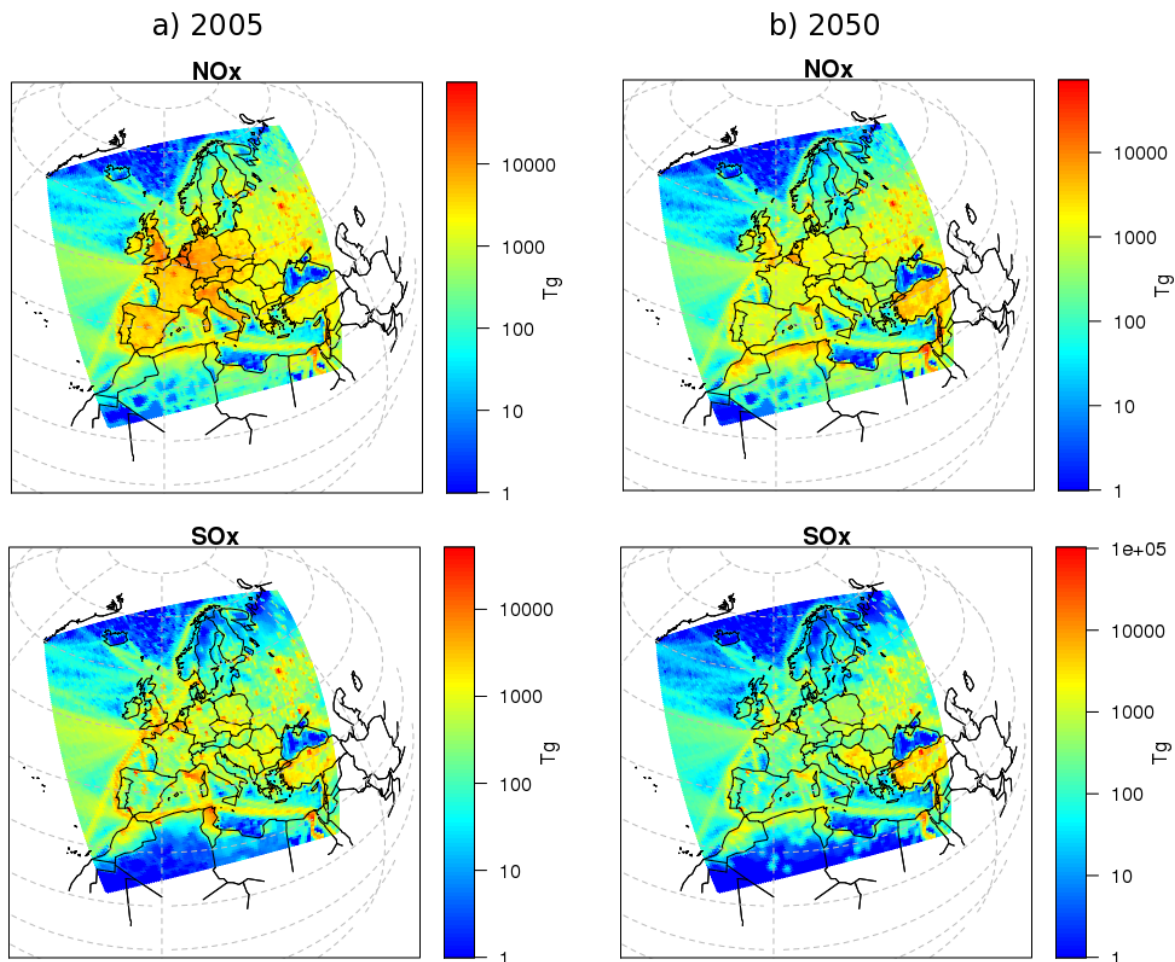


Figure 2: comparisons of NO_x and SO_x annual emissions (in Tg) between 2005 (a) and 2050 CLE scenario (b)

Model evaluation

The chemistry-transport models used in this project have been extensively evaluated in many intercomparisons (see eg. Solazzo et al., 2012a-b; Van loon et al., 2007, Kukkonen et al., 2012), for their ability to simulate daily fluctuations. Their ability to simulate trends due to emission changes has also been evaluated in several studies (Jonson et al., 2005; Vautard et al., 2006; Colette et al., 2011; Langner et al., 2012a; Stevenson et al., 2012). However this is difficult for PM due to the lack of early emission information and concentrations. In order not to duplicate previous efforts, we focused here on the ability of models to simulate the HINDCAST period when the CTMs were forced by non-nudged regional climate models of the EURO-CORDEX evaluation simulations, assuming constant emissions to check if the RCM forcing itself provides a variability that make simulations consistent with the observations (trends being removed) at various scales (daily, seasonal, and interannual, but not interdecadal). It is important to note that this is a different approach to the other intercomparison studies cited above, where real (forecast or reanalysis) meteorological data are used.

In order to evaluate the models, the EMEP (<http://ebas.nilu.no>) and AirBase (<http://acm.eionet.europa.eu/databases/airbase/>) databases have been used and compared to our HINDCAST simulations. We focus on ozone (O₃), nitrogen dioxide (NO₂) and particulate matter with a diameter smaller than 10 µm (PM₁₀) and 2.5 µm (PM_{2.5}). The measurements of nitrate, ammonia and sulphate from EMEP will serve for the analyses of particulate matter.

Statistics of PM and secondary inorganic aerosols

We evaluated PM₁₀ and PM_{2.5} concentrations with data from AirBase stations. Given the spatial resolution of the models (about 50 km × 50 km), not all the reporting sites are representative enough. We use an objective classification of the AirBase sites based on past measurements proposed by Joly and Peuch (2012) in order to overcome issues of lack of homogeneity and erroneous information in the metadata. This pollutant-specific classification based on past measurement data defines 10 classes of measuring stations, from the least polluted (class 1) through the most polluted (class 10). We chose to use the classes 1-5 to evaluate the performance of PM₁₀ as in Lacressonniere et al. (2012). Due to the lack of sufficient data of PM_{2.5} within the AirBase data set, there is no classification established for PM_{2.5} in Joly and Peuch (2012). We chose to use the classes 1-5, considering PM_{2.5} as a longer-lived species like PM₁₀. We also considered the stations providing data for at least 5 years of the period 1998-2008; the numbers of stations reach 358 and 26 for PM₁₀ and PM_{2.5}, respectively.

The measurements of sulphate, nitrate and ammonium were obtained through the EMEP database. A total of 16 stations have been selected for the inorganic components based on that they provide daily observations for at least 10 years over 1998-2008. For the evaluation of particulate matter concentrations, the model to data statistics mean bias (MB), root mean square error (RMSE) and sigma ratio (σ , i.e. modelled standard deviation divided by observed standard deviation) are selected for the present study. As suggested by Boylan and Russell (2006), we also considered the mean fractional bias (MFB) and the mean fractional error (MFE). They proposed that the model performance criteria would be met when both MFE $\leq 75\%$ and MFB $\leq \pm 60\%$, respectively. The model performance goal would be met when both MFE $\leq 50\%$ and MFB $\leq \pm 30\%$.

Time series of period-average monthly mean PM₁₀ concentrations from the HINDCAST simulation are presented in Fig.3. A common underestimation of PM₁₀ is observed for the MOCAGE, EMEP and MATCH models. For CHIMERE, PM₁₀ levels are slightly overestimated in winter and underestimated in summer. Table 3 summarizes the statistics of the daily mean PM₁₀ and PM_{2.5} levels, averaged for the annual and seasonal (JJA, DJF) periods of 1998-2008 over all the European stations considered. Negative mean biases are calculated in the models for the annual and seasonal periods. The greater underestimation of PM₁₀ in MOCAGE (Fig 3) is partly attributed to a lack of secondary organic and inorganic aerosols in the reaction scheme. The high sigma ratio calculated for wintertime indicates that the models do not simulate the range of variability as the measurements. The MFB for PM₁₀ do not meet the model performance goals, except for CHIMERE for the annual and JJA periods. However, the model performance criteria are met for the CHIMERE, EMEP and MATCH models. As seen in Table 3, lower biases are calculated for the PM_{2.5} daily mean in all the models by comparison with PM₁₀. For PM_{2.5}, the JJA MFE and MFB fall within the performance criteria recommended by Boylan and Russel (2006) for all the models.

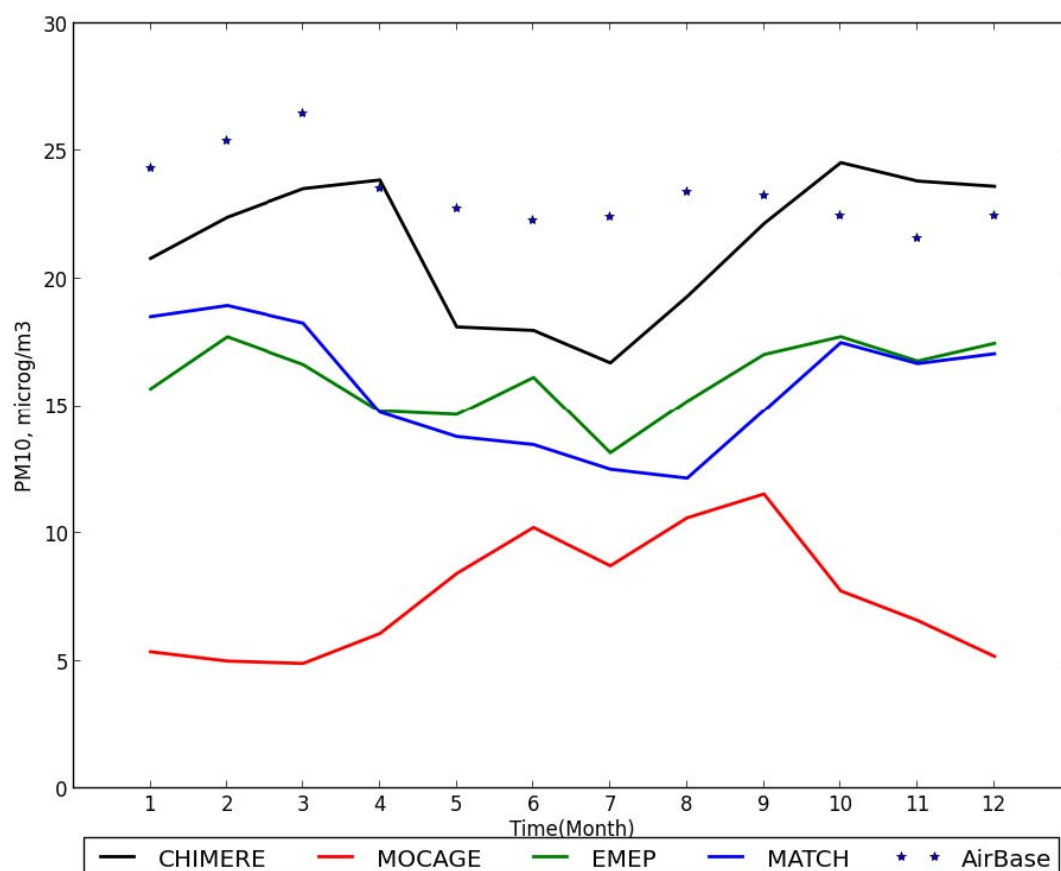


Figure 3: Time series of monthly average daily PM10 levels ($\mu\text{g.m}^{-3}$) over the period 1998-2008, simulated by CHIMERE (in black), MOCAGE (in red), EMEP (in green) and MATCH (in blue), driven by non-nudged regional climate model data; and measured by AirBase (blue stars). The time series are averaged over the stations.

		PM10 daily mean			PM2.5 daily mean		
		MB	σ	MFB	MB	σ	MFB
Annual	CHIMERE	-0.9	0.9	1.1	-0.5	1.6	0.9
	MOCAGE	-15.7	0.30	-104.6	-8.9	0.6	-72.1
	EMEP	-6.6	1.1	-28.4	-5.2	0.8	-34.4
	MATCH	-7.2	0.65	-29.4	-3.6	0.6	-12.7
JJA	CHIMERE	-3.5	1.06	-14.8	-0.9	1.6	-10.5
	MOCAGE	-12.6	0.65	-78.0	-4.2	1.6	-38.7
	EMEP	-7.3	2.3	-36.9	-3.4	1.6	-32.3
	MATCH	-9.5	0.6	-47.9	-3.5	0.8	-24.9
DJF	CHIMERE	0.1	1.4	8.3	-1.6	2.3	-2.2
	MOCAGE	-18.7	0.34	-130.9	-14.1	0.28	-111.6
	EMEP	-5.8	1.5	-18.9	-6.8	0.9	-36.4
	MATCH	-5.6	1.3	-14.9	-3.6	1.3	0.4

Table 3: Annual and seasonal (JJA: June, July and August, DJF: December, January and February) statistics over Europe at AirBase stations for PM2.5 and PM10 mean values. Statistics are averaged for the 10-yr

period. The calculated statistics are mean bias (MB, $\mu\text{g.m}^{-3}$), sigma ratio (σ), and mean fractional bias (MFB, %).

Results for the MB, standard deviation and mean are presented in Table 4 for the secondary inorganic aerosols (sulphate, nitrate and ammonium). The models well reproduce the mean sulphate concentrations, low biases are calculated. The variability of the observations (Std Dev= 1,8 $\mu\text{g.m}^{-3}$) is slightly underestimated by MATCH and overestimated by CHIMERE. The mean concentrations of nitrate simulated by the models are in the same range of values as the observation (Mean=1,7 $\mu\text{g.m}^{-3}$). The variability of CHIMERE and EMEP are higher than the observed variability (Std dev=1,6 $\mu\text{g.m}^{-3}$). For ammonium, the levels simulated by the models agree well with the observations.

	Sulfate			Nitrate			Ammonium		
	Mean	MB	Std Dev	mean	MB	Std Dev	Mean	MB	Std Dev
CHIMERE	3.1	0.8	2.4	2.1	0.4	2.9	1.6	0.6	1.4
EMEP	2.1	-0.2	1.9	2.2	0.5	2.0	1.0	0.0	0.9
MATCH	1.9	-0.4	1.4	1.7	0.0	1.4	0.86	-0.14	0.64
Observation	2.3		1.8	1.7		1.6	1.0		0.8

Table 4: Annual statistics obtained with CHIMERE, EMEP and MATCH over Europe at the EMEP stations. Statistics are averaged for 1998-2008 period. The computed statistics are mean, mean bias (MB, $\mu\text{g.m}^{-3}$), simulated standard deviation (Std Dev, $\mu\text{g.m}^{-3}$). Statistics are computed for the sulfate, nitrate and ammonium daily mean values. Daily mean values of sulfate, nitrate and ammonium simulated and observed, as well as observed standard deviations are computed.

Ozone Statistics

Modelled ozone concentrations were also evaluated against AirBase data. In order to select the monitoring sites that are most representative of the spatial resolution used in this study, the objective classification of AirBase monitoring stations, as developed by Joly and Peuch (2012), was used. As in Lacressonnière et.al. (2012), the measurement stations corresponding to classes 1-5 were selected to be most representative of O_3 values. Only the stations providing data for a minimum of 10 years during the period 1998-2008 were selected, so that there was a total of 543 stations used for the analysis of O_3 data. The model to data statistics of mean bias (MB), root mean square error (RMSE), sigma ratio, mean fractional bias (MFB), and mean fractional error (MFE) were used to evaluate the models' performance in comparison with observation data.

Time series of 1998-2008 monthly mean O_3 concentrations from the HINDCAST simulation, averaged over the 543 AirBase station locations, are presented in Fig.4. CHIMERE and EMEP generally produce concentrations of ozone that are higher than values measured at the selected stations all year round, while MATCH and MOCAGE generate values of ozone that are lower than measurements in the summertime. The springtime maxima produced by the four models range from 35-42 ppb, which is in line with the average observational maximum of 37 ppb in May. Table 5 summarizes the statistics of the hourly O_3 values, averaged for the annual and seasonal (JJA) periods for 1998-2008 over the European stations considered. Positive mean biases are calculated in CHIMERE and EMEP for the annual and seasonal periods, while negative biases are calculated for MATCH and MOCAGE in the summer. The sigma ratio, i.e. the standard deviation of the modeled time series divided by the standard deviation of the observed time series, shows how well the models are able to simulate a realistic variability in ozone concentrations. On an annual basis, CHIMERE and MATCH generally underestimate the observed variability of O_3 values ($\sigma=0.7$ and $\sigma=0.8$,

respectively), whereas EMEP and MOCAGE come close to matching the variability of the observations ($\sigma=0.9$ and $\sigma=1.0$, respectively).

The mean fractional biases (MFB) for all models are below 30 percent and the mean fractional errors (MFE) are all below 50 percent for both the annual and summer periods. MATCH has the lowest MFB (3.1%) and CHIMERE has the lowest MFE (34.6%) during the summer period.

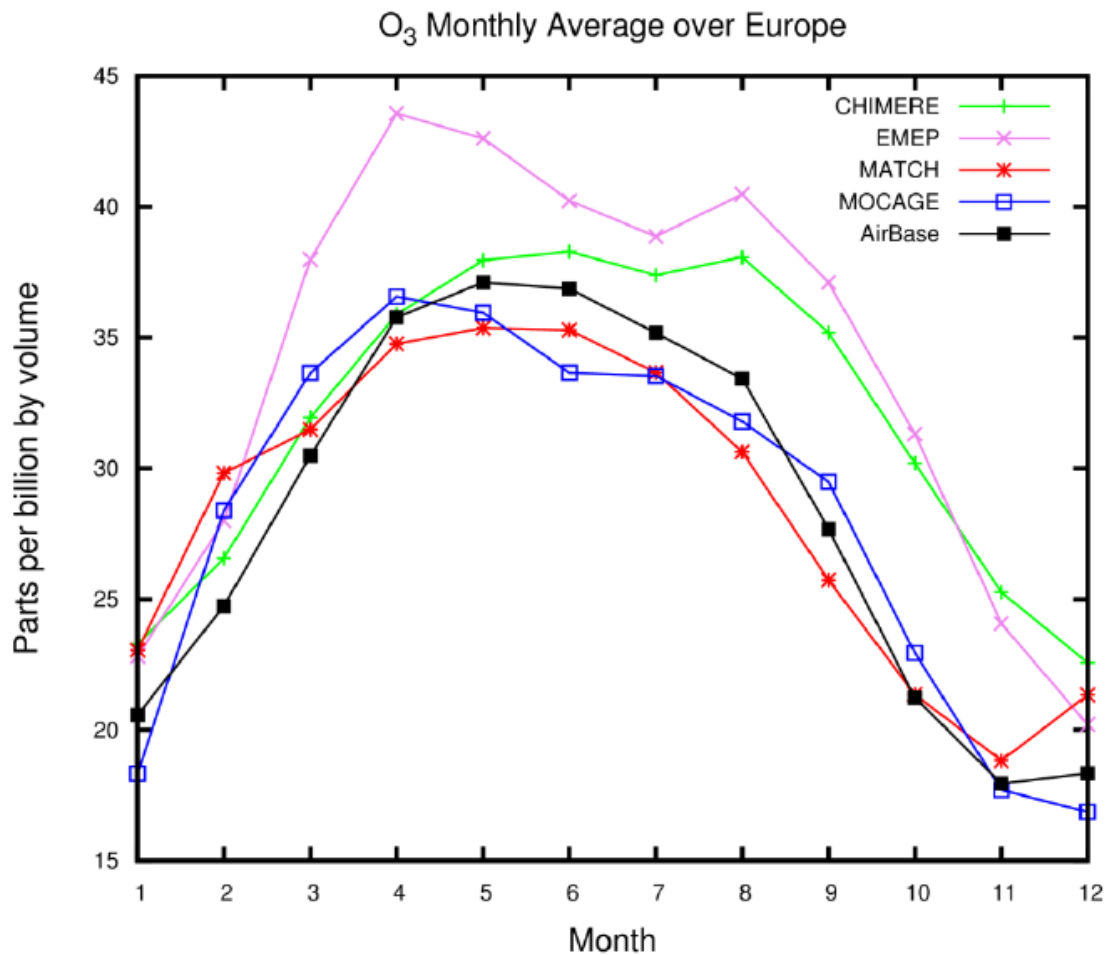


Figure 4: Time series of monthly average O₃ levels (ppb) over the period 1998-2008, simulated by CHIMERE (in green), EMEP (in pink), MATCH (in red), and MOCAGE (in blue), driven by non-nudged regional climate model data; and measured by AirBase (in black). The time series are averaged over the stations that correspond to pollution classes 1-5.

Hourly O ₃ Data	Model	RMSE ($\mu\text{g.m}^{-3}$)	MB ($\mu\text{g.m}^{-3}$)	Sigma	MFB	MFE
Annual	CHIMERE	13.0	4.7	0.7	27.1	44.0
	MOCAGE	15.0	6.6	0.9	29.0	47.4
	MATCH	12.8	1.0	0.8	11.4	44.8
JJA	CHIMERE	14.0	0.7	1.0	4.2	49.7
	MOCAGE	15.1	3.6	0.6	18.0	34.6
	MATCH	16.2	5.4	0.7	20.6	37.8

Table 5: Annual and seasonal (JJA: June, July and August) statistics over Europe at AirBase stations. Statistics are calculated over the period 1998-2008. The calculated statistics are root mean square error (RMSE, ppb), mean bias (MB, ppb), sigma ratio (σ), mean fractional bias (MFB, %) and mean fractional error (MFE, %). Statistics are computed for the hourly ozone values.

2.2 Changes in air pollutant concentrations

Ozone

Figure 5 shows the average concentration of ozone (O_3) at the surface, as simulated by the four models for scenario S1 for the summer period (June, July, and August) and the winter period (December, January, and February). The results for this future scenario are averaged over the 30 years corresponding to the time period in which the driving GCM for each model reaches 2 degrees above pre-industrial temperatures. In general, O_3 concentrations in the summer vary between 25 and 45 ppb over land. MATCH and MOCAGE show lower concentrations of O_3 in the summer over Europe (between 25 to 30 ppb on average) than CHIMERE and EMEP, due to the fact that MATCH and MOCAGE experience their peak values of O_3 earlier in the year. As expected, the greatest summer concentrations of O_3 occur in southern Europe. During the winter, O_3 values over Europe are generally less than 30 ppb for all models, while MOCAGE has significantly higher values of O_3 (around 50 ppb) over the ocean. The differences shown for MOCAGE may be attributed to numerous causes. In particular, MOCAGE is the only model out of the four which uses its own lateral boundary conditions, which have an inter-annual variation; the other three models use the same lateral conditions on the influx boundaries, which are taken from a multi-year average of chemical composition with monthly temporal resolution, simulated with the LMDz-INCA model.

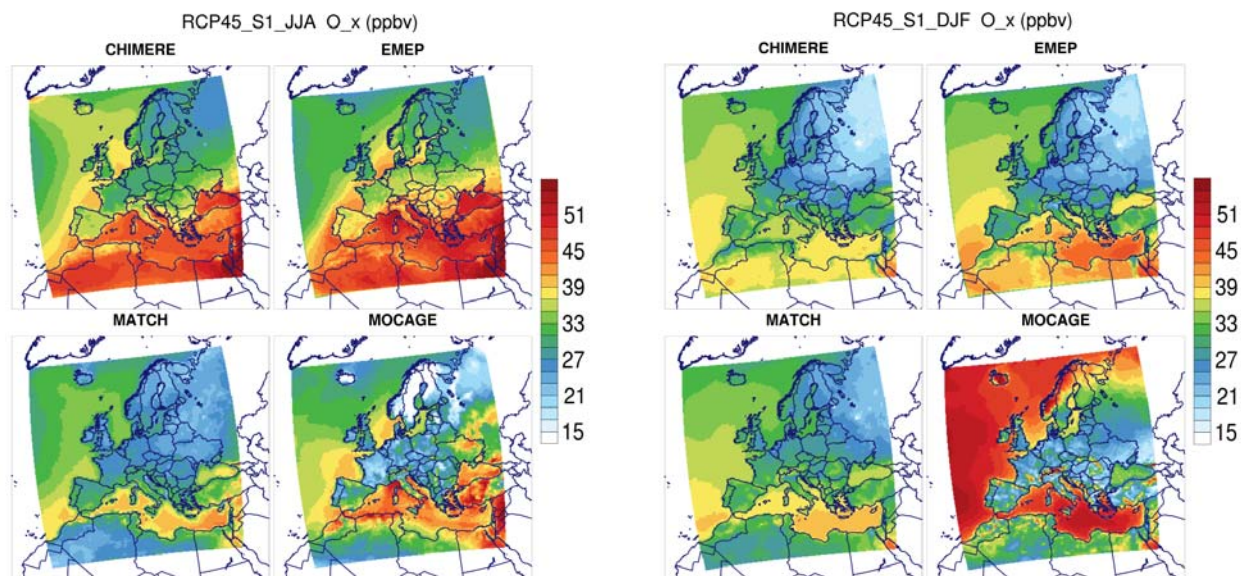


Fig.5: Average O_3 concentrations simulated for S1 by CHIMERE, EMEP, MATCH, and MOCAGE for summer (left) and winter (right).

Comparison between future and current climate

Figure 6 shows the difference in the average concentration of ozone at the surface for the future S1 scenario minus the control scenario (HISTORICAL), as simulated by the four models. The results for the future scenario are averaged over the 30 years corresponding to the time period in which the driving GCM for each model reaches 2 degrees above pre-industrial temperatures, whereas the results for HISTORICAL are averaged over the 1971-2000 time period. The differences between the future and control simulations vary greatly depending on season. In winter, ozone concentrations are higher over Europe in the future scenario; however, in the summer, ozone concentrations are significantly lower in the future scenario over all of Europe for all models. The decrease of ozone during the summer is linked to the reduction in anthropogenic emissions observed from 2005 to 2050, while during winter continental changes are most likely driven by reductions in titration of ozone with NO_x , coupled with the increase in temperature.

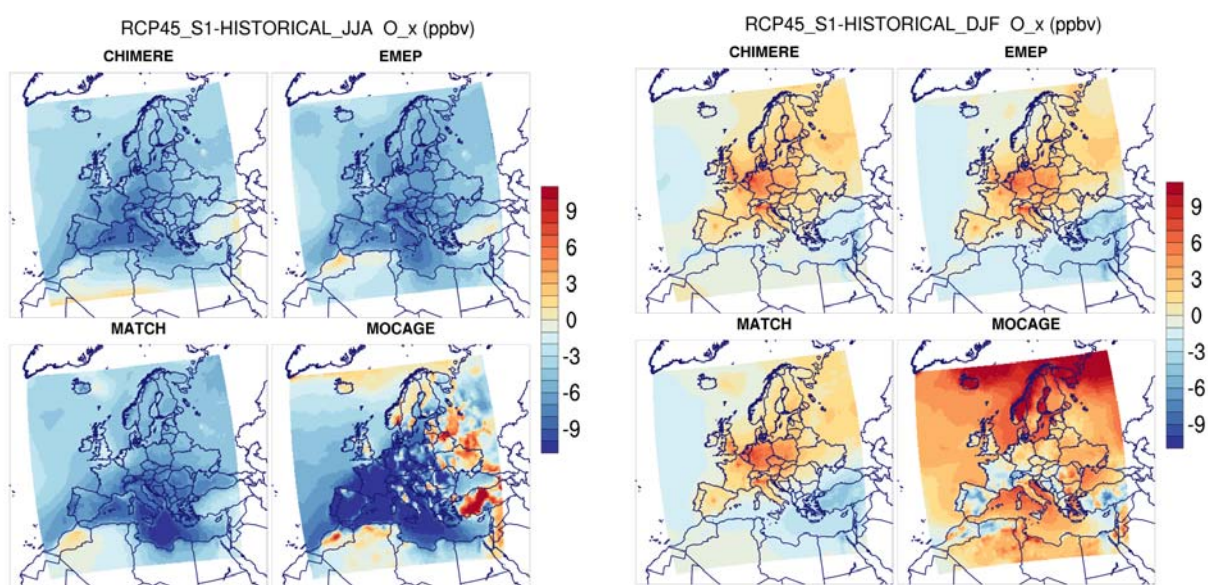


Fig.6: Differences in average O_3 concentrations (in ppbv) between S1 and HISTORICAL simulated by CHIMERE, EMEP, MATCH and MOCAGE for summer (left) and winter (right).

Climate change effect

The difference between S1 and S2 shows the influence of climate change only on expected changes in future air quality, sometimes called the « climate penalty ». Figure 7 shows the difference between S1 and S2 for surface ozone for the summer months (June, July, and August) and the winter months (December, January, and February) for the four models. S2 is averaged over 1971-2000, whereas S1 is averaged over the 30 years corresponding to the time period in which the driving GCM for each model reaches 2 degrees above pre-industrial temperatures. In the summer, the climate change effect for all four models is positive and less than 2 ppbv over most of Europe. In the wintertime (December, January, and February), the climate penalty for all four models is similar in magnitude to the summer. These results indicate that, when not taking into account differences in emissions (because these two scenarios both use the same 2050 ECLIPSE v4a emission data), the future climate, on average, has a tendency to cause greater values of ozone at the surface in comparison with the current climate. This conclusion is consistent with other studies, which note a strong correlation between ozone concentrations and temperature in polluted regions (Jacob and Winner, 2009, and references therein).

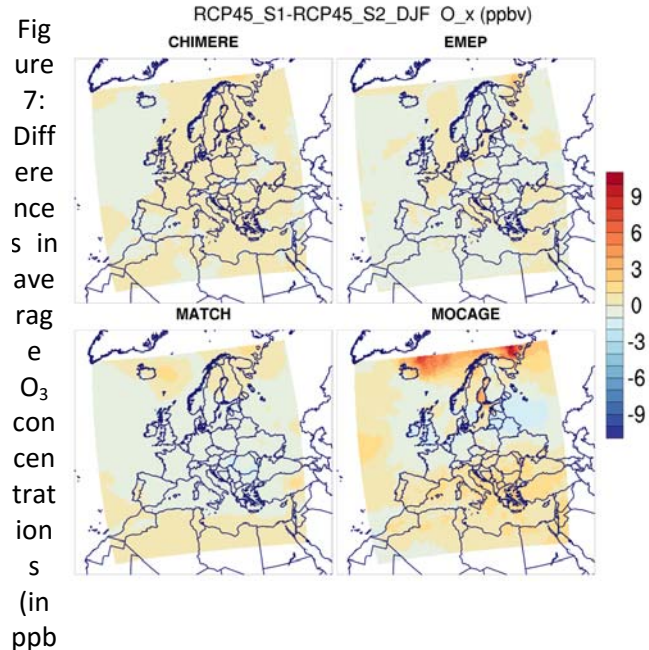
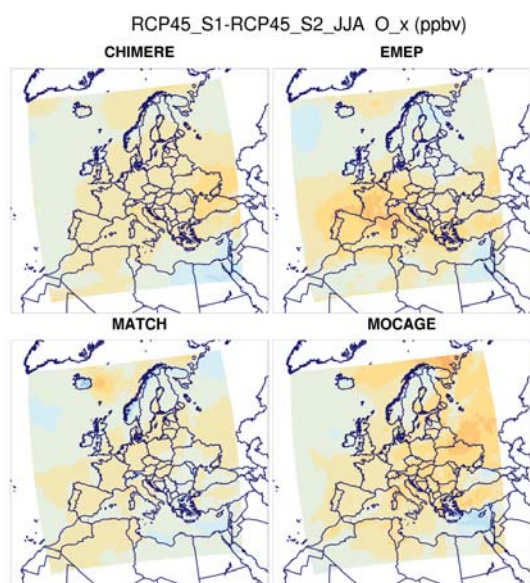


Figure 7: Difference in average surface O₃ concentrations (in ppb)

) between S1 and S2 simulated by the models for

summer (left) and winter (right).

Effect of a more ambitious emission abatement scenario

Simulation S3 was performed with the MFR ECLIPSE v4a emission data in order to show the potential impacts of technically feasible reductions in anthropogenic emissions. Figure 8 shows the effect of the mitigated emissions upon surface-level ozone as the difference between S1 and S3, averaged over the 30 year future +2°C period for each model. The results show that the mitigated mitigation emission scenario results in noticeable reductions in surface ozone in the summer. CHIMERE, EMEP, and MATCH show a decrease in ozone of around 1 ppb in the United Kingdom and Scandinavia, 2 ppb in central Europe, and up to 4 ppb in Eastern Europe. For MOCAGE, the reductions are much more dramatic, with a reduction of up to 10 ppb in Spain, Eastern Europe, and North Africa. In the winter, the mitigated scenario causes more minimal reductions in O₃ in the south-western part of Europe (e.g. Spain) and northern Africa. The remainder of the European domain experiences a slight increase in surface O₃ during the winter months. These results show that efforts to reduce anthropogenic emissions could play a significant role in mitigating surface O₃, particularly in the summer, with consequent implications for the protection of public health.

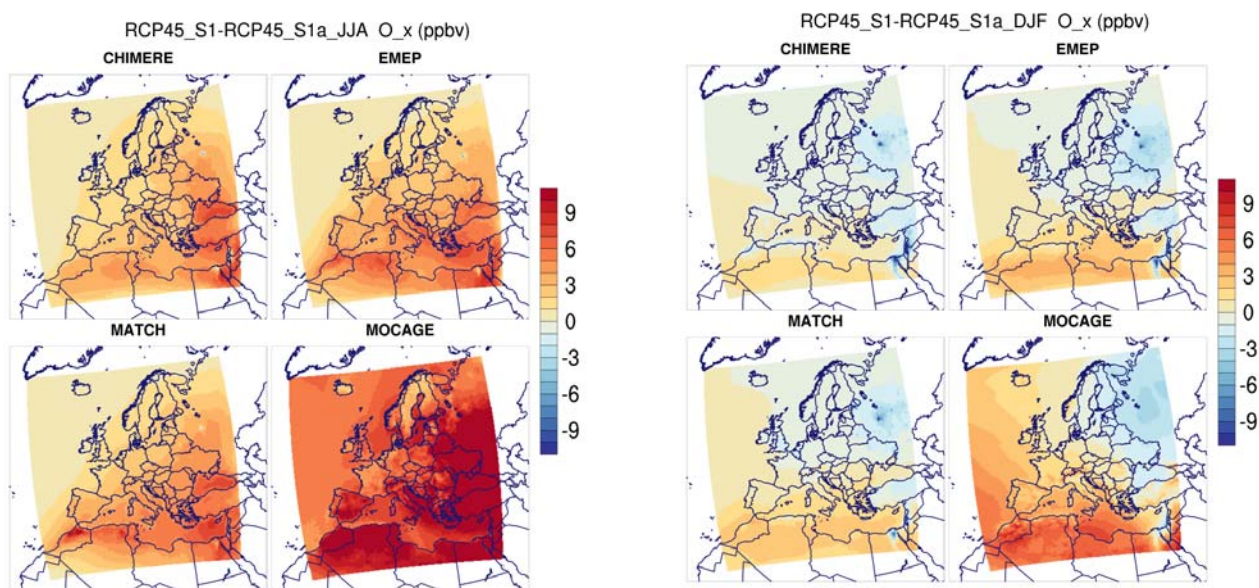


Fig.8: Differences in average O₃ concentrations (in ppbv) between S1 and S3 simulated by CHIMERE, EMEP, MATCH, and MOCAGE for summer (left) and winter (right).

Particulate Matter and aerosols

The average fields of annual PM₁₀ for the HISTORICAL simulation (Fig.9) display higher concentrations over central Europe, near pollution sources, and over the southern domain, due to the incoming flux of desert dust. However, MATCH only includes Saharan dust from the boundaries in the simulations and thereby simulates lower values over the southern domain. In addition to soil dust within-domain emissions, this version of MATCH also lacks secondary organic aerosols. The differences between the models mainly originate from differences in the dynamical emissions of desert dust and sea salt. The highest values of PM_{2.5} are simulated in CHIMERE and EMEP, up to 25 $\mu\text{g.m}^{-3}$, over central Europe, while the levels of PM_{2.5} are notably lower in MOCAGE. The lack of secondary aerosols in MOCAGE explains these differences.

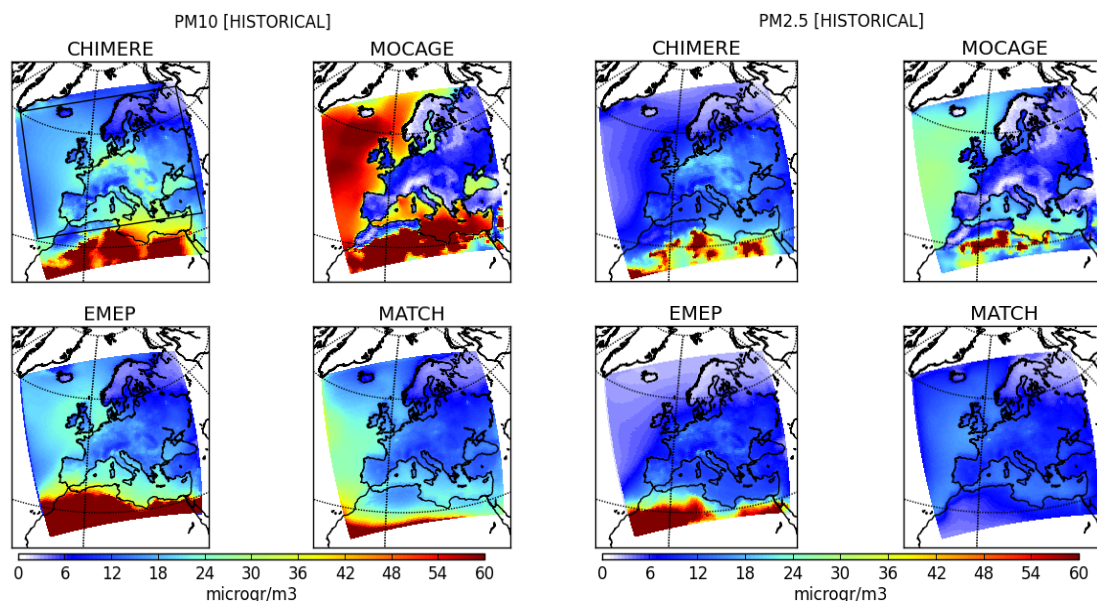


Fig. 9: Average of annual mean PM10 (left) and PM2.5 (right) simulated by CHIMERE, MOCAGE, EMEP and MATCH in the HISTORICAL simulation.

The impact of a +2°C climate and of associated emission change is demonstrated when S1 is compared to the control (HISTORICAL) scenario (Fig. 10). The decrease of PM10 in S1 is simulated over continental Europe, with the largest decreases of PM10 over Western Europe. All the secondary inorganic aerosols decrease in the future as a result of decreasing anthropogenic emission of precursors. However, the highest changes are observed over North Africa in CHIMERE, MOCAGE and EMEP. These differences can mainly be attributed to the changes in dust emissions, due to changes in precipitation and winds. Weaker changes of dust concentrations are simulated in MATCH.

The comparisons between S2 and HISTORICAL (Fig. 10b) display the contribution of global and regional anthropogenic emission changes. The concentrations of PM10 over Europe largely decrease in scenario S2 in the CHIMERE, EMEP and MATCH models. In case of MOCAGE, higher changes of PM10 levels are simulated over North Africa, which is due to the boundary conditions, while the dynamical emissions (desert dust, sea salt and biogenic COV) have been calculated with the same meteorology of the current climate.

The differences between S1 and S2 show how the +2°C climate affects surface PM in the absence of emission changes, under the regional climate change only (Fig. 10). The projected changes of PM10 concentrations vary greatly between the models. According to the analysis of PM components, the changes in PM10 are mainly due to changes in natural emissions, such as desert dust, sea salt and biogenic emissions, affected by changes in meteorology. Over continental Europe, slight changes of PM10 are observed.

Compared to the CLE scenario, the mitigation scenario (use of MFR emissions scenario) enhances the decrease of PM10 compared to the current legislation over Europe in all the models (Fig. 10d), with largest decrease over Eastern Europe, up to 5 $\mu\text{g}\cdot\text{m}^{-3}$.

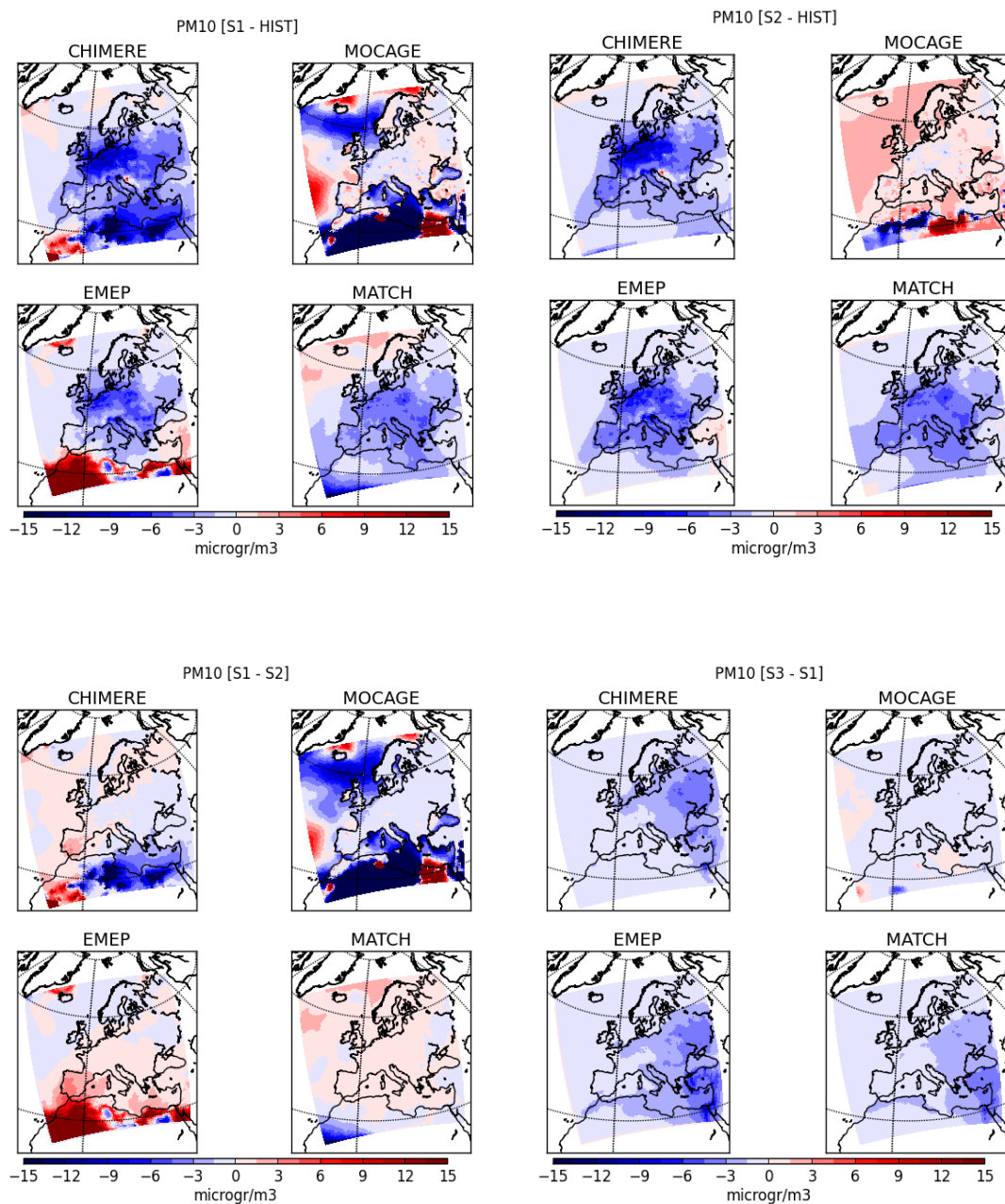


Fig. 10: Differences in annual PM10 between the future scenario S1 and HISTORICAL (top left), the future scenario S2 and HISTORICAL (top right), the future scenarios S1 and S2, and the future scenario S3 and S1, simulated by CHIMERE, MOCAGE, EMEP and MATCH.

The same comparisons are displayed for PM2.5 between HISTORICAL and the future scenarios (Fig. 11). The decrease of PM2.5 concentrations is large in the future CLE scenario (S1), in CHIMERE, EMEP and MATCH, and even more with the implementation of the MFR emission scenario (S3). Regional climate change has minor effects on PM2.5 concentrations (S1-S2) over continental Europe as it mainly affects coarser particles (desert dust and sea salt) as observed in PM10 differences.

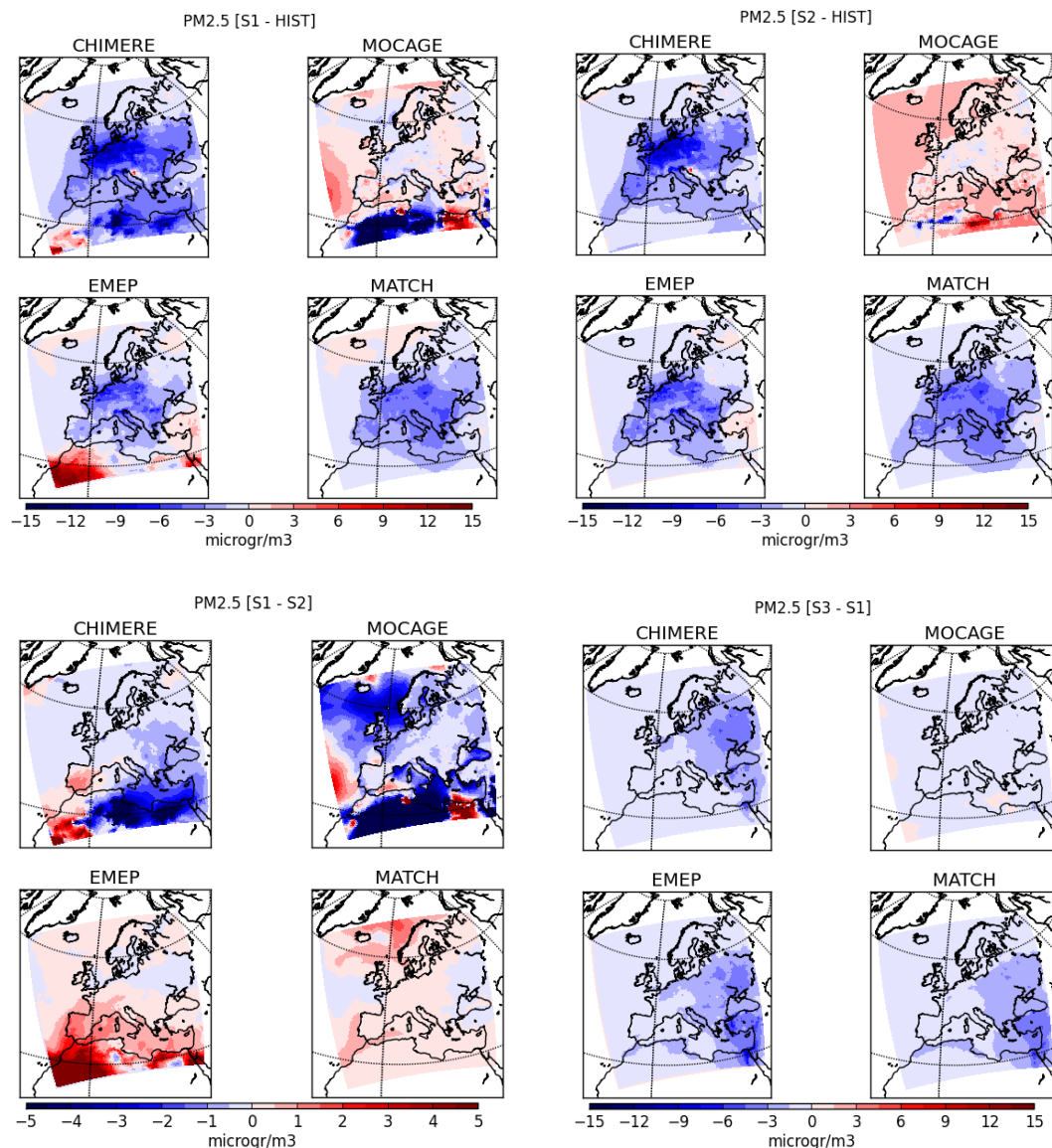


Fig. 11: Same as Fig.4.2.6 for PM2.5

The aerosol composition is presented in Fig. 12 over Europe (only continental surfaces are used in the calculation of averages) for the CHIMERE, EMEP and MATCH models. All three models simulate the secondary inorganic aerosols (sulphate, nitrate, ammonium), sea salt, primary organic matter (POM), black carbon (BC), and desert dust (BC). The formation of secondary organic aerosols (SOA) is only included in the CHIMERE and EMEP models.

All the secondary aerosols decrease in the future scenarios, and most notably in S1 and S3, as the emissions of anthropogenic precursors decrease. The small increase in NH₃ emissions between 2005 and 2050 CLE scenario is not seen in the formation of ammonium. The ammonium concentrations decrease from HISTORICAL to S2 in the three models. This feature is likely related to decreased formation of ammonium sulphate following the large reductions in available SO₂ in all future scenarios (Engardt and Langner, 2013). This projection of aerosol compositions shows increasing relative contribution of sea salt and dust aerosols in the future.

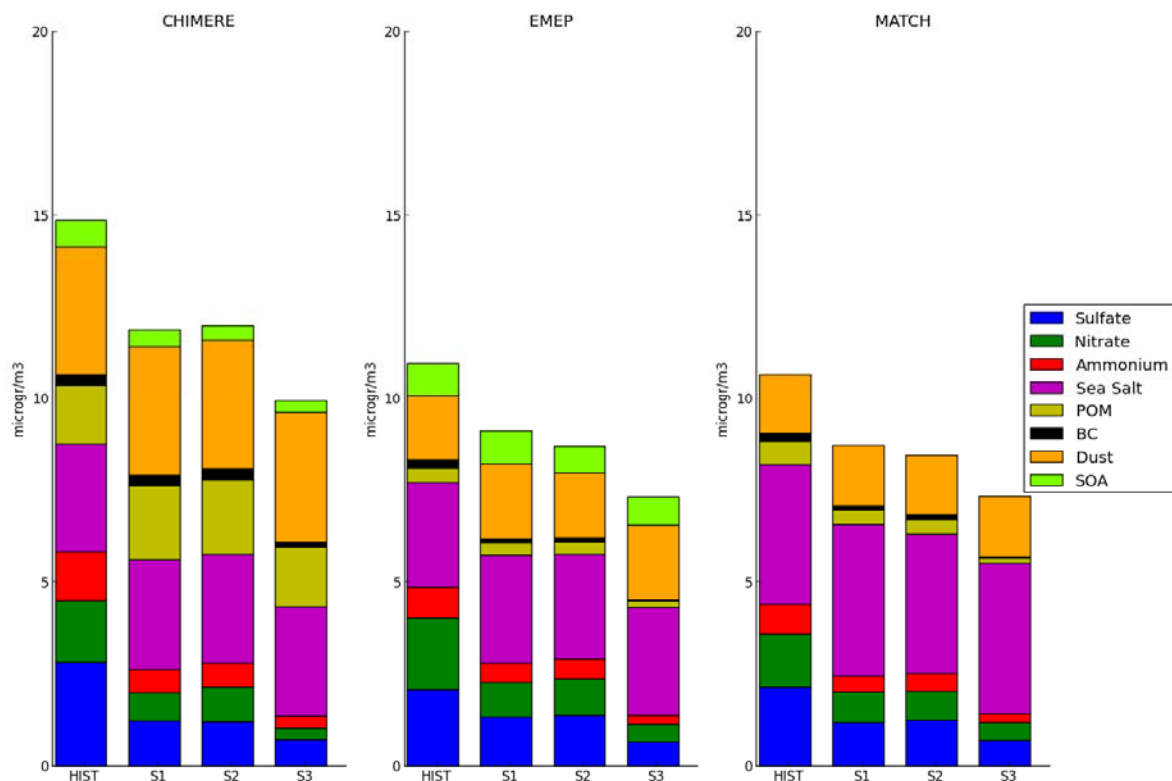


Fig. 12: Aerosol composition over Europe (see Fig.4.2.5 for the domain considered, sea surface excluded) in HISTORICAL, and the future scenarios S1, S2 and S3.

Deposition changes

Figures 13-15 show total deposition of sulphur, total deposition of oxidised nitrogen and total deposition of reduced nitrogen averaged over the 30 years in the HISTORICAL experiment (i.e. current situation based on meteorology from GCMs) for the four participating models. Areas with large emissions stand out with increased deposition. Sulphur deposition is, for example, particularly large in high-emission areas in Western Europe and in south-eastern Europe while the deposition of oxidised and reduced nitrogen is largest in north-western continental Europe. The volcanic SO_2 emissions from Etna are not included in CHIMERE but stand out very clearly in EMEP and MATCH. MOCAGE includes volcanic SO_2 emissions but since these occur high above the surface and remain in the gas-phase very little is being deposited to the ground.

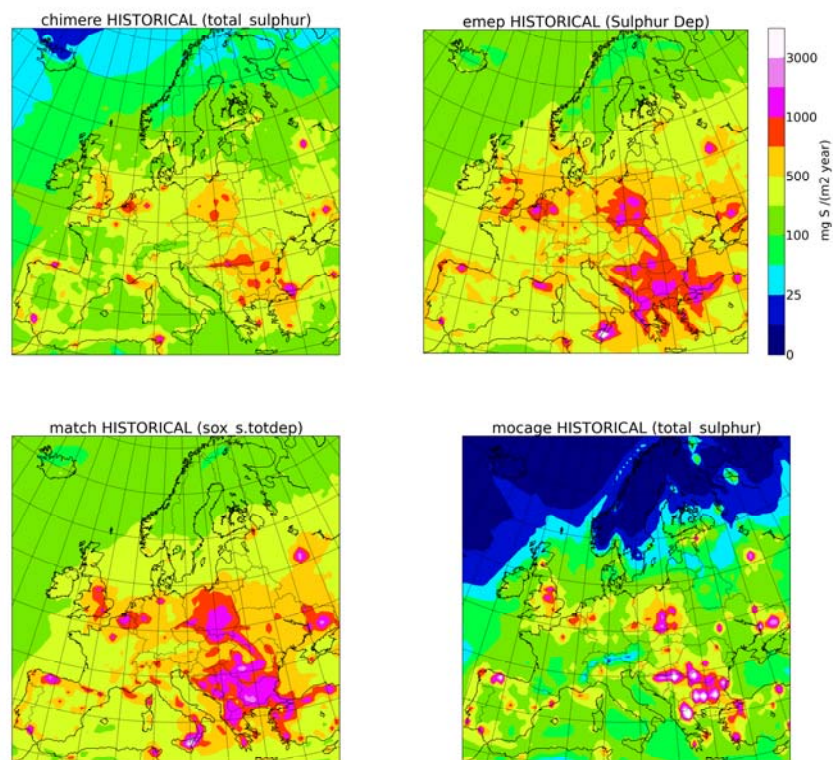


Figure 13 Annual average total deposition of sulphur in the HISTORICAL experiment.

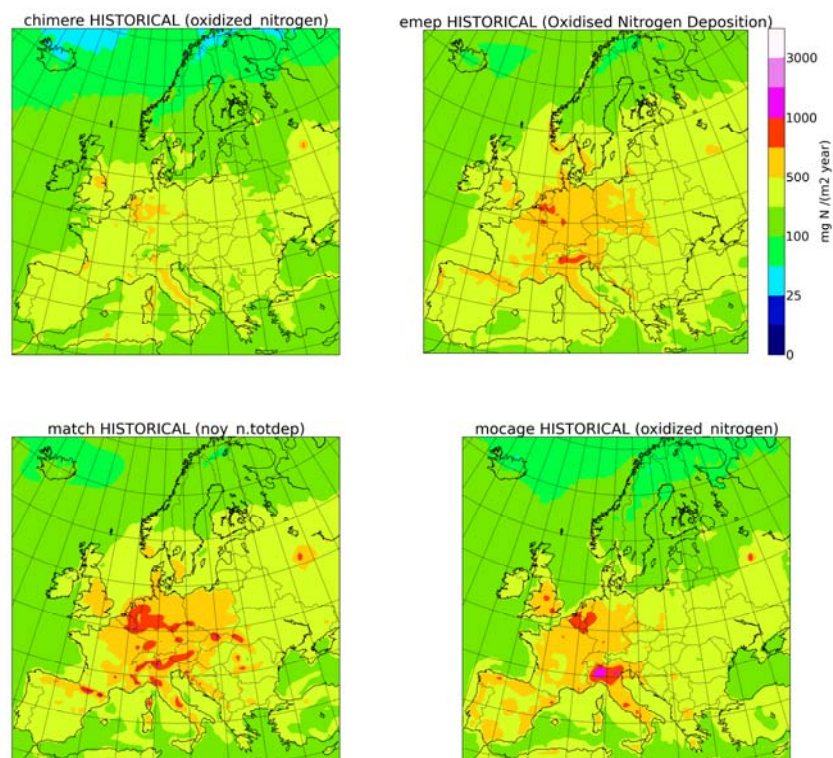


Figure 14 Annual average total deposition of oxidised nitrogen in the HISTORICAL experiment.

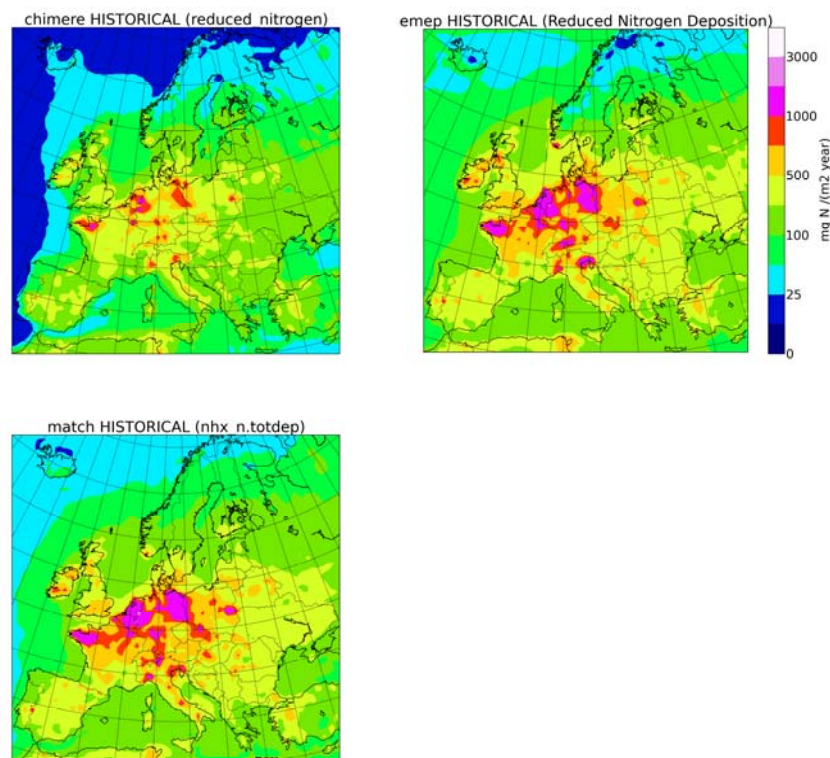


Figure 15 Annual average total deposition of reduced nitrogen in the HISTORICAL experiment.

EMEP and MATCH display very similar spatial patterns and levels for the deposition all components. CHIMERE and MOCAGE feature lower deposition for all components, although MOCAGE has a number of localized areas with very high sulphur deposition. Away from the high emission areas, on the other hand, is the deposition of total sulphur unreasonable low in MOCAGE implying that sulphur is deposited too efficiently. This is related to the fact that reduced nitrogen (i.e. NH_3 and ammonium) is not treated in MOCAGE and that all emitted sulphur remains as gaseous SO_2 . The low total deposition in CHIMERE is caused by too low wet deposition in that model.

Figs. 16-18 show changes in deposition from 1971-2000 (experiment HISTORICAL) to a future time period when the global mean temperature has increased 2°C in the respective global GCM (experiment S1). Changes in deposition emanate from changes in climate, European emissions and global emissions (manifested as alternative boundary concentration of the regional CTMs).

For sulphur and oxidised nitrogen the deposition is projected to decrease substantially over Europe but increase in Turkey and parts of North Africa. The pattern of the deposition changes are similar between all models although MOCAGE display areas in east and southern Europe with increasing sulphur depositions that are not evident in the other models. For reduced nitrogen, the three models that included this component all project that the depositions will increase in Europe up to the period when global mean temperatures reach $+2^\circ\text{C}$.

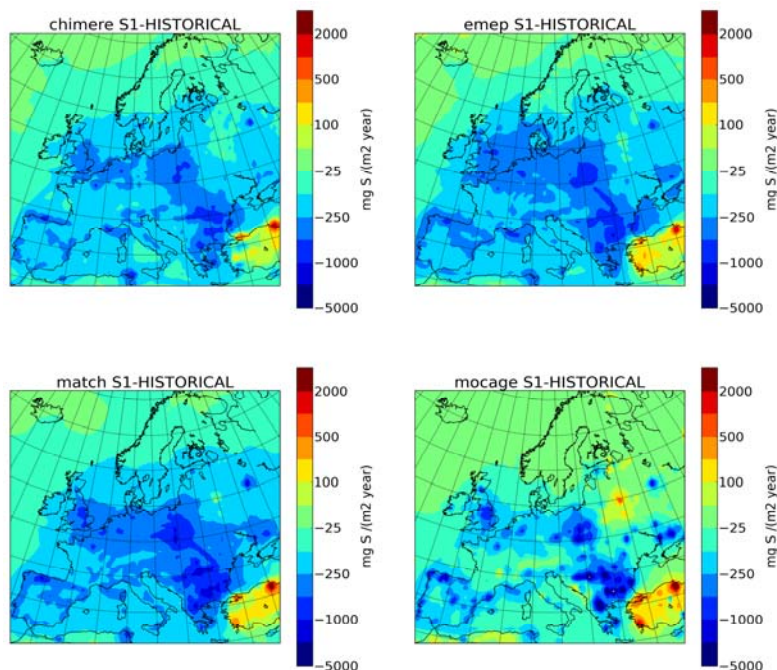


Figure 16 Change in average total deposition of sulphur from HISTORICAL to the period when the global mean temperature increases by +2°C (experiment S1; "future situation").

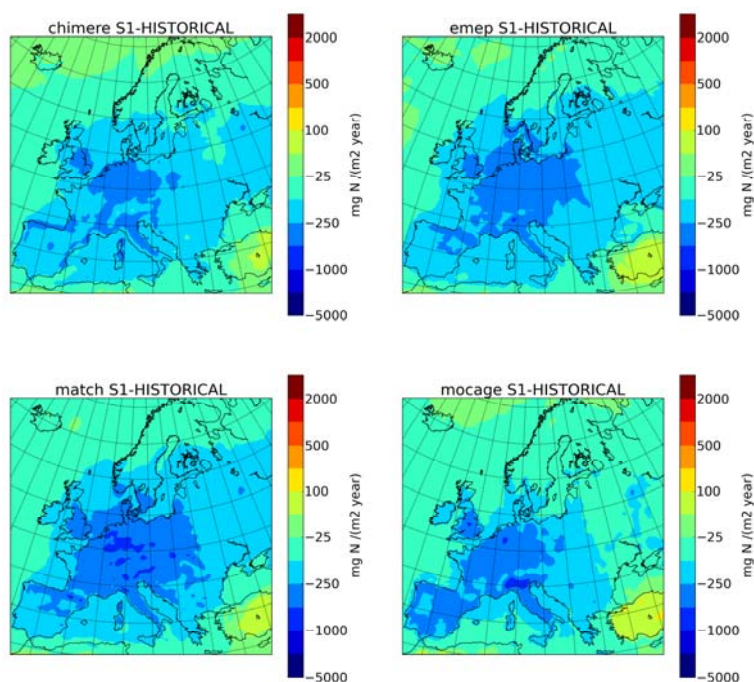


Figure 17 Change in average total deposition of oxidised nitrogen from HISTORICAL to the period when the global mean temperature increases by +2°C (experiment S1; "future situation").

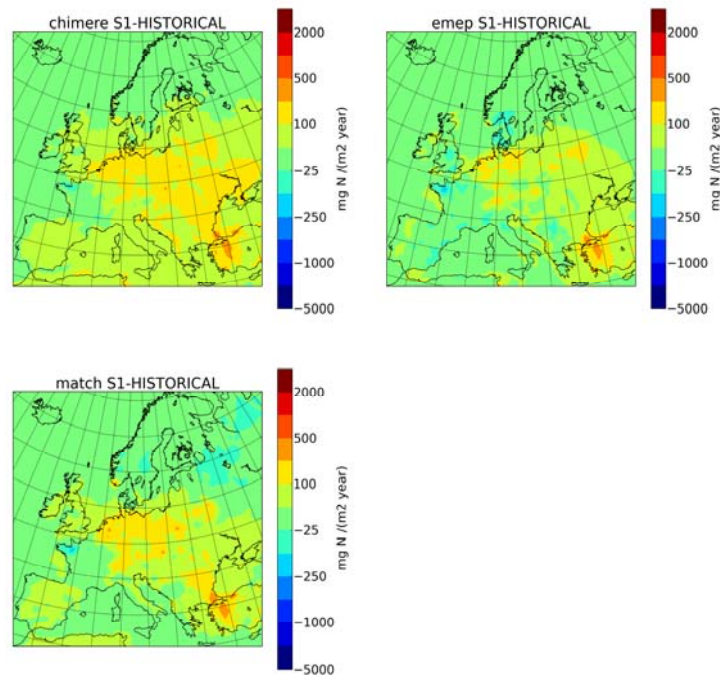


Figure 18 Change in average total deposition of reduced nitrogen from HISTORICAL to the period when the global mean temperature increase by +2°C (experiment S1; “future situation”).

In order to unravel the effects of climate change and changing emissions a number of additional experiments were performed.

The “climate penalty” on total deposition of sulphur and nitrogen components following an increase of the global mean temperature by +2°C (i.e. experiment S1 minus S2) is shown in Figures 19-21. From the figures it is apparent that the associated climate change only results in small ($\pm 25 \text{ mg m}^{-2} \text{ year}^{-1}$) changes in total deposition of all species. This finding applies to all four models.

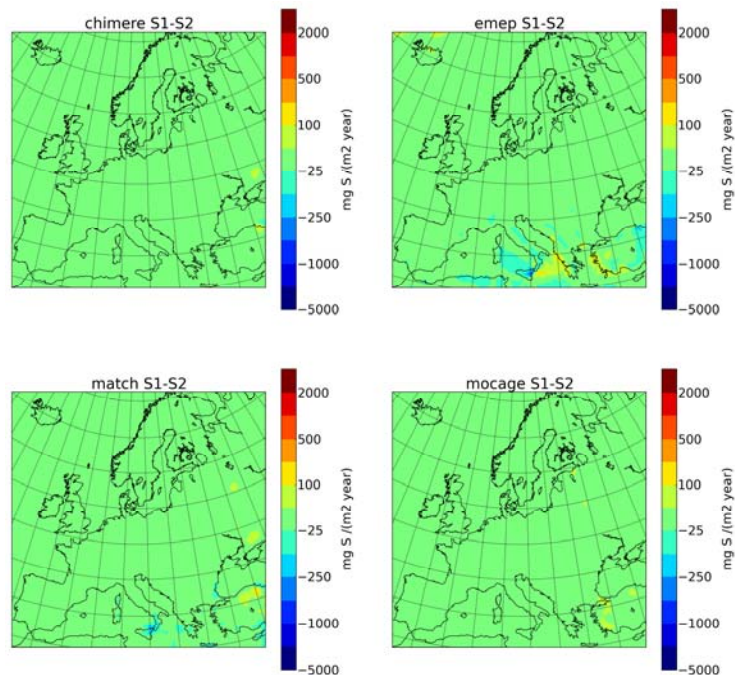


Figure 19 The effect of a global climate change, defined as a +2°C temperature increase, on the total sulphur deposition over Europe (“climate penalty”). Emissions and background concentrations are kept at the levels of 2050.

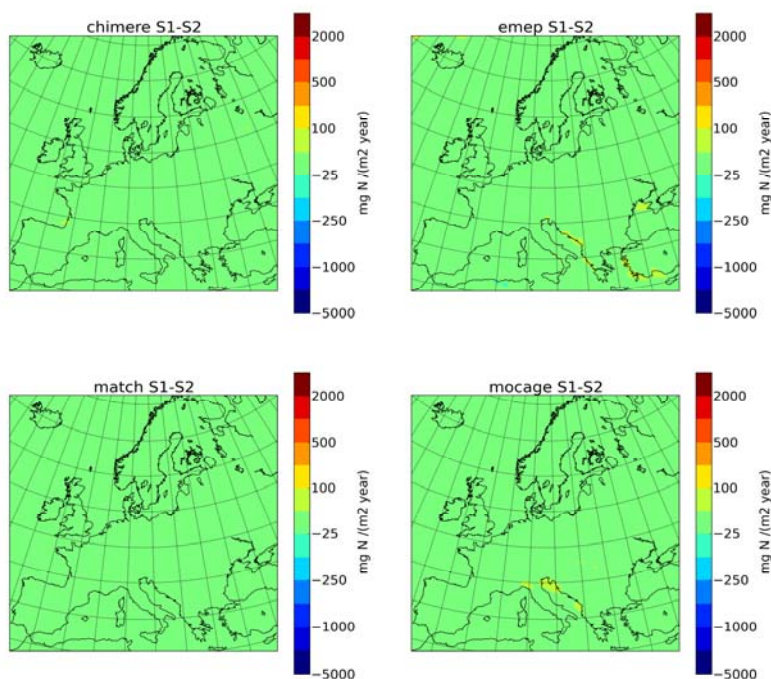


Figure 20 The effect of a global climate change, defined as a +2°C temperature increase, on the total deposition of oxidised nitrogen over Europe (“climate penalty”). Emissions and background concentrations are kept at the levels of 2050.

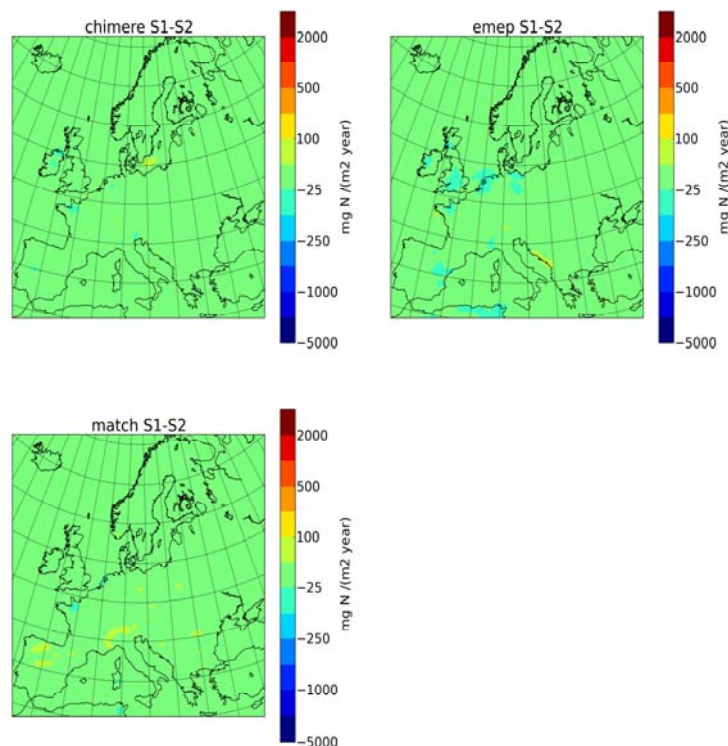


Figure 21 The effect of a global climate change, defined as a +2°C temperature increase, on the total deposition of reduced nitrogen over Europe (“climate penalty”). Emissions and background concentrations are kept at the levels of 2050.

The effects of changing air pollutant emissions from present times to the period of a +2° C warmer world can be deduced by comparing simulations with climate change only (Figs 19-21) and the results with climate and emission changes (Figs. 16-18). The comparison clearly show that most of the change in the deposition of all species, in models, emanates from changes in air pollutant emissions rather than changes in climate.

Climate change has considerably smaller impacts on the deposition of sulphur and nitrogen containing species than changes in emissions in a +2 °C warmer world. The magnitude of the future emissions are, however, highly uncertain and depend on political decisions and technical achievements made over the coming decades. As an indication of the uncertainty of the emission inventories and, in particular, addressing the effect of following what is defined as maximum technically feasible reduction (MFR), we have calculated how much better the situation could be compared with the situation with only effective implementation of existing emission control legislation (CLE; current legislation). All models agree (not shown), not surprisingly, that decreased emissions throughout the modelling domain result in decreasing deposition of all species. It is interesting to note, however, that the magnitude of the decrease is not identical in all models. The gains, in terms of modelled decreased deposition, are very similar in EMEP and MATCH. CHIMERE generally prescribes a smaller improvement for all species and MOCAGE calculates a smaller improvement for sulphur deposition and larger improvements for oxidised nitrogen deposition, although identical emissions are used by all models.

2.3 Uncertainty in air pollution changes

The uncertainty in air pollution changes is estimated using the spread of the four regional chemistry-transport models (CTMs), i.e. CHIMERE, EMEP MSC-W, MATCH and MOCAGE. Here we further analyse

several contributions to this overall uncertainty. Both uncertainties in the whole model chain (i.e. regional CTM, regional climate models (RCM) and global climate models (GCM)) and with respect to the length of the present and future climate projections are considered. It is beyond the purpose of the study to evaluate the specific source of the uncertainty in the model formulation. Instead, we wish to assess the robustness/uncertainty of model predictions, by comparing the inter-model spread to the climate change signals. Two long period simulations of 30-years have been conducted, one that covers the present period (1971-2000) and one that covers the +2°C period under the RCP4.5 scenario. We focused on annual PM2.5 and SOMO35, two indicators commonly used in health impact studies (HRAPIE, 2014), to evaluate the uncertainties associated to this future air quality projection. In a second part, we use the 30 year periods as a benchmark to assess the uncertainty in using shorter decadal time periods for predicting the effects of climate change on air pollution. The results presented here are from Lacressonnière et al. (2015b).

Method

We formed a small ensemble in order to assess the uncertainty in air quality projections under climate change. All four CTMs were used in the ensemble for the analysis of the SOMO35 index. On the contrary, only the models that produce the complete PM composition (CHIMERE, EMEP and MATCH) were used for the analysis of annual PM2.5.

We use the ensemble spread (max-min) and the “ensemble mean” in order to quantify the inter-model uncertainty:

- Ensemble mean = $\frac{1}{n} \sum_{i=1}^n (S1 - S2)$
- Ensemble spread = $|Max((S1 - S2)_n) - Min((S1 - S2)_n)|$

n is the number of the members in the ensemble

The ratio between the ensemble mean of climate change signal and the spread in the ensemble is calculated and its value above 1 is set as a criterion for confidence in the climate impact ensemble simulation. A second criterion is the sign of the changes among the models, we consider that the climate change signal is robust when all three models agree on the sign of PM2.5 and three of the four models (of the SOMO35 simulations) agree on the sign of SOMO35.

Finally, we use the 30 years period of the scenarios to evaluate the inter-annual variability and compare the decadal and climate period signals. For both air pollution indicators, we choose to focus on decades, such as the periods of 1970s (1971-1980), 1980s (1981-1990) and 1990s (1991-2000) for S2. For the S1, the 2 degree warming period was considered for each CTM. For each model, we form an ensemble of all combinations of considered decades (Table 6): 6 members for CHIMERE, EMEP and MOCAGE; and 9 members for MATCH.

	CHIMERE	MOCAGE	EMEP	MATCH
S1 - decadal periods	2031-2040 2041-2050	2041-2050 2051-2060	2061-2070 2071-2080	2041-2050 2051-2060 2061-2070

Table 6: Decadal periods used by each CTM to create an ensemble of differences between S1 and S2 : 6 members for CHIMERE, EMEP and MOCAGE and 9 members for MATCH.

Results

The comparisons between the S1 and S2 scenarios show that regional climate change only slightly impacts PM2.5 levels (Fig. 22). The ensemble mean of PM2.5 displays a regional climate change signal that ranges from -0.5 to $1.1 \mu\text{g.m}^{-3}$. Over some parts of Europe, the three models agree on the climate change signal (Fig. 2, black bullets): a decrease of PM2.5 is simulated over the south of Europe (notably Spain and south of France) while a decrease is found over some parts of eastern and central Europe. However, the amplitudes of the changes vary among the models as shown by the ensemble spread (max-min).

The effects of climate change on SOMO35 (Fig. 23 and 24) are stronger, notably for two of the models (MOCAGE and EMEP). The ensemble mean of SOMO35 ranges from -171 to 322 ppbv.day . Despite an agreement of increasing SOMO35 in the future scenario of S1, the spread between the models is high over most of Europe (Fig. 23).

Our results highlight that, for both indicators, the inter-model variability is higher than the regional climate change signals. However, the three CTMs simulate a decrease of PM2.5 over southwestern Russia and an increase of PM2.5 in the south of Spain, that can be stated with confidence (following our criteria) as the climate change signal is stronger than the inter-model variability. On the contrary, the future projections of SOMO35 are more uncertain as the climate signal/model spread ratio is less than 1 over the entire domain despite 3 models predict an increase.

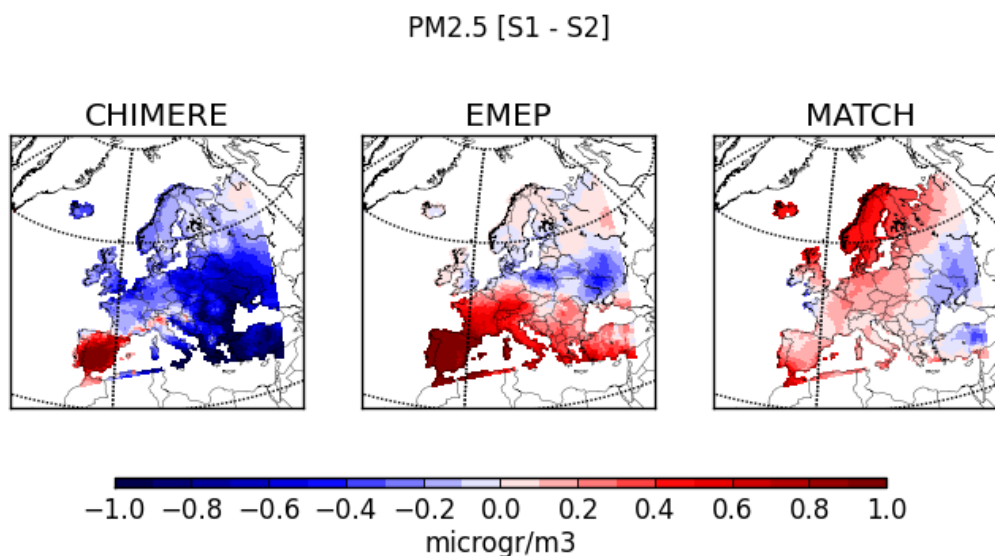


Fig. 22 Differences in PM2.5 concentrations due to climate change (S1-S2)

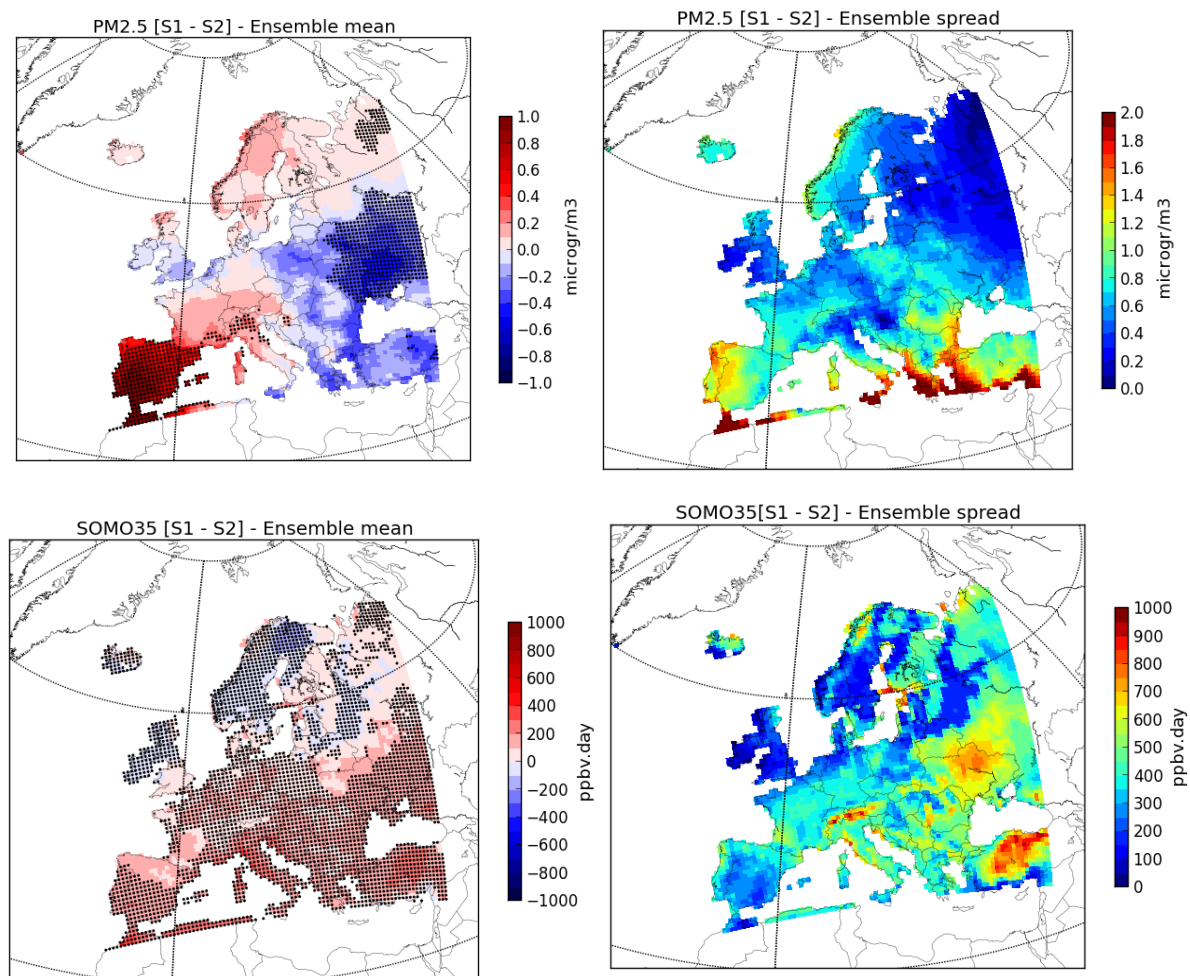


Fig.23: Top: Annual PM2.5. Bottom: SOMO35. (left) Ensemble mean of climate change (S1-S2). Black bullets are shown when all three models agree on the signal of PM2.5 changes, and at least three of the four models agree on the signal of SOMO35 changes. (right) Ensemble spread ($|\text{Max}-\text{Min}|$). Only grid cells where there are significant changes according our criteria are plotted (ensemble mean of $\Delta(\text{PM2.5}) \geq 0.1 \mu\text{g.m}^{-3}$ and $\Delta(\text{SOMO35}) \geq 50 \text{ ppbv.day}$)

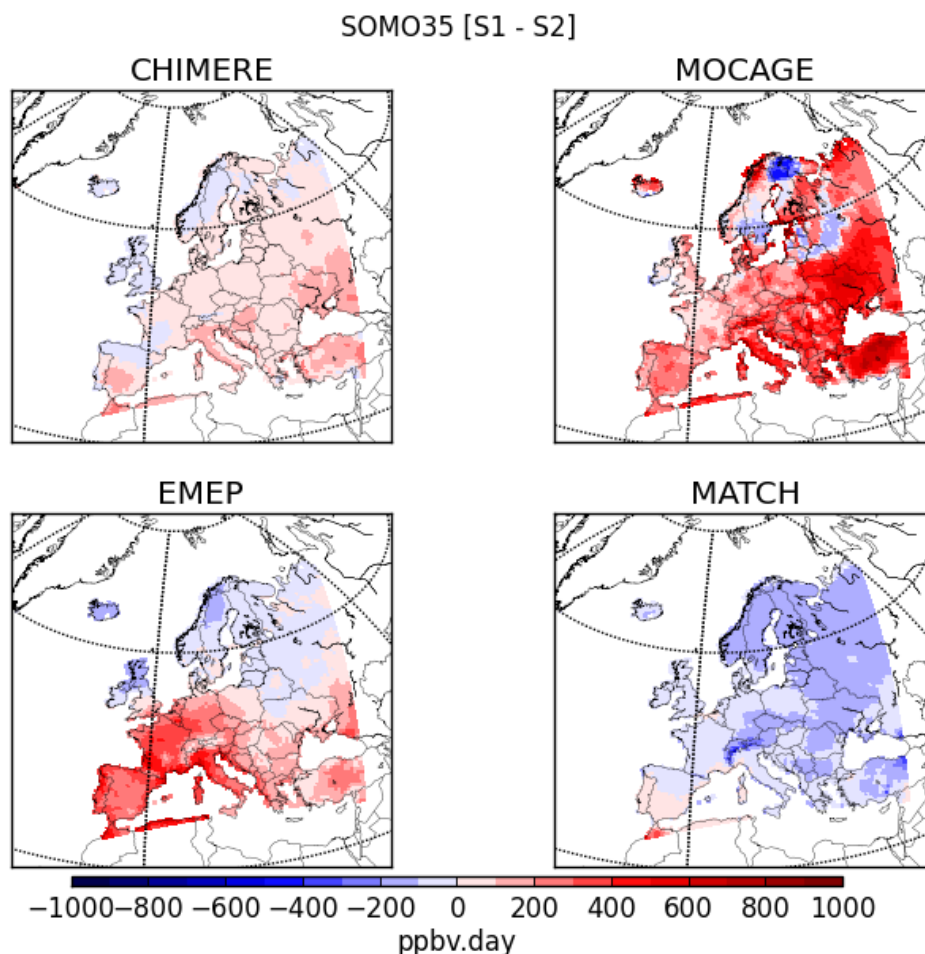


Fig.24: Differences in SOMO35 due to climate change (S1-S2)

A closer look at the individual aerosol compounds of PM_{2.5} shows that regional climate change mainly affects the compounds of PM_{2.5} due to changes in dust, sea salt and SOA in all CTMs, and which are all not directly linked to anthropogenic emissions. Competing effects of the meteorological processes on primary and secondary compounds of PM_{2.5}, explain the large spread and variability between the CTMs. A common increase of PM_{2.5}, simulated over south-western Europe (Spain, southern France) in the three CTMs, is mainly due to the increase in dust levels. On the contrary, the decrease in PM_{2.5} over southwestern Russia can be explained by that of SIA.

The regional climate change leads to increasing SOMO35 levels in three of the CTMs. However, the changes in ozone greatly vary depending on the season. An increase in temperature is simulated by all the RCMs and appears as a predominant parameter in the enhanced levels of ozone in summer. The processes involved in the winter changes of ozone are titration, deposition and transport. Changes especially in summertime ozone are modulated by absolute concentrations to affect changes in SOMO35.

We then investigate if the projected impacts of climate change are affected by the use of decadal periods instead of longer (30-year) periods. This allows us to understand whether long-term climate variability is an importance source of uncertainty as compared to inter-model spread.

For each model and for PM_{2.5}, we calculate the mean climate change for the ensemble of decade periods (6 members for CHIMERE and EMEP; 9 members for MATCH); and compare it to the spread between pairs of decadal simulations (Fig.4). When the signal of climate change has mean values above 0.5 $\mu\text{g.m}^{-3}$, all

decade periods agree on the sign of the changes (Fig. 25, a), such as over Spain in the CHIMERE and EMEP models. However, over the same areas, the max-min values (spread) show that the amplitude of the changes indicating the dispersion of the signal can highly vary among the decades. For particular locations, the ensemble spread reaches $2.6 \mu\text{g.m}^{-3}$, $3.5 \mu\text{g.m}^{-3}$ and $1.2 \mu\text{g.m}^{-3}$ for CHIMERE, EMEP and MATCH respectively.

In Fig. 25(c), we show the ratio between the climate signal simulated by the 30-year periods and the spread of the ensemble. Where the climate change signal of a 30-year period is significant (above $\pm 0.5 \mu\text{g.m}^{-3}$, black bullets), the average climate change signal is in most cases stronger than the uncertainty of the decade periods. In case of EMEP and CHIMERE, for example, the decadal periods all reproduce the increase of PM_{2.5} over Spain.

The same analysis has been conducted for SOMO35 (not shown). The results are quite different among the models. The ensemble of decadal simulations agrees on the climate change signal over most of Europe in MOCAGE and MATCH, and over eastern Europe only (where the climate change is significant) in EMEP. Finally, for CHIMERE, the ensemble agrees on the projection of future SOMO35 over a few grid cells only, spread all over the domain. The ensemble spread reaches 400 ppbv.day in CHIMERE, 1141 ppbv.day in MOCAGE, 866 ppbv.day in EMEP and 277 ppbv.day in MATCH. The 30-year climate signal/ ensemble spread ratios, calculated for each model, show that over the area where the climate change simulated by the 30-years periods of S1 and S2 is significant (above $\pm 100 \text{ ppbv.day}$), the climate signal is again higher than the decadal uncertainty. Depending on the model this appears for about 5% to half of the grid cells.

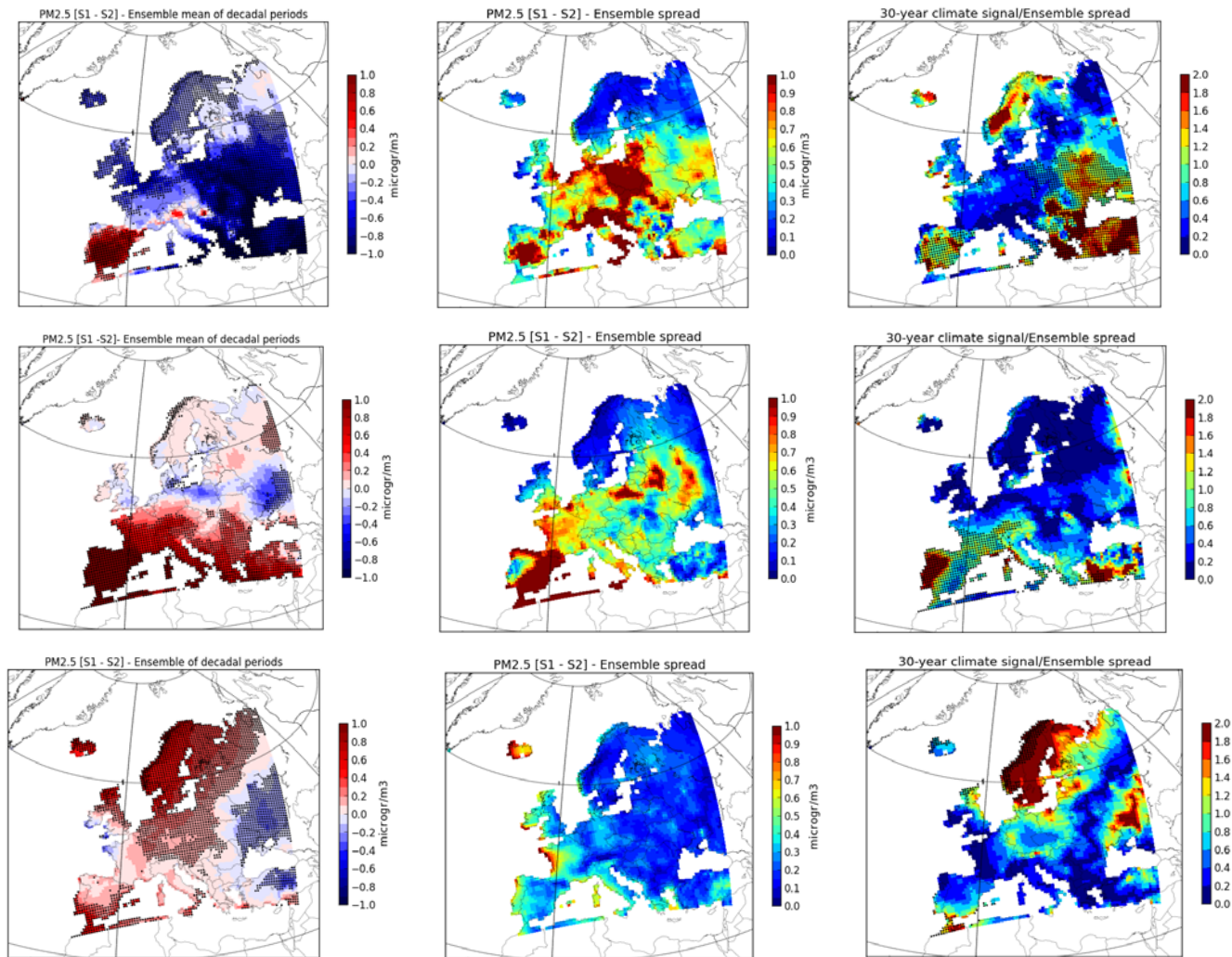


Fig.25: From top to bottom: CHIMERE, EMEP and MATCH models.(b) Ensemble mean (decade periods) of annual PM2.5. Black bullets are plotted when all the members of the ensemble agree on the signal of the PM2.5 projections. (c) Spread ($|Max-Min|$) of the ensemble. (d) Ratio between the 30-year climate signal (a) and the ensemble spread (c). Black bullets are shown where the climate change of 30-year period is such as $\Delta (PM2.5) \geq 0.5 \mu_g.m^{-3}$.

Conclusion

The levels of PM_{2.5} are only slightly affected by regional climate change: the ensemble mean change range from $-0.5 \mu\text{g.m}^{-3}$ to $1.1 \mu\text{g.m}^{-3}$ over Europe. An increase of PM_{2.5} levels can be robustly predicted over Spain where all three models agree on the sign of the changes. According to the analysis of separate components, this increase is mainly due to changes in dust emission. The decrease of PM_{2.5} over southwestern Russia is simulated by the models and is linked to the SIA compounds. Over these two areas, the model spread is smaller than the climate change signal. However, over the other parts of Europe, the projected changes of PM_{2.5} are not robust, judging by the inter-model variability. Our results allow concluding that the impact of regional climate change on PM mainly proceeds by modifying natural emissions, such as desert dust, sea salt and biogenic VOCs. The largest changes in PM_{2.5} are indeed attributed to these natural or biogenic compounds, which cannot easily be controlled by policy measures.

The induced changes of SOMO35 and ozone can be large, depending on the season, area and model considered. However a large variability among the models is simulated for SOMO35: three of the models simulate an average increase of this indicator over Europe while one model predicts a decrease. In summer, the increase of ozone levels is simulated by three of the models when averaged over Europe and the ensemble mean changes range from -1.7 to 1.6 ppbv. The increase in summer ozone is correlated to increased temperature, and also linked to elevated isoprene emissions. Projected changes of winter ozone are weaker and processes other than photochemistry lead the changes in ozone, such as dispersion and titration by NO. For SOMO35, the variability between the models is higher than the ensemble climate change signal, because the meteorological parameters and processes that lead to O₃ differences differ between the models. For this reason, we cannot state a clear conclusion about changes of SOMO35 in the future climate.

The use of decade periods instead of climate periods has smaller effects on PM_{2.5} projections than for ozone and SOMO35. In the case of PM_{2.5}, there is only small decadal variability over the southern part of the domain, and over eastern Europe, where significant trends are observed in all three models. By contrast, stronger decadal variability appears over central Europe. For SOMO35, the decadal variability is very different among the models. This is probably due to the strong impacts of the meteorological parameters, such as temperature, on excess ozone levels measured by SOMO35. Our results confirm (see Langner et al., 2012) the importance of studying sufficiently long time periods to extract robust signals of climate change impacts on surface ozone concentrations and that 10-year periods may not be sufficient for the calculation of the impacts of climate change for a 2°C warming. Finally, we show that the use of decade periods can lead to uncertainty, but this decadal variability is small compared to the 30-year signal over the area where the regional climate change trend is significant. In addition, our results highlight that the uncertainty associated with decadal variability is lower than the inter-model variability.

2.4 City-scale changes

In order to examine the impact of climate change on city-scale air pollution, a focus has been put on two cities: Stockholm and Paris. It was not possible to evaluate the uncertainties as only one model was running for each city. The CHIMERE model chain simulated air pollution for Paris and the MATCH model chain simulated air pollution for Stockholm.

Experiments have been coordinated with the ERANET ACCEPTED project and results are summarized in a submitted article (Markakis et al., 2015).

Figures 26-29 show the change in concentrations of SOMO35, NO_x , PM10 and PM2.5. In these simulations PM in MATCH includes SOA as well as the other components. Under the influence of this climate projection, with current emissions, climate change causes a small decrease in SOMO35 whereas future emission change further decreases the SOMO35 by 0.5-1 ppm(v) d. For NO_x and PM10, climate causes very small changes, some areas positive and some negative, but future emission decreases are strong enough to decrease the future concentrations by up to 3 $\mu\text{g}/(\text{N}) \text{ m}^{-3}$. For PM2.5 both climate change and emission changes cause decrease in urban background concentration.

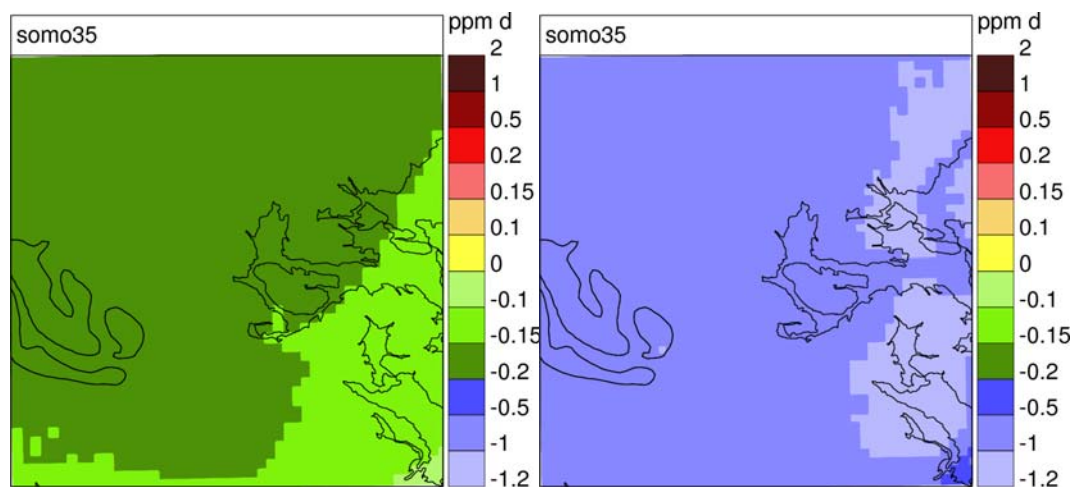


Figure 26 Change in SOMO35 in Stockholm from present (1991-2000) to future (2046-2055) under the influence of climate change (left), and climate and emission change (right) modelled with MATCH on 1kmx1km resolution.

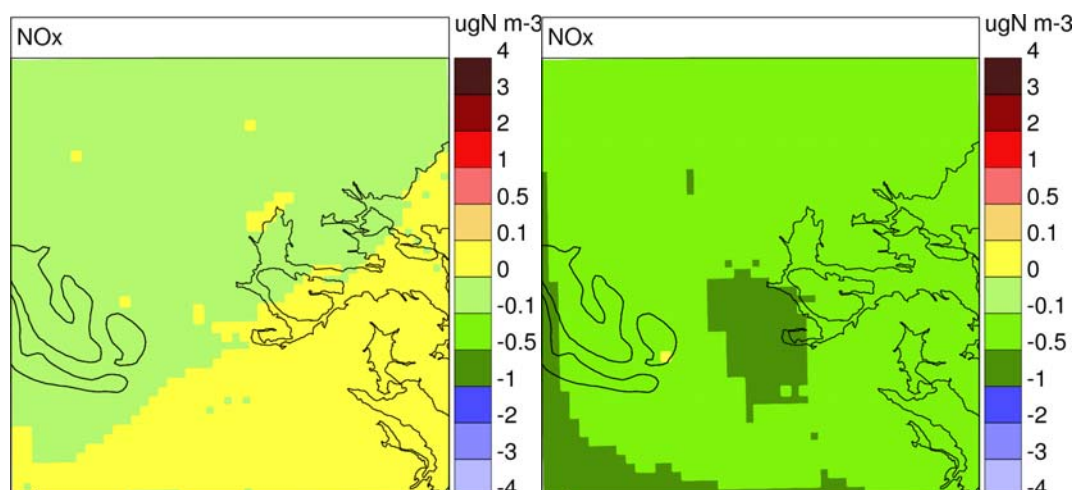


Figure 27 Change in NO_x in Stockholm from present (1991-2000) to future (2046-2055) under the influence of climate change (left), and climate and emission change (right) modelled with MATCH on 1kmx1km resolution.

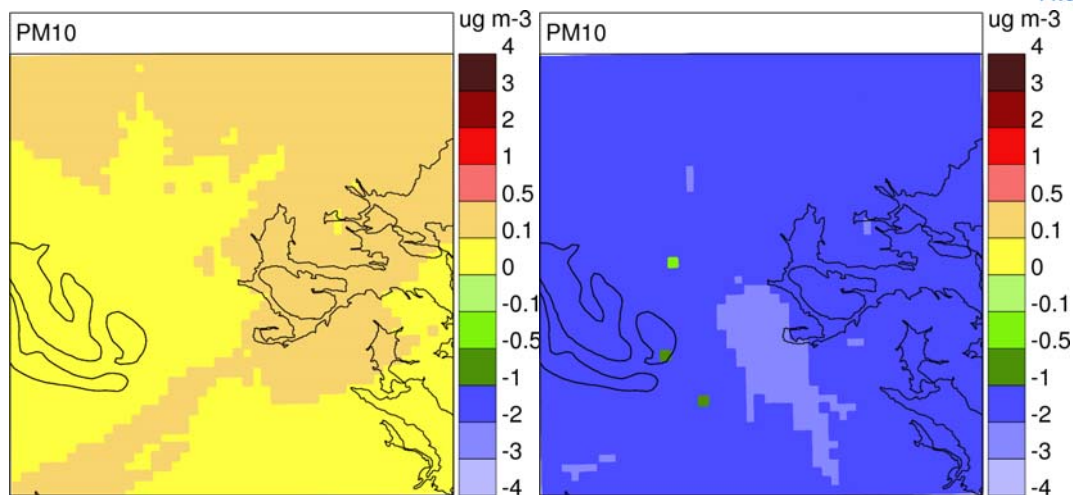


Figure 28 Change in PM10 in Stockholm from present (1991-2000) to future (2046-2055) under the influence of climate change (left), and climate and emission change (right) modelled with MATCH on 1kmx1km resolution.

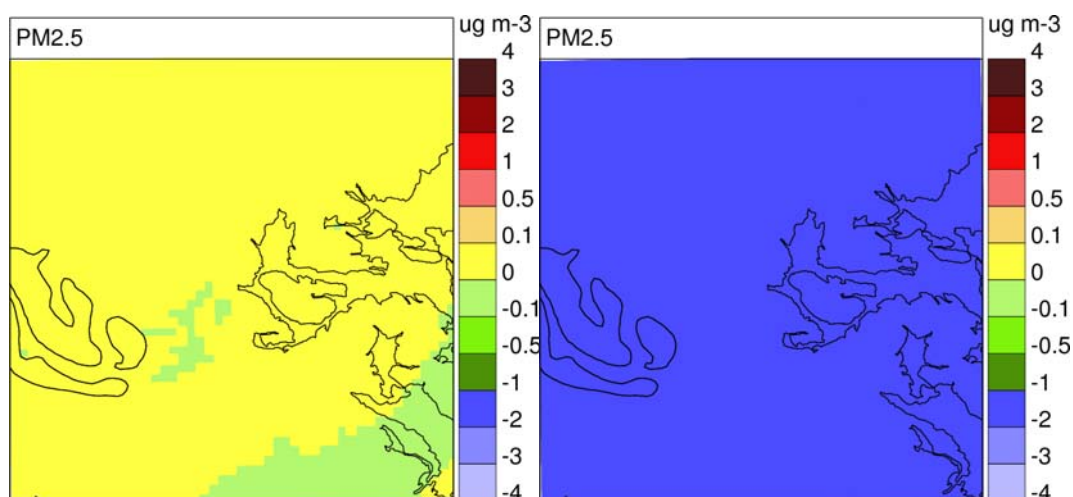


Figure 29 Change in PM2.5 in Stockholm from present (1991-2000) to future (2046-2055) under the influence of climate change (left), and climate and emission change (right) modelled with MATCH on 1kmx1km resolution.

Paris

The influences of climate change have been evaluated over Paris for Ozone, NO_x, PM10, PM2.5 and SOMO35.

Fig. 30 shows that climate change causes little change to O₃. A small decrease of PM10 and PM2.5 concentrations are observed over Paris due to climate change (Figure 31). The NO_x levels decrease over Paris and western Ile-de -France while the levels slightly increase over the eastern domain (not shown).

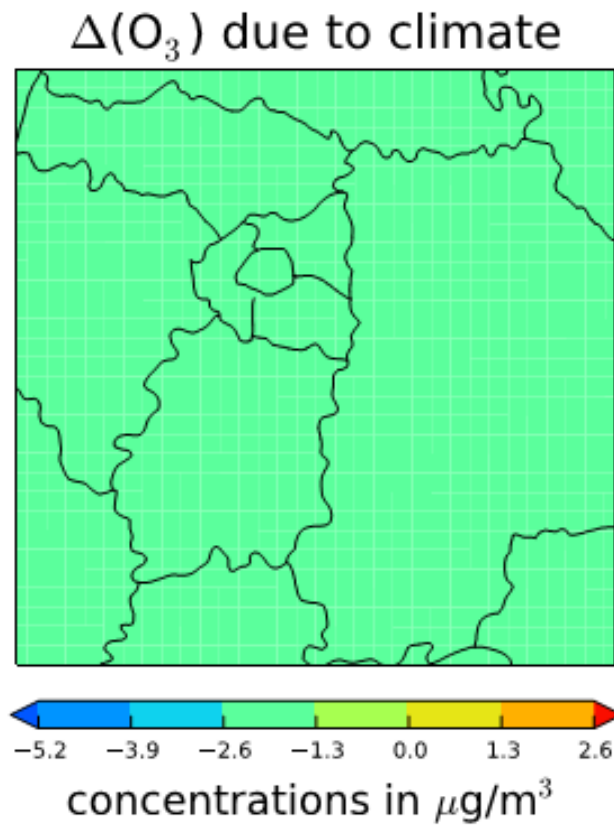


Figure 30: Change in Ozone in Paris between future (2027-2056) and present (1971-2000) under the influence of climate change for the whole year modelled with CHIMERE on 4kmx4km resolution.

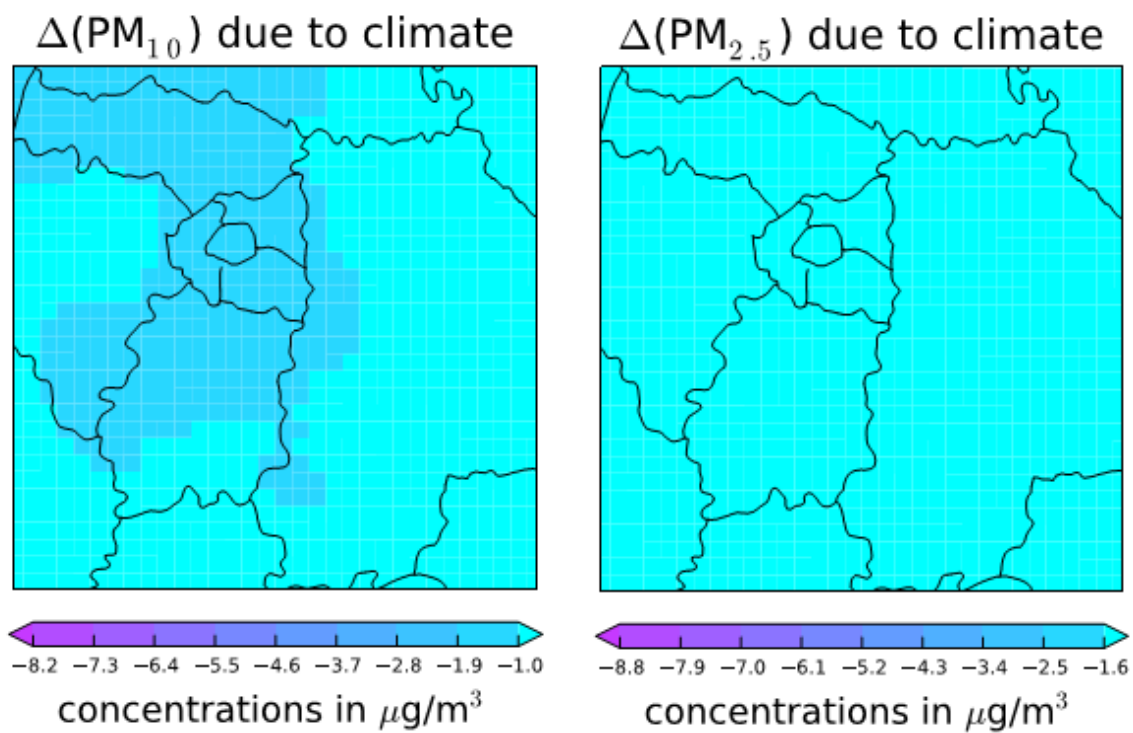


Figure 31 Change in annual PM10 (left) and PM2.5 (right) in Paris between future (2027-2056) and present (1971-2000) under the influence of climate change modelled with CHIMERE on 4kmx4km resolution.

2.5 Impact of a 3°C change

We present the impact of a global climate change of +3°C compared with a +2°C on air quality. This allows the quantification of the difference and of the possible non-linearity affecting the pollutants concentrations (for ozone and particles) between these two scenarios. We introduce the S4 scenario that uses the regional climate projection using the RCP8.5 scenario, boundary conditions from RCP4.5 centered on 2050 and projected European emissions for the year 2050. We choose this particular scenario to estimate the impact of regional climate change only (same emissions and same boundary conditions as S1 scenario). Two models of the initial four models group have run this additional scenario: CHIMERE and EMEP.

Name	Climate	Boundary conditions	Emissions	Simulated Period	
				CHIMERE	EMEP
S4	+3°C RCP4.5	2050	V4a 2050 CLE*	2040-2069	2058-2087

Table 7. Description of the simulations performed for the +3°C experiment. *Current legislation emissions

Particulate matter (PM_{2.5} concentrations)

Figure A1 shows the impact of a +3°C (S4-S1) regional climate change against the +2°C (S4-S2) on PM_{2.5} mean annual concentrations for both models. Even if both models have very different response to climate change (cf Deliv. D333), only slight differences are observed between both scenarios for CHIMERE and EMEP. The patterns of PM_{2.5} changes are indeed slightly strengthened under the +3°C scenario. However, **the impact of both a +2°C or a +3°C regional climate change on PM_{2.5} future concentrations is weak**. More precisely, for CHIMERE differences between both scenarios are always below 1 µg.m⁻³ over the European domain while for EMEP higher differences can be observed especially associated to changes in North African dust emissions. Nevertheless, differences remain lower than a few µg.m⁻³ over Europe.

Ozone concentrations

Figure 32 shows the impact of a +3°C (S4-S1) regional climate change against the +2°C (S4-S2) on ozone concentrations for both models. S4 scenario presents higher differences than S1 (ranging respectively from -2 to 3 ppbv for CHIMERE, and from -2 to 1 ppbv for EMEP), **indicating that a +3°C regional climate could have an impact of about ± 5% on ozone concentrations with respect to present climate**. The highest differences are seen over Northern Europe, where a decrease of ozone levels is projected by both models, and over North Africa for CHIMERE. It should be noted that, for ozone, higher differences between both climatic scenario are expected in the case when regional

models are forced with boundary conditions taken into account RCP 8.5. Indeed, tropospheric ozone has an average life time of 3 weeks and large scale changes will impact Europe.

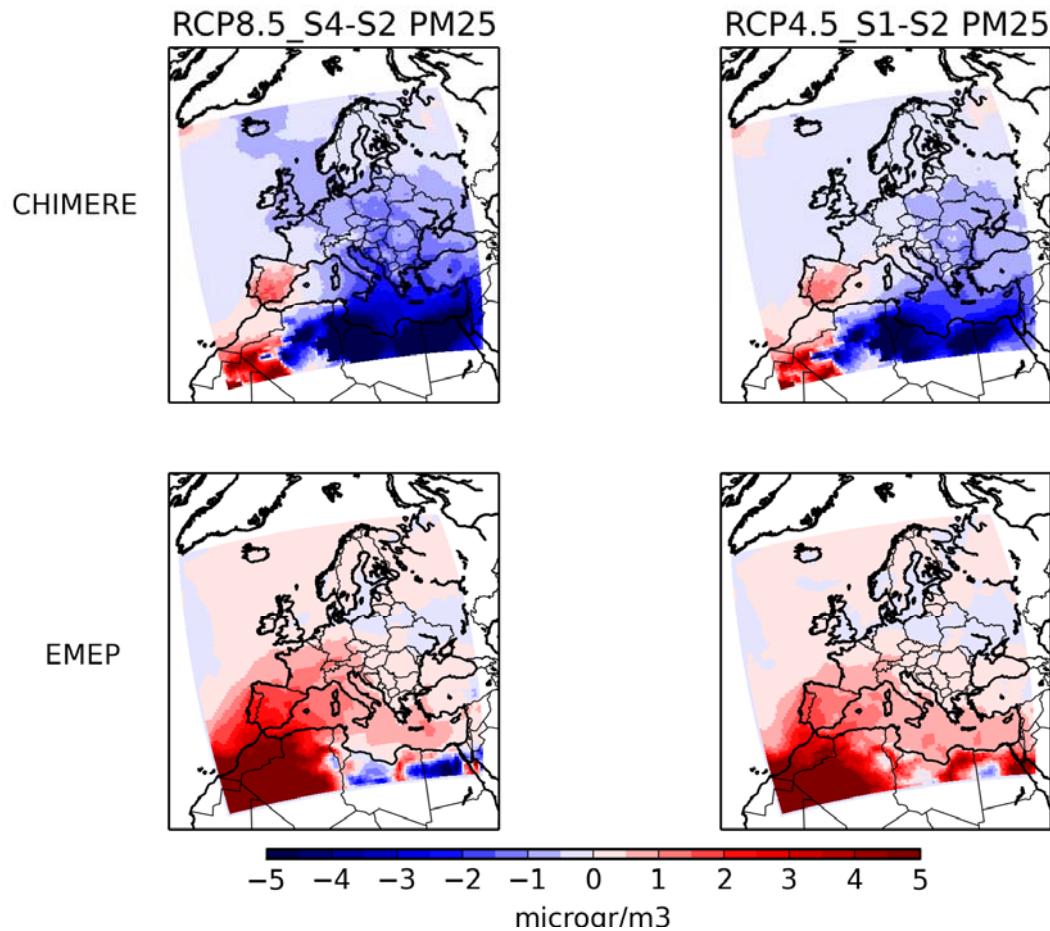


Figure 32. Differences in annual $PM_{2.5}$ concentrations between (left) future +3°C scenario S4 and scenario S2 and (right) future +2°C scenario S1 and scenario S2, simulated by CHIMERE and EMEP, in $\mu g.m^{-3}$.

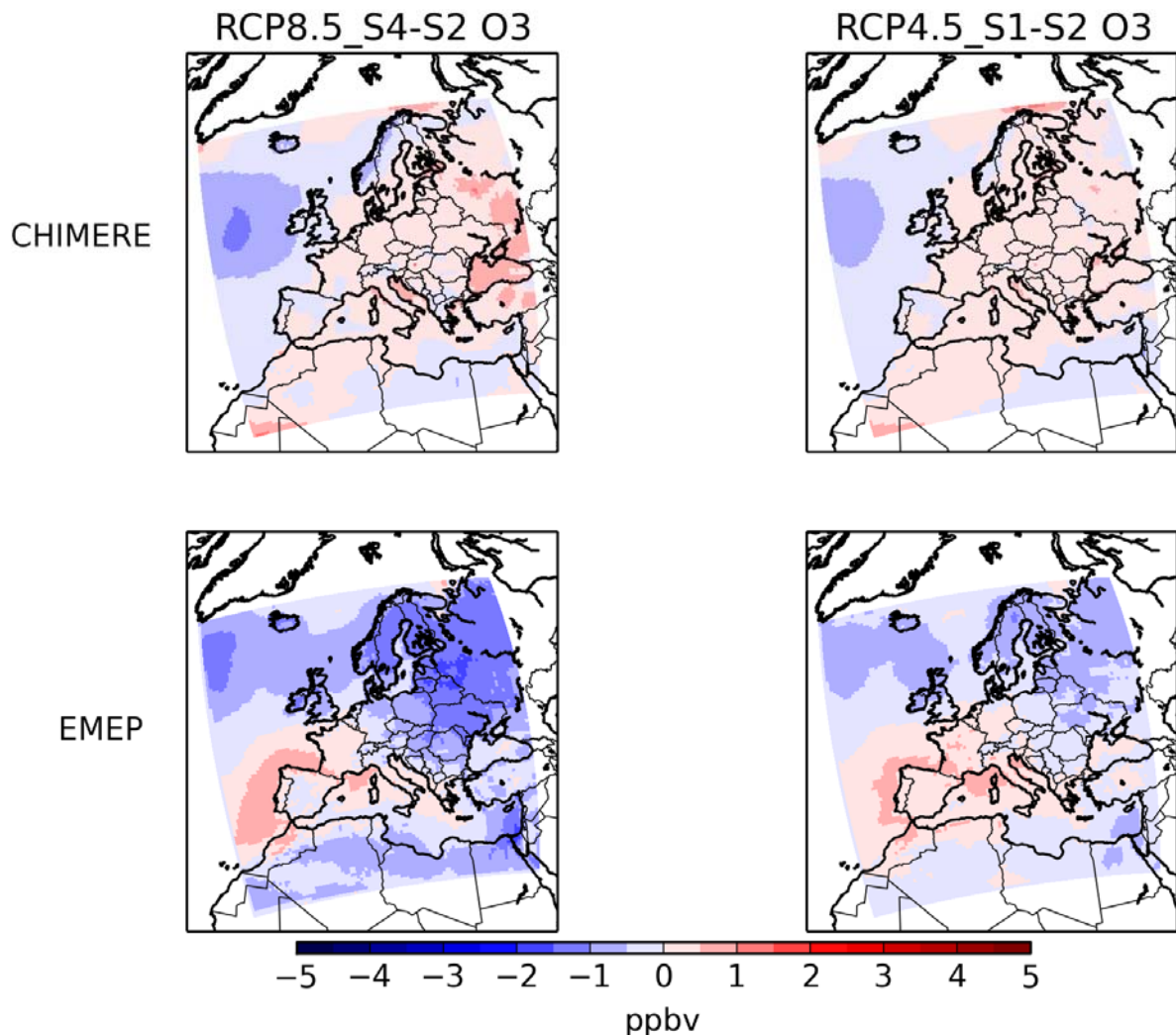


Figure 33. Differences in annual O_3 concentrations between (left) future +3°C scenario S4 and scenario S2 and (right) future +2°C scenario S1 and scenario S2, simulated by CHIMERE and EMEP, in $\mu g \cdot m^{-3}$.

2.6 Conclusions

The comparisons between the present and future scenario have been carried out for the four CTMs models.

Concerning the particulate matter, the future scenarios highlight that the decrease of annual PM10 and PM2.5 over Europe is mainly induced by the decrease of anthropogenic emissions of precursors, while the changes caused by regional climate changes are comparatively small. Maximum technically feasible emission reduction would further improve PM levels and air quality. Our results also highlight that the changes in PM under regional climate change are mainly due to natural components, such as desert dust, sea salt and biogenic emissions. The changes in ozone depend on the season considered. A decrease of ozone concentrations is observed in summer, mainly due to the decrease in anthropogenic emissions, while the levels increase over Europe in winter. The climate change appears to increase ozone in both seasons. Finally, the MFR emission scenario shows that further reductions in anthropogenic emissions play a significant role in mitigating ozone.

The comparisons of the deposition of oxidised sulphur, oxidised nitrogen and reduced nitrogen deposition between the HISTORICAL and the future scenarios show that decreasing emissions result in decreasing deposition of all species, and that deposition is much more sensitive to changes in emissions than climate change.

To conclude, the experiments show that, if the 2°C global warming occurs near the middle of the 21st century, such as predicted from climate simulations using the RCP4.5 scenario, the current legislation, together with improvements in global ozone concentrations should help reduce air pollution in Europe. Using all maximum technically feasible reduction possibilities would further improve air quality by a large factor. It is also found that consequences of a 2°C warming would not hinder such improvements, as they would induce changes smaller than those obtained by emission reductions.

3. Impacts of air pollution on health

Air pollution has a number of important impacts on human health, as well as on the natural and man-made environment. These include impacts of short-term and long-term exposure to air pollution on health, damage to building materials, effects on crops and impacts on natural and semi-natural ecosystems (Holland et al, 2005). Concerns over these impacts have led to the introduction of air quality policies in Europe over the past few decades. These were initially driven by the need to reduce impacts on ecosystems (acidification and eutrophication). More recently, they have focused on reducing the significant impacts of air quality on human health, including the shortening of life expectancy. These policies, which includes the Thematic Strategy on Air Pollution (CEC, 2005), have led to substantial reductions in emissions – and improvement of air quality.

Nevertheless, current levels of air pollution in Europe still lead to widespread health and environmental impacts (CEC, 2013). To address this, new measures to reduce air pollution have recently been adopted (EC, 2013): this includes a new Clean Air Programme for Europe (with further measures to meet current targets, as well as new air quality objectives for the period up to 2030) and revised national emission ceilings. However, these policies have not considered the potential effects of future climate change, which has the potential to impact on air pollution by changing emissions (biogenic and fire related), altering patterns of atmospheric dispersion and chemistry, and affecting the frequency of extreme weather such as heat waves. In the future, therefore, a changing climate could potentially counteract the beneficial effects of current and planned policy.

To investigate this, the IMPACT2C project has assessed the impacts of climate change on air quality in Europe for 2°C of warming, relative to pre-industrial levels (Vautard et al, 2014). The analysis focused on fine particulate matter (PM_{2.5}) and ozone, as these have been associated with the highest health impacts (WHO, 2013). Four state-of-the art modelling suites were used to simulate global and regional European climate and then air quality.

Method

Air pollution has a number of important impacts on human health, as well as on the natural and man-made environment. These include impacts of short-term and long-term exposure to air pollution on our health, damage to building materials, effects on crops, and impacts on natural and semi-natural ecosystems (both terrestrial and aquatic). These impacts have a number of important economic costs – known as external costs or externalities - as they are not included in the price of goods or services that lead to air pollution.

The usual approach taken for the detailed quantification of the benefits of air pollution emissions through to monetisation is often referred to as the ‘impact pathway approach’. This is a logical progression from emissions, through the estimation of the modelled dispersion and change in air quality concentrations, to exposure and quantification of impacts and their valuation. This approach was advanced through the series of EC Research projects under the ExternE series (EC, 1995, 1999) and was applied previously in EC policy impact assessment (CEC, 2005) in relation to new proposed air quality (as part of the CAFÉ CBA project, Holland et al, 2005).

In order to undertake the analysis a series of steps are undertaken:

1. Quantification of emissions;
2. Analysis of pollutant dispersion and chemistry across the EU28 (plus Switzerland and Norway, i.e. EU28++) and the change in air pollution concentrations;

3. Quantification of exposure of people, environment and buildings that are affected by air pollution, i.e. linking the pollution concentrations with the 'stock at risk' e.g. population data;
4. Quantification of the impacts of air pollution, using response relationships linking pollution concentrations with physical impacts such as crop damages, or epidemiological studies linking pollution to health impacts;
5. Monetary valuation of the impacts, where possible, to represent impacts on human welfare.

The overall damages are thus calculated using the following relationships:

$$\text{Impact} = \text{pollution} \times \text{stock at risk} \times \text{response function}$$

$$\text{Economic damage} = \text{impact} \times \text{unit value of impact}$$

The appropriate measure of pollution is dependent on the impact under consideration. The focus of the air quality modelling has been on PM_{2.5} and ozone. The term 'stock at risk' refers to the population exposed to pollution. The analysis described here was performed at the resolution provided by the climate models. Although the general form of these relationships does not change between different types of impact, the precise form of the analysis varies depending on the nature of the stock at risk. For example, quantification of certain health impacts requires assessment of exposure of only certain parts of the population (e.g. those aged over 65 or incidence rates for chronic bronchitis or the use of respiratory medication).

The final stage, monetary valuation, is generally performed from the perspective of 'willingness to pay' (WTP). For some effects, such as damage to crops or to buildings of little or no cultural merit, this is implemented using appropriate market data. Some elements of the valuation of health impacts can also be quantified from 'market' data (e.g. the cost of medicines and care), though other elements such as WTP to avoid being ill cannot. In such cases the findings of alternative, non-market, valuation methods have to be used.

Emission and Air Quality scenarios

Steps 1 and 2 in the methodological framework were undertaken by the modeling experiments described above. The analysis considered a number of future emission scenarios, taking account of future changes in air pollutant emissions reductions out to 2050, associated with current and planned legislation, and also explored a scenario with more stringent emission reduction measures (a Maximum Technically Feasible Reduction).¹ They then compared four state-of-the art modelling suites (CHIMERE, MATCH, EMEP and MOCAGE) to simulate global and regional European / air quality, looking at future emission scenarios as below.

The modelling results provide key insights. Future levels of air pollution in Europe in the coming decades will be primarily determined by the emission improvements from European and national policies – and combined with improvements in global ozone concentrations – these lead to large improvements in air quality by the time 2°C warming is reached (approximately 2050 under RCP4.5). The effects of climate change warming in this period will induce some changes in ozone and particulate matter concentrations, but a robust finding is that these effects will be modest.

¹ The air pollutant emission scenarios used in the study were developed by IIASA under the EU-FP7 project ECLIPSE (Project no. 282688), with additional support from EU-FP7 PEGASOS (Project no. 282688).

Stock at Risk including socio-economic change

The first step in the analysis was to take the change in air quality concentrations, and link this with population to estimate the population-weighted-exposures. In the assessment of the future effects of climate change, assumptions have to be made about future conditions, which require socio-economic scenarios. This is important, for example, because the future population of Europe will change, and in turn, this will change the population at risk to air pollution. In line with the IMPACT2C project, the analysis has considered the new SSPs (Shared Socio-economic Pathways) (van Vuuren et al, 2012). Within the air quality analysis, the use of the new SSPs has been focused on the consideration of the changes in population. This was chosen as the key driver, though other factors (i.e. GDP, income and WTP for health) would also have potential effects. The information on the SSPs was taken from the SSP site.

<https://secure.iiasa.ac.at/web-apps/ene/SspDb/dsd?Action=htmlpage&page=about>.

However, the relevant data for the SSPs is only available at the country level. For air quality, the grid resolution of population needs to be higher than this, so existing gridded population data for Europe was combined with the SSP country data, to interpolate to future 2050 population. This was combined and re-gridded with the air pollution data within a GIS environment.

This proved quite an intensive exercise, so for the analysis of health impacts, the analysis has focused on SSP2. SSP2 is the central scenario, which could be referred to as a Business As Usual (BAU) scenario, as it relies on the extrapolation of current trends into the future. The health functions require some information on the age split of the population. The population level in the EU28++ under SSP2 is projected to remain broadly stable between current and 2050. However, population ageing is very significant and the numbers of elderly and very elderly are projected to increase. By 2050, over one third of the population will be aged over 65 (around 160 million people).

Analysis of Impacts

The health impact assessment approach used here is based on methods and quantification steps developed over a number of years, in Europe, the USA, and globally for the World Health Organization (WHO). These methods have been subject to extensive review (e.g. Krupnick et al, 2005) and found to be fit for purpose and reflective of the current state of science. Following the advice of an earlier expert group convened by WHO-Europe under the CAFE Programme², the Health Impact Assessment is performed against exposure to ozone and fine particles, considering the acute effects on mortality – as reflected by premature mortality (ozone) – and the longer-term changes in life expectancy (sometimes termed chronic mortality) from particles. Note that the particles considered include primary particulate emissions (emitted directly) and secondary particulates that form in the atmosphere following the release of SO₂, NO_x and NH₃. In line with WHO advice, the analysis treats all particles, irrespective of source and chemical composition, as equally harmful. The outputs are reported as the cumulative years of life lost (YOLL) from PM pollution. For acute mortality from ozone, the analysis quantifies the number of ‘premature deaths’ (deaths brought forward)³. The method used here was based on the CAFE CBA methodology (Holland et al, 2005a; b; Hurley et al, 2005) and response functions developed as part of the EC CAFE programme. Response functions, data on incidence rates, etc. are described in detail by Hurley et al (2005) for each effect. Hurley et. al. (2005) based their quantification on a function developed by applying a risk factor from

² The recommendations of WHO-CLRTAP Task Force on Health (TFH) (<http://www.unece.org/env/documents>) and the WHO “Systematic Review of Health Aspects of Air Quality in Europe” (<http://www.euro.who.int/document/e79097.pdf>).

³ This wording signifies that many people whose deaths are brought forward by acute exposure to ozone in particular have serious pre-existing cardio-respiratory disease and so in at least some of these cases, the actual loss of life is likely to be small – the death might have occurred within the same year and, for some, may only be brought forward by a few days.

Pope et al (1995, 2002) for all-cause mortality (excluding accidents and other violent deaths) using life tables for the population of England and Wales.

Health effects are quantified against exposure to annual average $PM_{2.5}$ concentrations and ozone expressed as SOMO35 (the sum of mean hourly ozone levels over 35 parts per billion). Of the effects listed, the most significant in economic terms is mortality from long-term exposure to fine particles. This is quantified in terms of impact on life expectancy and valued using the value of a life year lost, but for sensitivity also in terms of deaths brought forward by pollution exposure, valued using the value of statistical life (VSL). Preference here is given to the life expectancy/VOLY approach on the grounds that exposure to air pollution, particularly at levels typical of the EU28, is only one of a number of determinants of life expectancy and seems unlikely to be the primary cause of death in affected individuals in the way that traffic or workplace accidents clearly are. Against this, the VSL is a better established metric within the economics literature and is used extensively in North America to quantify the benefits of reducing chronic exposure to fine particles (OECD, 2012).

It is highlighted that PM and ozone also have impacts on morbidity, particularly on respiratory illnesses, which are additional to the mortality related impacts quantified here. There overall health burden of climate change will therefore be higher.

It is also stressed that in 2013, the World Health Organisation (WHO) undertook a review on the Health Risks of Air Pollution in Europe (HRAPIE). This review recommended new concentration–response functions for estimating health impacts of particulate matter, ozone and NO_2 for cost–benefit analysis. The project is complete but the findings – and impacts – are yet to be considered within European impact assessment methodologies. Of particular importance is the emergence of a relationship between NO_2 and mortality, which indicates a much higher overall health burden.

Valuation

The impacts on human health are difficult to value, because there are no observed market prices. However, it is possible to derive monetary values for this non-market sector, by considering the total effect on society's welfare. This requires analysis of three components which each capture different parts of the total effect. These are the resource costs i.e. medical treatment costs; the opportunity costs, in terms of lost productivity; and dis-utility i.e. pain or suffering, concern and inconvenience to family and others.

The first two components can be captured relatively easily. Techniques are also available to capture the third component, by assessing the 'willingness to pay' or the 'willingness to accept compensation' for a particular health outcome. These are derived using survey-based "stated" preference methods and/or "revealed" preferences methods that are based on observed expenditures such as on consumer safety.

However, there is substantial debate concerning the correct approach to valuation of mortality risks in the context of air pollution. As outlined above, these can be valued using a long-established metric, the value of statistical life (VSL) - also known as the value of a prevented fatality, VPF - but changes in life expectancy can also be valued using the value of a life year (VOLY), which provides a way of accounting for differing lengths of remaining life expectancy. Both approaches are used in the literature and both have strengths and weaknesses. Impact2C has used both.

The main results reported below use a VOLY of €63,000. These values are taken from Hurley et al (2005), for which an extensive review of the valuation literature was carried out, and updated to 2010 price levels. They have also been updated to take account of subsequent literature, for

example by Alberini et. al (2006) and Desaiques et al (2011). The values shown are interpreted as being average values for the EU region, and hence are applied without adjustment by country. The VSL is also applied, using values of €1.16 million⁴. Consistent with all sector-based analysis in IMPACT2C, the economic valuation results below are presented in terms of constant 2010 prices in Euros over future years, without any adjustments or discounting to facilitate direct comparison, over time, and between sectors. However, subsequent policy analysis that looks at the costs and benefits of adaptation or mitigation policy would need to work with present values (i.e. values that are adjusted and discounted as with standard economic appraisal).

Results

The results are presented below, with the results for the EU28 plus Norway and Switzerland.

Particulate matter

The health impacts for particulate matter follow from and mirror the results presented in section 1. This found climate change has minor effects on PM_{2.5} concentrations (S1-S2) over continental Europe. The projected changes of PM concentrations also vary greatly between the models, which leads to a very large range – varying even in sign when aggregated at the European scale – thus while some models project a small increase in PM, others project a decrease. The results of the four models – expressed as the change in life years lost per year in 2050 due to climate change (from the baseline) – are shown in the table below.

Change in life years lost/year in 2050 from the additional impact of climate change on PM2.5 concentrations (S1-S2) EU + Norway and Switzerland.

	MOCAGE	MATCH	EMEP	CHIMERE	Average
S1-S2	-136883	35435	63671	-72754	-27633

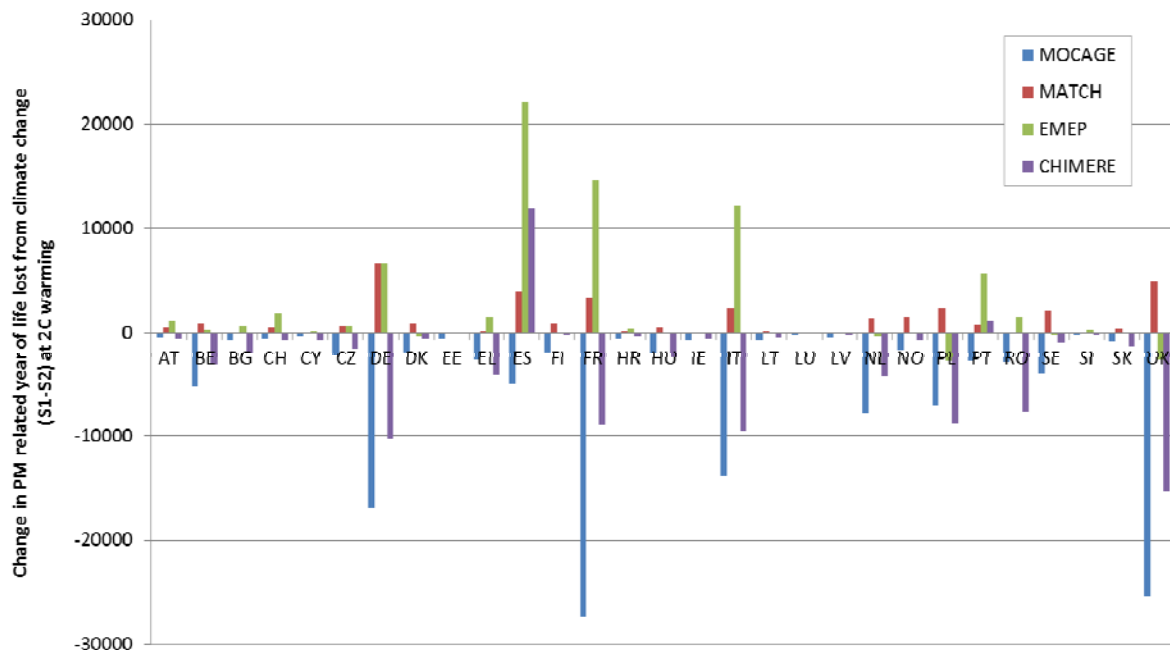
-ve = a reduction in health impacts (benefit), +ve an increase in health impacts (impact)

It is stressed that while these values involve large number of life year lost, the changes are small when compared to the future baseline levels, even in 2050 (which are of the order of one and half million years of life lost/year, even with existing pollution control policies – though they are much higher at current baseline levels in 2015).

The results reflect the patterns shown in the Figure, with MOCAGE showing (relatively) large decrease in PM (hence a beneficial effect of climate change), MATCH and EMEP generally showing increases (impacts of climate change). CHIMERE shows different changes across Europe. The results on a country basis are shown in the figure below for the four models, noting that in all cases the results are heavily biased by the country population size, thus large effects are seen for the major populated countries. Nonetheless, it can be seen that the EMEP model projects larger relative impacts (increases in health impacts) in the South, particularly in Spain and Italy. For those models that project benefits, large benefits are projected in North-West Europe, notably in France and the UK.

Change in life years lost/year in 2050 from the additional impact of climate change (S1-S2) on PM2.5 concentrations. Positive values represent increases in health impacts (additional impacts from climate change), while negative values represents decreases (benefits)

⁴ This value is towards the lower end of the range suggested by a recent OECD review, which indicates values of low 1.85million, central 3.75million and high 5.55million.



The analysis has also estimated the potential economic costs of these changes. These are shown in aggregate in the Table below.

Monetary valuation (Million Euro/year) of the change in life years lost/year in 2050 from the additional impact of climate change (S1-S2) on PM_{2.5} concentrations. EU + Norway and Switzerland. Current (2010) prices, with no discounting.

	MOCAGE	MATCH	EMEP	CHIMERE	Average
S1-S2	-8624	2232	4011	-4583	-1741

-ve = a reduction in health impacts (benefit), +ve an increase in health increase. Valuation using the value of a life year lost.

The economic costs are potentially quite large, i.e. billions of Euros per year (and would be much higher if a full VSL was used). However, the wide range of results – even in terms of the sign - across the models prevents firm conclusions being made on the likely effects of climate change.

Ozone

The health impacts for ozone also follow from and mirror the results presented in section 1. This found climate change has minor effects on ozone.

In contrast to PM, there was found to be a more consistent increase in surface ozone during the summer months, although this was low in absolute terms. The net result is an increase in ozone related deaths for the three models considered. The aggregated changes – across the year – are shown below.

Change in ozone related premature deaths/year in 2050 from the additional impact of climate change (S1-S2) EU + Norway and Switzerland

	MOCAGE	EMEP	CHIMERE	Average
S1-S2	594	68	200	287

+ve an increase in health impacts (impact)

It is stressed that while these values involve large number of premature deaths, the changes are small when compared to the future baseline levels (which are of the order of twenty thousand [20000] premature deaths/year).

The analysis has also estimated the potential economic costs of these changes. These are shown in the Table below.

Monetary valuation (Million Euro/year) of the change in ozone related premature deaths/year in 2050 from the additional impact of climate change (S1-S2). EU + Norway and Switzerland. Current (2010) prices, with no discounting.

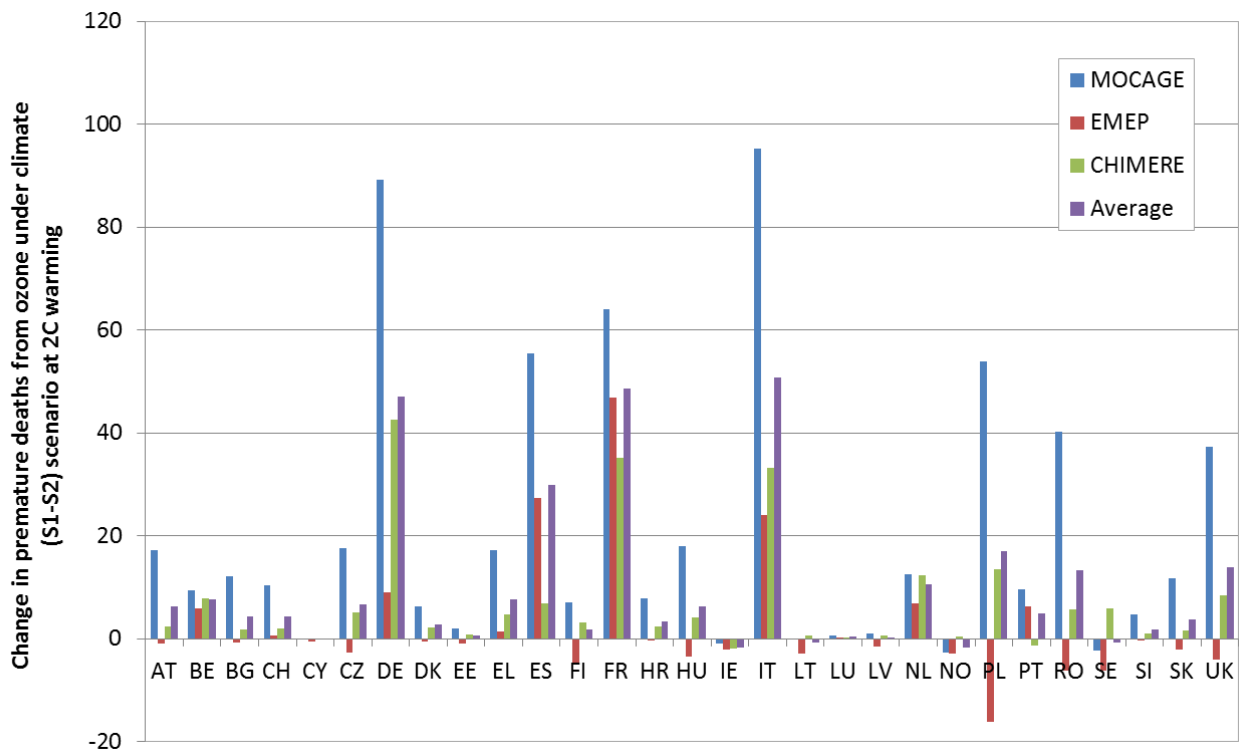
	MOCAGE	EMEP	CHIMERE	Average
S1-S2	75	9	25	36

+ve an increase in health increase (impact). Valuation using the value of a life year lost and assuming 2 years of life lost on average.

The economic costs are much smaller in size compared to the potential PM effects, reflecting the larger PM effects (and the fact that premature deaths are adjusted here for life expectancy losses – they would be much higher if a full VSL was used). There is a greater confidence in the sign of change, with all models reflecting a similar change overall.

However, as highlighted earlier in this report (Figure 7) there are differences across Europe in terms of the change in average O₃ concentrations for the climate scenario (S1-S2). These are reflected through into differences in the distributional patterns of health impacts across Europe, and these do vary with the models. The results on a country basis are shown in the figure below for the models, noting that in all cases the results are heavily biased by the country population size, thus large effects are seen for the major populated countries.

Change in ozone related premature deaths/year in 2050 from the additional impact of climate change (S1-S2). Positive values represent increases in health impacts (additional impacts from climate change), while negative values represents decreases (benefits)



Conclusions

The analysis of health impacts from climate change follows the pattern of the air quality model runs. The analysis indicates an increase in ozone related health impacts (premature mortality) from climate change at 2C warming in Europe, with higher impacts found in the south. However, this increase is low when compared to future baseline air pollution health impacts, i.e. the impact of climate change is very modest compared to the future baseline conditions, and future air quality policy. For PM, a more complex picture emerges, with some models projecting increases in health impacts at 2C warming in Europe, while others projecting a decrease. However, as with ozone, the magnitude of these changes are very small when compared to the future baseline air quality, and are low when compared to the changes that will arise from air quality policy over future decades.

4. Impacts of climate change on health

The purpose here is to describe both, the qualitative findings from intensive systematic literature review on climate change impact in Europe, and experiments that have been carried out so far in IMPACT2C for the estimation of heat mortality.

4.1 Qualitative survey

A comprehensive literature search was conducted in accordance with the Preferred Reporting Items for Systematic Reviews and Meta-analysis (PRISMA) methodology (Liberati et al., 2009). The search was designed to identify recent research papers relevant to the effects of climate change on health in Europe. We reviewed the literature of studies on climate change and health by searching the PubMed and ScienceDirect databases from January 2007 on to September 5, 2014. Four search algorithms were designed for use in the PubMed and ScienceDirect databases, allowing a basic search as well as searches specific to different health outcomes and risks. Original research papers were identified, with further material obtained by way of screening the references of the identified papers. The reference lists of selected key papers were reviewed, and relevant citations obtained from the mentioned scientific databases. Additionally, grey literature search was conducting and documents were included in research database, e.g. WHO, IPCC, EEA etc. The European Commission Community Research and Development Information Service (CORDIS) website was used to identify relevant European Commission-funded projects and publications (EU CORDIS, 2014). The initial search performed using the four search algorithms in PubMed returned a total of 6,550 results, with an additional 2,740 identified using ScienceDirect. First screening (by way of automatic filters in PubMed and manual screening of ScienceDirect search results) returned a total of 617 papers. Second screening using the established eligibility criteria and assessment of published abstracts returned 181 results and further assessment of full text versions (using the same eligibility criteria) excluded another 65 articles. An additional 37 original studies were identified from the hand search, leaving a final total of 169 studies included for review.

	TOPIC	IDENTIFIED STUDIES
Direct health effects	Heat and high temperature	24
	Low temperature and cold	10
	Floods and storms	11
	Wildfires	11
Indirect health effects	Vector-and rodent borne infectious diseases	40
	Food- and water-related diseases	5
	Air quality	35
	Allergic diseases	28
	Ultraviolet radiation exposure	5
	TOTAL	169

Table 8: Screened results of literature search

3.2 Quantitative survey

Heat-mortality function

The city-specific heat-mortality functions reported by Baccini et al. (2008) for the 15 European cities participating in the PHEWE project were used. These functions refer to the effect of maximum

apparent temperature on natural mortality (all ages) during the 90s and they are summarized by a threshold (corresponding to the minimum of the heat-mortality curve) and a slope above the threshold. In order to account for geographical heterogeneity, new random effects meta-analyses of these city-specific thresholds and slopes, separately for Mediterranean cities (Athens, Barcelona, Ljubljana, Milan, Rome, Turin, Valencia), Northern cities (Dublin, Helsinki, London, Paris, Stockholm, Zurich) and Eastern cities (Budapest, Prague) were performed. In the table 9 below, the overall meta-analytic estimates are reported.

Region	Threshold (°C) for maximum apparent temperature	Slope above the threshold (b) (% variation associated to 1°C increase of maximum apparent temperature above the threshold)
Mediterranean countries	29.4	3.12
North-western countries	23.9	1.84
Eastern countries	22.6	1.84

Table 9: Overall meta-analytic estimates

Exposure definition

The baseline climate (1971-2000) and meteorological projections for two future time periods (2°C and 3°C), obtained using five different models, as provided by partners (website: impact2c.dmi.dk) were considered:

Models (RCP8.5)		Temperature	Precipitation	historical	2°C	3°C
CSC REMO	MPI ESM LR r1	Cooler	Driest		X	X
SMHI RCA4	HadGEM2 ES r1	Hottest	Wettest		X	X
KNMI RACMO22E	EC EARTH r1	Median	Mid	X	X	X
MOHC-SMHI-RCA4	EC-EARTH-r12	Hot	Mid		X	X
MOHC-SMHI-RCA4 (RCP4.5)	HadGEM2-ES-r1	Hot	Mid		X	X

Table 10: Models

Meteorological data consisted in daily time series (one for each year of interest) at a fine spatial resolution. The daily mean apparent temperatures (AT), by combining mean temperature (from the “CORRECTED” data sets) and relative humidity (from the “REGRIDDED” data sets) according to the following formula was calculated:

$$AT = c_1 + c_2 * T + c_3 * RH + c_4 * T * RH + c_5 * T^2 + c_6 * RH^2 + c_7 * T^2 * RH + c_8 * T * RH^2 + c_9 * T^2 * RH^2$$

where T and RH are temperature (°F) and relative humidity (%), respectively, and c_i , $i=1...9$ are fixed coefficients ($c_1=-42.38$, $c_2=2.04901523$, $c_3=10.14333127$, $c_4=-0.22475541$, $c_5=-0.00683783$, $c_6=-0.05481717$, $c_7=0.00122874$, $c_8=0.00085282$, $c_9=-0.00000199$). Apparent temperature was set to T if $T < 80^\circ\text{F}$ and $RH < 40\%$.

Maximum apparent temperature – mean apparent temperature conversion

Thresholds reported in table 11 refer to maximum apparent temperature and they cannot be used if exposure is measured in terms of mean apparent temperature. This is the reason why a constant from each estimated threshold in table 11 were subtracted. The constants (one for each region) were estimated from the original PHEWE data set. First, a simple regression model to compare daily maximum apparent temperature (outcome variable) and daily mean apparent temperature (explanatory variable) for each of the 15 cities were specified; then, after having found that the slope was always very close to 1, the constant terms arising from the regressions, separately by region were averaged. In table 12 the constant terms were used are reported together with the “new” lower thresholds (Threshold*).

Region	Threshold (°C)	Constant (°C)	Threshold* (°C)
Mediterranean countries	29.4	3.7	25.7
North-western countries	23.9	2.8	21.1
Eastern countries	22.6	3.3	19.3

Table 11: Thresholds

Attributable Fraction at the cell level

For each day d belonging to the “warm season” (april 1st-september 30th), the daily attributable fraction (AF) (i.e. the fraction of deaths attributable to mean apparent temperature above the threshold) were calculated:

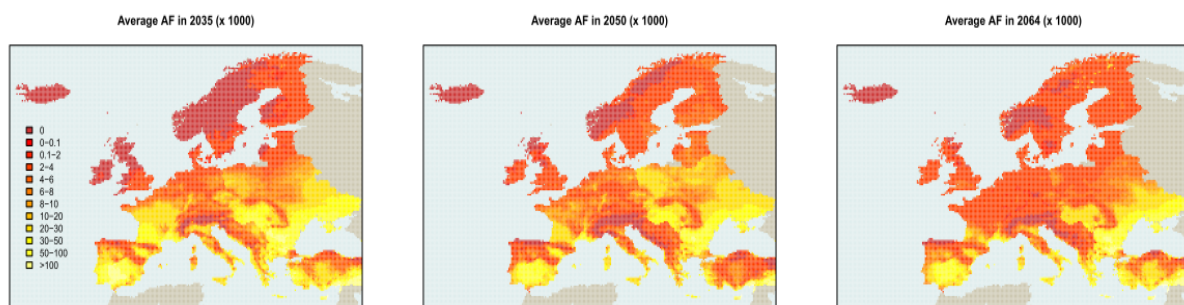
$$AF_d = 1 - 1/\exp(b(AT_d - \text{Threshold}^*)) \text{ if } AT_d > \text{Threshold}^*$$

$$AF_d = 0 \text{ if } AT_d \leq \text{Threshold}^*$$

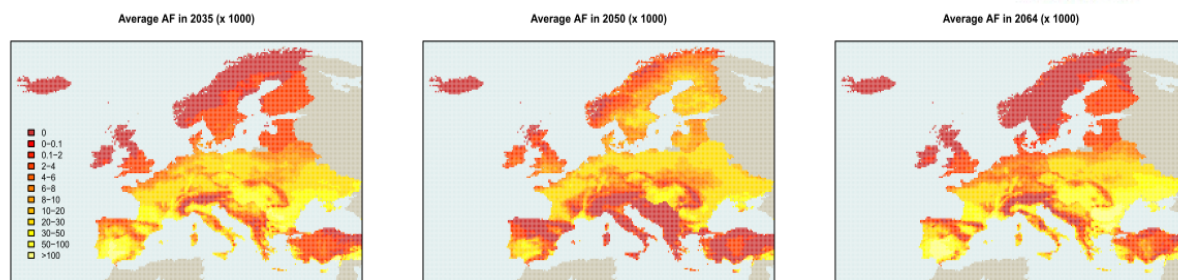
Then the average AF during each warm season for each cell of the map was calculated:

$$\overline{AF}_{cell} = \sum_{d=1}^{183} AF_{cell,d} / 183.$$

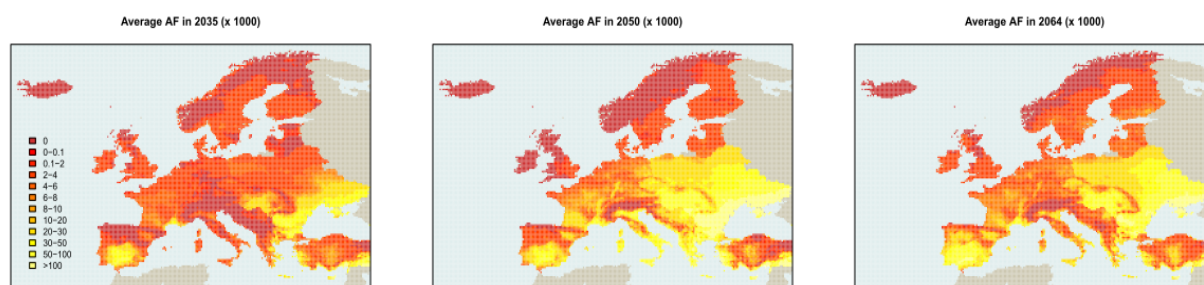
This value expresses the “overall” relative impact of heat during the year and it allows comparison among cell/areas (see Figures 1-6).



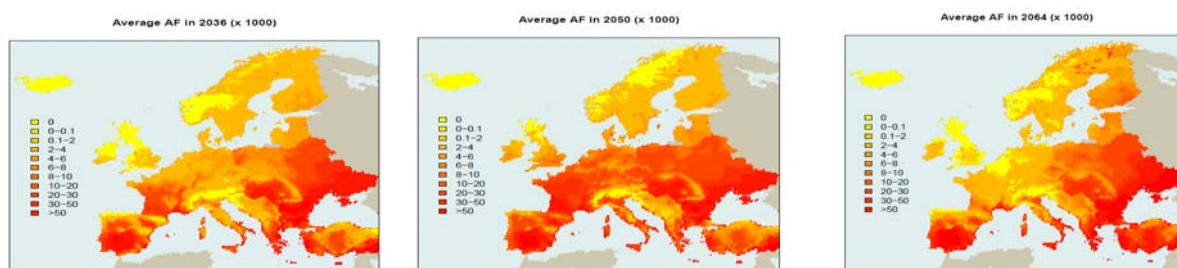
Figures 36: SMHI model



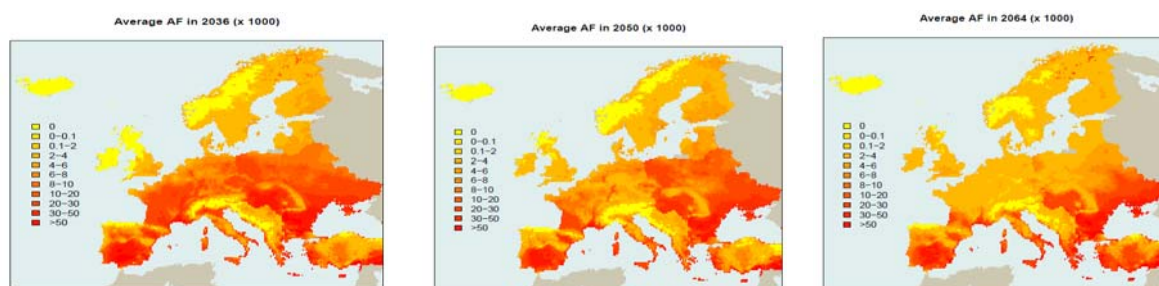
Figures 37: KNMI model



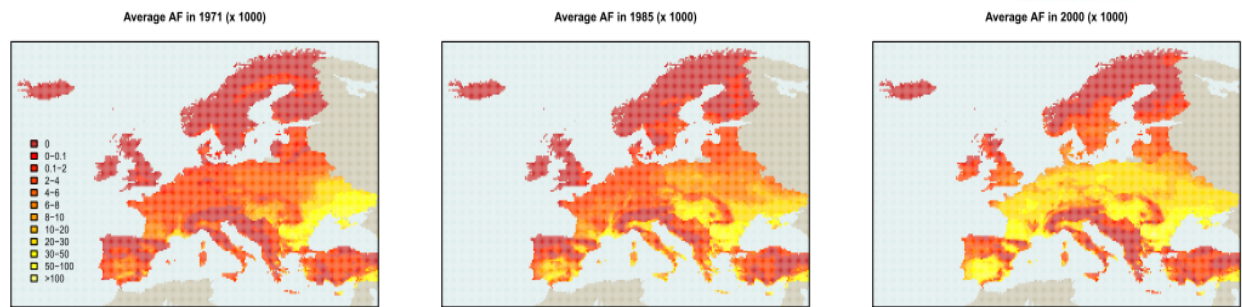
Figures 38: CSC model



Figures 39: MOHC model



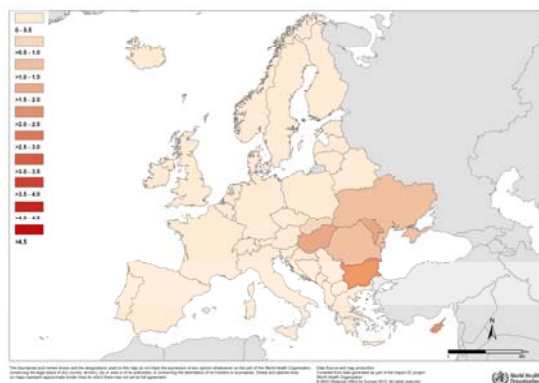
Figures 40: MOHC model (RCP4.5)



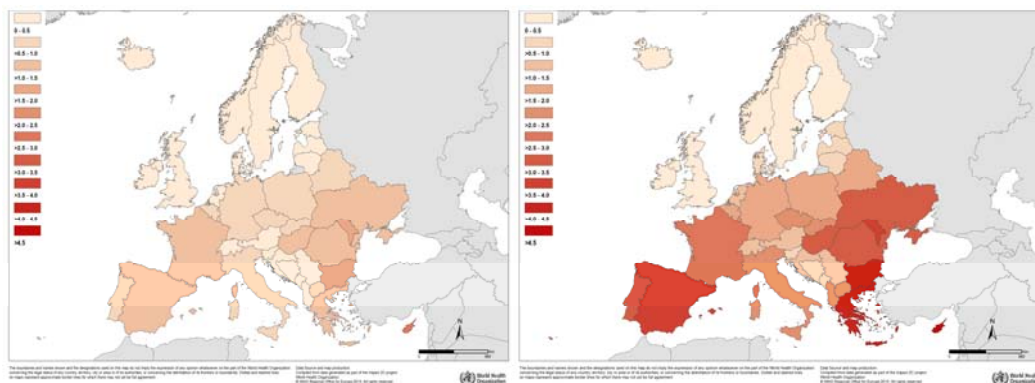
Figures 41: Historical: 1971-2000

Country-level AF

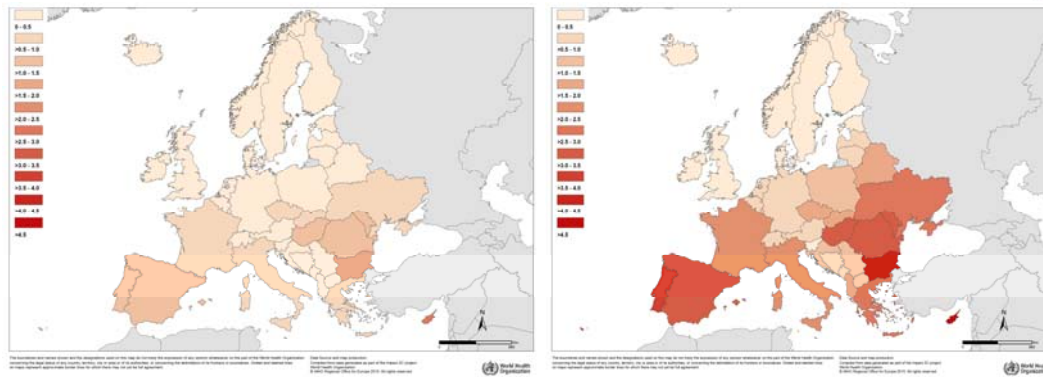
In order to obtain an estimate of AF at the country level were collapsed AF_{cell} belonging to the same country by calculating their mean. It was done separately for each year, so that the final result for each country was an annual time series of AFs. We reported mean, minimum and maximum AFs for each country during the two periods ($2^{\circ}C$ and $3^{\circ}C$), and under different climate models.



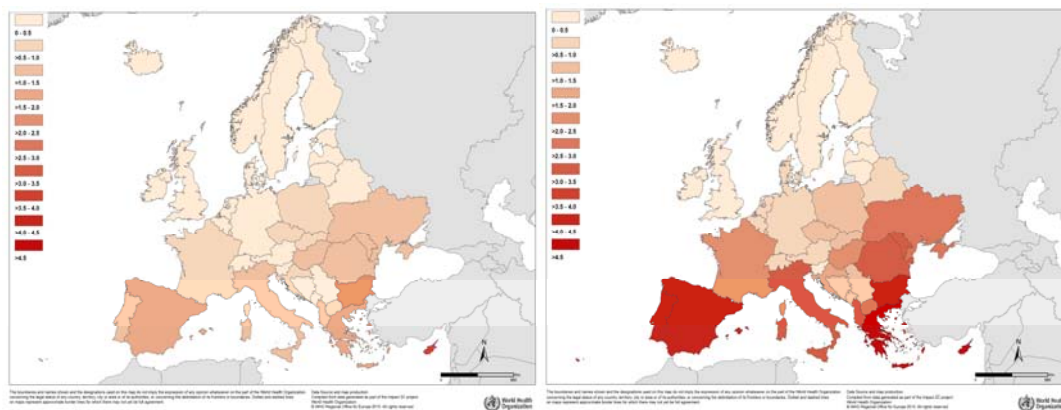
Figures 42: Historical: 1971-2000



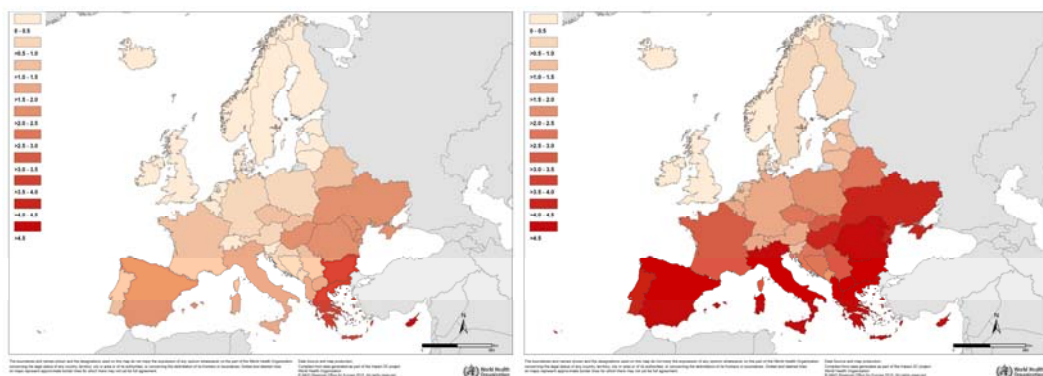
Figures 43: SMHI model ($2^{\circ}C$ and $3^{\circ}C$)



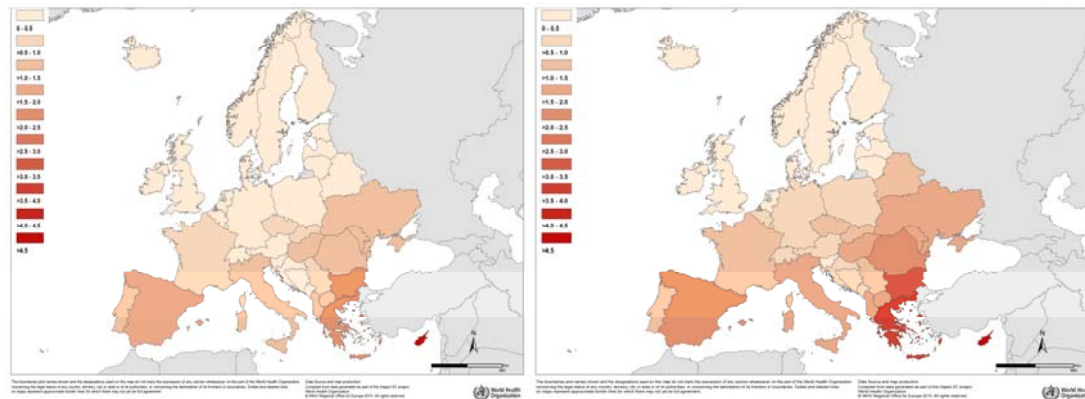
Figures 44: KNMI model (2°C and 3°C)



Figures 45: CSC model (2°C and 3°C)



Figures 46: MOHC model (2°C and 3°C)



Figures 47: MOHC model (RCP4.5) (2°C and 3°C)

To estimate the attributable deaths, the total heat-attributable deaths by models minus the estimated deaths without climate change were calculated. This was then converted into a percentage above the threshold, called the attributable fraction (AF) at country levels (Figures 40-46).

Attributable deaths (AD)

Indicating with $AF_{c,m,ts}$ the mean AF for country c , climate model m and time period ts (see last statement of the previous section), the number of attributable deaths per year (AD) according to this formula were calculated:

$$AD_{c,ts,m} = AF_{c,m,ts} * pop_{c,ts} * r_{c,ts} * p,$$

where $pop_{c,ts}$ is the average population of country c during time slice ts ; $r_{c,ts}$ is the average annual crude mortality rate for c during ts ; p is the proportion of deaths observed during warm season.

Proportion p was estimated using the PHEWE original data; it was approximately equal to 0.45. Population was assumed to change over time according to OECD scenario SSP2 (data downloaded from <https://secure.iiasa.ac.at/web-apps/ene/SspDb>). The crude mortality rate was projected under the assumption of constant fertility (source: United Nations).

Attributable community rate (ACR)

Finally, for each country and scenario the attributable community rate (ACR), which is the ratio between the number of AD and the population were calculated.

Preliminary results

Qualitative survey

Climate change differs from many traditional European local and regional environment and health issues, in that it is a global man made phenomenon for which local, regional and global solutions are required. It acts over long periods, is subject to multiple uncertainties, is strongly mediated by social,

economic and environment determinants, causes diverse and interacting health impacts as well as provides new challenges and opportunities at all levels of society.

If climate change continues as projected across the Representative Concentration Pathway (RCP) scenarios, the major changes in ill health compared to no climate change will occur through:

- Greater risk of injury, disease, and death due to more intense heat waves and fires
- Increased risk of under-nutrition resulting from diminished food production in poor regions
- Consequences for health of lost work capacity and reduced labour productivity in vulnerable populations
- Increased risks of food- and water-borne diseases (very high confidence) and vector-borne diseases
- Modest reductions in cold-related mortality and morbidity in some areas due to fewer cold extremes, geographical shifts in food production, and reduced capacity of disease-carrying vectors due to exceedance of thermal thresholds. These positive effects will be increasingly outweighed, worldwide, by the magnitude and severity of the negative effects of climate change” (Smith et al., 2014)

In the first Burden of Disease study WHO estimated for the year 2000, that climate change has caused the loss of over 150,000 lives and 5,500,000 DALYs (0.3% of deaths and 0.4% of DALYs, respectively). This is a relative small burden compared with effects of other stressors. However only four health outcomes were included based on known sensitivity to climate variation, predicted future importance, and availability of quantitative global models (or the feasibility of constructing them): episodes of diarrhoeal disease, cases of *Plasmodium falciparum* malaria, fatal accidental injuries in coastal floods and inland floods/landslides, the non-availability of recommended daily calorie intake (as an indicator for the prevalence of malnutrition). Limited adjustments for adaptation were included in the estimates (McMichael et al, 2004)

The WHO (2014), estimated approximately 250 000 additional deaths, per year due to climate change between 2030 and 2050, globally. The second study of global burden of disease attributable to climate change considers heat-related mortality, coastal flood mortality, diarrhoeal disease, malaria, dengue and under-nutrition. WHO projects a decline in child mortality, and this is reflected in declining climate change impacts from child malnutrition and diarrhoeal disease between 2030 and 2050. On the other hand, by the 2050s, deaths related to heat exposure (over 100 000 per year) are projected to increase. Impacts are greatest under a low economic growth scenario because of higher rates of mortality projected in low- and middle-income countries. This study showed that climate change in WHO Regional Office for Europe is associated with increase in heat-related mortality and the impacts were restricted to mortality in people aged over 65 years.

The health impacts of climate change will depend on the underlying health of affected populations, which will in turn depend on future socioeconomic conditions and other important factors, such as universal health coverage and environmental regulation.

This WHO study from 2014 showed that climate change is associated with a significant increase in heat-related mortality. The global estimate for increases in heat-related deaths (annual estimate) is 92207 (64458–121464) additional deaths in 2030 and 255486 (191816–364002) additional deaths in 2050 (assuming no adaptation) (Figure 41).

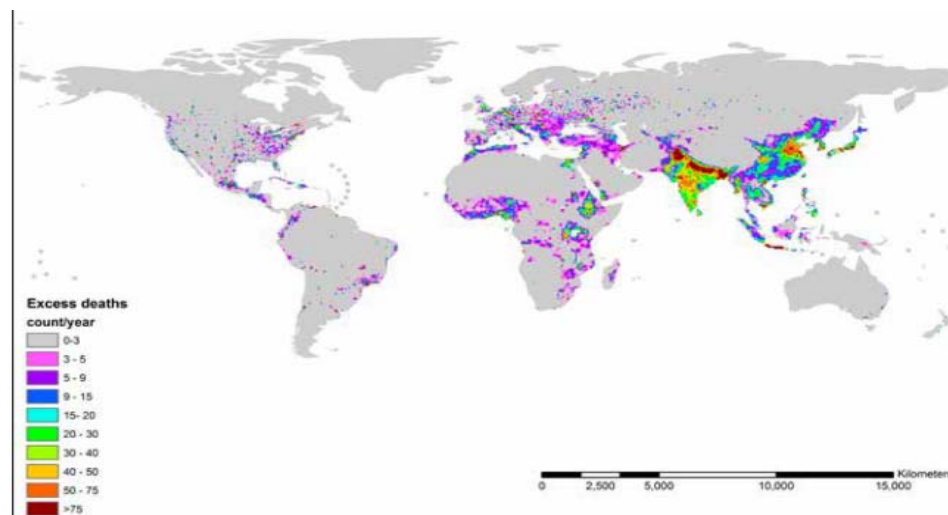


Figure 48: Estimated annual counts of heat-related deaths in people aged 65 years and over, by 0.5° grid cell, for BCM2 in 2050, with no adaptation assumed. Source: WHO (2014)

For Europe the estimation without and with adaptation are showed on Table 8 and 9 respectively.

WHO results are consistent with a previous study that used this modelling approach (Takashi et al, 2007). The present model has the following improvements: risk function is nonlinear with 95% confidence bands rather than wide category point estimates; WHO addressed mortality displacement; and the model is based on a longer observation period.

The proportion of heat-related respiratory admissions is expected to approximately double, from 0.18% in the baseline period (1981-2010) to 0.4% in the period 2021-2050. This equates to an increase in the number of heat-related respiratory hospital admissions (RHA) from 11 000 per year at baseline to 26 000 per year. The greatest increases are expected in southern European countries, with the proportion of heat-related admissions for respiratory conditions expected to approximately triple in this region (Åström et. Al., 2013).

While heat-related mortality in Europe is project to increase in all regions, there are relatively higher levels of climate change attributable heat deaths in southern Europe. It is estimated that 90 000 additional heat-related deaths are projected each year by the 2050s (under the A1B scenario), with an expected welfare cost of €30 billion per year (Watkiss, 2011). Other study estimated that by the 2080s, heat-related mortality rates in Europe are likely to increase by 12–33 per 100 000 per year, totalling approximately 50 000 to 160 000 additional deaths yearly. The highest increase in mortality is expected in central and southern Europe (Ciscar et al., 2009).

A study performed across 10 cities in central Italy, projects that all cities will demonstrate an increase in heat-related mortality. The greatest increases are predicted in Italian coastal regions, with mortality expected to increase by up to 11.8% by 2031-2050, compared with baseline 1999-2008, for each 1°C increase above the estimated temperature threshold (Morabito et al., 2012)(Morabito et al., 2012).

There were close to 11,000 excess deaths from non-accidental causes during interactions between high temperatures and air pollution from wildfires in excess of an additive effect during the Moscow major heat wave in summer 2010 (Shaposhnikov et al., 2014). The risk of wildfires is expected to increase in Europe. Projections show an increase in wildfire risk in many parts of Europe, including France, Germany, Belgium, Romania and Bulgaria, plus southern parts of the Netherlands, Sweden

and Finland. Areas of high and very high wildfire risk will increase by the period 2041–2070. Fire risk is expected to increase most significantly in Greece, Portugal, Spain and southern parts of Italy (Amatulli, Camia & San-Miguel-Ayanz, 2013; Lung et al., 2013).

Extreme weather events and climate-sensitive infectious diseases also pose occupational risks to health workers, which may in turn undermine health protection for the wider population (WHO, 2009). Other mechanisms include elevated occupational exposures to toxic chemical solvents which evaporate faster at higher temperatures (Bennett & McMichael, 2010). Projections have been made of the future effects of heat on work capacity (Dunne, Stouffer, & John, 2013; T. Kjellstrom, Holmer, & Lemke, 2009). By 2100, under RCP4.5, (Dunne et al., 2013) project up to a 20% loss of productivity globally. There is an unfortunate trade-off between health impact and productivity, which creates risks for poor and disenfranchised labourers working under difficult working conditions and inflexible rules (T. B. Kjellstrom & Lemke, 2011; T. Kjellstrom et al., 2009; Sahu, Sett, & Kjellstrom, 2013).

The evidence on the climatic influence on infectious disease in Europe is significant, particularly for vector-borne diseases, and food-and water-borne diseases as summarized as follows:

- Climate change-induced ecosystem changes will affect disease vectors (as well as intermediate hosts and hosts) that can transmit serious infectious diseases. Climate modelling suggests that the geographic range of *Ixodes ricinus* ticks will increase during the 21st century. Projections using the SRES A2 and B2 emissions scenarios show an increase in the vegetation period and associated tick activity by 2071–2100, with the ticks likely to be distributed across Norway, Sweden and Finland by 2100. A resultant increase in tick-borne disease may occur (Jaenson & Lindgren, 2011). However, other contributors to changing disease distribution require further assessment, including alterations to vegetation and habitat, human behaviour, density and distribution of non-human hosts (such as deer and rodents), and health interventions including vaccination programs (Semenza & Menne, 2009).
- The *Anopheles atroparvus* mosquito is a potential vector for malaria in many parts of Europe, with re-establishment of transmission a possibility. The observed and projected risk of Malaria were explored for Portugal (Benali et al., 2014), Turkey (Dogan, Cetin & Egri, 2010), Spain (Sainz-Elise et al., 2010) and Germany (Schröder & Schmidt, 2008). However, numerous factors make the re-emergence of malaria in Europe unlikely, including health system functionality, building and development regulations, and patterns of land use (Semenza & Menne, 2009).
- As dengue risk is not dependent purely on vector distribution, modelling of risk in terms of disease occurrence rather than mosquito presence has also been performed, with projections based on global and regional climate models under the SRES A1B scenario. An overall increase in dengue risk is predicted, with the greatest increase expected in southern Europe, particularly coastal areas. Central parts of Europe, including France, Germany and Hungary, may also see an increase in dengue fever incidence, while the British Isles and northern Europe are predicted to remain at near-zero risk even by 2071–2100 (Bouzid et al., 2014).
- Climatic changes in central Asia favour conditions for the propagation of plague; it has been projected that only a 1°C increase in spring temperatures could result in a 50% increase in *Yersinia pestis* prevalence in its reservoir host. Plague epizootics may become more frequent in central Asia and pose a threat to eastern European countries (Semenza and Menne, 2009).
- Regarding the food-borne diseases, from the period 2071–2100 salmonella may increase from 24 000 to 50 000 reported cases per year (an increase of 1–5%) with estimated

economical costs up to €0.2 billion per year (Watkiss et al, 2009). An increase in the risk of campylobacter is also predicted (ECDC, 2012).

- An increase in extreme precipitation events is expected in Europe as the climate changes (Watkiss et al., 2013), with associated increased risks of water-borne diseases such as cryptosporidiosis (ECDC, 2012).

Climate change is likely to trigger further changes in pollen concentration, volume and distribution, with an associated increase in the prevalence and severity of allergic diseases in many parts of Europe. While increasing temperatures may prompt earlier flowering and hence prolongation of the pollen season, rising atmospheric carbon dioxide concentrations will result in increased plant growth and pollen production. Furthermore, changing weather patterns may prompt an increase in the geographic range of many allergenic plants, with increasing population risk of allergic disease (Weber, 2012; Cecchi et al., 2010; Shea et al., 2008).

EU countries

Residents of the European Union are at risk to both direct and indirect impacts of climate change. Heat-waves, flooding, and poor air quality, exacerbated by climate change can directly impact health in this region, while increased risk of infectious diseases, food safety, and increased vector distribution may indirectly affect human health as a result of climate change (Kovats et al., 2014)

In the European Union, high levels of urbanisation, a comparably old population and synergistic effects of air pollution increase the health risks associated with high temperatures, but future cold-related mortality is likely to be reduced with climate change (Ballester et al., 2011) (HPA, 2012).

Flooding has severe acute and long term health effects such as drowning, injury and infection and PTSD and mental health implications respectively. By the year 2080, coastal flooding is projected to affect an additional 775,000 and 5.5 million people per year and river flooding an additional 250,000-400,000 under current projection scenarios (Ciscar et al., 2011). River flooding may more than double annual average damages, with Central and Northern Europe and the United Kingdom most affected (Ciscar et al., 2009) (Ciscar et al., 2011).

The changing climate alters ecosystems for infectious disease vectors such as mosquitos, ticks and rodents. Emerging or re-emerging infections include dengue and chikungunya, tick borne diseases, leishmaniasis and malaria (Kovats et al., 2014). Leishmaniasis for example, is currently present in the Mediterranean region and climate change could facilitate the spread of either vectors or current parasites northwards (Ready, 2010).

The cases of salmonellosis and campylobacteriosis (only climate change-attributable ones) are projected to increase from 28438 per year in 2010-2040, to 32501 in 2041-2070 for EU total. Resource costs are calculated for both additional hospital admissions and additional cases of salmonellosis and campylobacteriosis are calculated to be around 700 M Euros in 2041-2170 period in A1B scenario and around 650 M Euros in the E1 scenario (Paci, 2014) .

Climate change could promote intoxications related to agricultural products such as mycotoxin production and regional expansion of ochratoxin A, patulin and Fusarium toxin contamination (Paterson and Lima, 2010). Exceeding temperature thresholds may also increase the risk of marine biotoxins in seafood (Miraglia et al., 2009).

Quantitative survey 2° C world

In EU 28 the average population during the period 2036-2064 under different models will be 537.226.000 and the number of deaths during each warm season will be on average 3.186.760. Part of these will be due to heat (attributable deaths- AD): total AD are: 0.94% under the KNMI scenario, 1.27% under the CSC scenario, 0.87% under the SMHI scenario, 1.19% under MOHC scenario, and 1.65% under RCP4.5 MOHC scenario. In absolute terms, these fractions correspond to 27178, 37473, 25765, 37314 and 47349 attributable deaths, respectively (except for Malta-data not available) (Table 12).

EU28	Total AD.SM HI	Total AD.CS C	Total AD.KM NI	Total AD.MOH C	Total AD.MOH C (RCP4.5)	No CC	2° C AD.SM HI	2° C AD.C SC	2° C AD.K MNI	2° C AD.M OHC	2° C AD.MOH C (RCP4.5)
Austria	276	184	159	283	356	71	205	113	88	212	285
Belgium	270	227	252	281	380	93	177	134	159	188	287
Bulgaria	2624	2122	1858	2551	3158	1150	1474	972	708	1401	2008
Croatia	161	140	97	160	233	28	133	112	69	132	205
Cyprus	716	455	378	710	919	211	505	244	167	499	708
Czech Republic	862	669	643	843	1051	312	550	357	331	531	739
Denmark	57	51	52	62	93	16	41	35	36	46	77
Estonia	14	10	13	15	28	4	10	6	9	11	24
Finland	36	19	40	38	62	8	28	11	32	30	54
France	4724	2932	3507	4763	5399	1499	3225	1433	2008	3264	3900
Germany	3073	2532	2671	3186	3993	1044	2029	1488	1627	2142	2949
Greece	1907	1120	731	1908	2872	277	1630	843	454	1631	2595
Hungary	1986	1659	1712	1929	2348	1043	943	616	669	886	1305
Ireland	11	6	4	12	20	0	11	6	4	12	20
Italy	5298	3258	2340	5311	6956	857	4441	2401	1483	4454	6099
Latvia	24	18	29	26	52	10	14	8	19	16	42
Lithuania	47	38	61	50	99	21	26	17	40	29	78
Luxembou rg	20	16	17	20	27	6	14	10	11	14	21
Malta	NA	NA	NA	NA	NA	NA	NA	NA	NA	NA	NA
Netherlan ds	309	311	334	326	439	136	173	175	198	190	303
Poland	2446	2228	2167	2400	3378	1148	1298	1080	1019	1252	2230
Portugal	997	766	787	972	1253	224	773	542	563	748	1029
Romania	4046	3746	3271	3931	5136	1959	2087	1787	1312	1972	3177
Slovakia	556	465	452	542	716	237	319	228	215	305	479
Slovenia	16	11	8	16	27	1	15	10	7	15	26
Spain	6721	3987	3978	6681	7872	1474	5247	2513	2504	5207	6398
Sweden	28	19	44	31	59	6	22	13	38	25	53
UK	248	189	160	267	423	46	202	143	114	221	377
Total EU28	37473	27178	25765	37314	47349	11881	25592	1529	13884	25433	35468

Table 12: The average number of heat additional deaths per warm season per year for EU countries for the 2⁰ C world

The average attributable fraction (AF) for EU 27 during the period 1971-2000 was 0.43% (on average 43 deaths due to heat every 10'000 deaths during the warm season). We assume that this AF does not change over time (i.e. there is not climate change): there will be 11881 attributable deaths per warm season during the future time slice 2036-2064 corresponding to 0.1 death per 10.000 inhabitants).

To estimate the attributable deaths in 2⁰ C world, we estimate the total heat attributable deaths by models minus estimated deaths without climate change. For EU27 (without Malta) in 2⁰ C world, yearly, per warm season, we estimate that under the KNMI model there will be 13884 more heat attributable deaths, for CSC model 15297 more heat attributable deaths; for SMHI model more 25592 heat attributable deaths; for MOHC model more 25433 heat attributable deaths; and for MOHC (PCR4.5) model more 35468 heat attributable deaths.

	Heat attributable fraction (AF)		
	0-1%	1-1.9%	2-7%
Mediterranean countries	Croatia, Slovenia	France, Italy, Portugal,	Cyprus, Greece, Spain
North-western countries	Austria, Belgium, Denmark, Finland, Germany, Ireland, Luxemburg, Netherlands, United Kingdom, Sweden		
Central-eastern countries	Estonia, Latvia, Lithuania	Czech Republic, Poland, Slovakia	Bulgaria, Hungary, Romania

Table 13: Percentage of heat attributable deaths in Europe for 2⁰C

In 2⁰ C world, both, citizens from Mediterranean (Cyprus, Greece, Spain) and Eastern EU countries (Bulgaria, Hungary and Romania) will be most affected by heat.

Other Mediterranean countries (Italy, Portugal and France) as well as other Eastern EU countries (Slovakia and Czech Republic) will be affected by heat too.

Even the risk from heat will be lower for the citizens in North-western EU countries compared with others, in 2⁰ C world there will be still registered heat deaths during the warm season.

As a risk reduction strategy in EU, several member states introduced heat wave early warning systems with response plans as an approach to reducing the human health consequences of heat waves. Early warning systems involve forecasting the heat wave event, predicting possible health outcomes, triggering effective and timely response plans targeting vulnerable populations, notification of heat wave events, communication of prevention responses and evaluation and revision of systems (Lowe et al, 2011).

3⁰ C world

In EU 28 the average population during the period 2050-2085 under different models will be 523.779.600 and the number of deaths during each warm season will be on average 3.194.667. Part of these will be due to heat (AD): total AD are 2.09% under the KNMI scenario, 2.25% under the CSC scenario, 2.42 % under the SMHI scenario, 3.48% under MOHC scenario, and 1.71% under RCP4.5 MOHC scenario. In absolute terms, these fractions correspond to 65602, 71556, 78394, 107146 and 49148 attributable deaths, respectively (except for Malta-data not available) (Table 14).

EU28	Total AD.SM HI	Total AD.CS C	Total AD.KM NI	Total AD.MOH C	Total AD.MOH C (RCP4.5)	No CC	3 ⁰ C AD.SM HI	3 ⁰ C AD.C SC	3 ⁰ C AD.K MNI	3 ⁰ C AD.M OHC	3 ⁰ C AD.MOH C (RCP4.5)
Austria	617	461	453	970	386	69	548	392	384	901	317
Belgium	1112	637	683	1100	451	93	1019	544	590	1007	358
Bulgaria	3298	3302	3085	4494	2773	1031	2267	2271	2054	3463	1742
Croatia	400	479	395	716	232	26	374	453	369	690	206
Cyprus	638	783	602	1169	711	160	478	623	442	1009	551
Czech Republic	1950	1355	1519	2526	1206	327	1623	1028	1192	2199	879
Denmark	330	206	178	308	118	17	313	189	161	291	101
Estonia	49	20	41	98	36	4	45	16	37	94	32
Finland	140	51	139	300	93	9	131	42	130	291	84
France	12502	9040	10051	14247	6311	1572	10930	7468	8479	12675	4739
Germany	9367	5861	5880	9666	4259	973	8394	4888	4907	8693	3286
Greece	2969	3569	2199	5762	2606	260	2709	3309	1939	5502	2346
Hungary	2876	2320	2838	3540	2101	953	1923	1367	1885	2587	1148
Ireland	59	45	30	111	28	1	58	44	29	110	27
Italy	9743	11668	8338	18668	7359	808	8935	10860	7530	17860	6551
Latvia	89	31	67	134	56	8	81	23	59	126	48
Lithuania	176	71	133	236	107	18	158	53	115	218	89
Luxembourg	116	71	71	117	48	9	107	62	62	108	39
Malta	NA	NA	NA	NA	NA	NA	NA	NA	NA	NA	NA
Netherlands	1289	840	841	1186	530	134	1155	706	707	1052	396
Poland	5716	3834	4624	6743	3440	1132	4584	2702	3492	5611	2308
Portugal	2710	3619	3147	3484	1344	249	2461	3370	2898	3235	1095
Romania	5334	5217	5117	7071	4002	1639	3695	3578	3478	5432	2363
Slovakia	1160	853	1056	1525	766	249	911	604	807	1276	517
Slovenia	93	70	50	145	31	1	92	69	49	144	30
Spain	13905	16052	12948	20929	9586	1599	12306	14453	11349	19330	7987
Sweden	251	79	150	351	100	6	245	73	144	345	94
UK	1504	1022	967	1550	518	52	1452	970	915	1498	466
Total EU28	78394	71556	65602	107146	49198	11399	66995	60157	54203	95747	37799

Table 14: The average number of heat additional deaths per warm season per year for EU countries for the 3⁰ C world

The average AF for EU 28 during the period 1971-2000 was 0.43% (on average 43 deaths due to heat every 10'000 deaths during the warm season). We assume that this AF does not change over time (i.e. there is not climate change): there will be 11399 attributable deaths per warm season during the future time slice 2050-2085 corresponding to 0.1 death per 10.000 inhabitants).

To estimate the attributable deaths in 3⁰ C world, we estimate the total heat attributable deaths by models minus estimated deaths without climate change. For EU27 (without Malta) in 3⁰ C world, yearly, per warm season, we estimate that under the KNMI model there will be 54203 more heat attributable deaths, for CSC model 60153 more heat attributable deaths; for SMHI model more 66995 heat attributable deaths; for MOHC model more 95747 heat attributable deaths; and for MOHC (PCR4.5) model more 37799 heat attributable deaths.

Conclusions

Climate change affects human health and well-being. In the near future it will lead to an amplification of current health problems, as well as new risks and pressures for the environment and the social and economic determinants of health. Some risks of climate change, such as risks to unique and threatened systems and risks associated with extreme weather events, are moderate to high at temperatures 1°C to 2°C above pre-industrial levels (IPCC, 2007).

Our estimations under different models on heat mortality due to climate change in 2⁰C and 3⁰ C worlds in EU countries are presented (Table 15)

EU28*	2 ⁰ C World	3 ⁰ C World
AD.SMHI model	25592	66995
AD.CSC model	15297	60157
AD.KMNI model	13884	54203
AD.MOHC model	25433	95747
AD.MOHC (RCP4.5)	35468	37799
Average	23135	62980

Table 15: Distribution of heat attributable deaths by models for 2⁰ C and 3⁰C Worlds in EU countries. *Data for Malta not available

In the WHO European Region, health effects have already been observed from more frequent and intense extreme weather events as well as changes in the geographic range of some infectious disease vectors.

Sustainable development, population health and equity provide a basis for assessing climate adaptation and mitigation policies, measures and strategies. In the near term protection of health against climate change risks can be enhanced through including health measures into national adaptation plans, including ensuring better and more equitable access to services that mitigate and improve the social and environmental determinants of health, strengthening of basic public health interventions, and interventions targeted at specific climate-related risks. In the longer term, however, climate change risks will require a transformational thinking of society as a whole and

within an all of government approach. Greater rates and magnitude of climate change increase the likelihood of exceeding adaptation limits.

An increase of 2°C above pre-industrial levels is often used as a (politically-determined) benchmark target of climate mitigation policy. Deep cuts in GHG emissions to limit warming to 2°C relative to pre-industrial levels remain possible, yet will entail substantial technological, economic, institutional, and behavioural changes. Similar challenges would have to be faced for less ambitious mitigation, but over a longer period of time. Delaying mitigation efforts beyond those in place today through 2030 is estimated to substantially increase the difficulty of the transition to low longer-term emissions levels and narrow the range of options consistent with maintaining temperature change below 2 C relative to pre-industrial levels (IPCC, 2007).

Measures, technologies and policies for reducing greenhouse gas emissions are well known. Some can have significant local and immediate benefits for human health, in particular through reducing non-communicable diseases and improving universal health access. The opportunity exists for policies in particular in household energy, electricity generation, transport, urban planning and land use, buildings, food and agriculture. The health sector can also improve its own environmentally friendly practices and at the same time minimize its carbon emissions.

The WHO European Regional Framework for Action, has set a good bases for action in the “era of committed climate change” however will require some rethinking of incorporating the larger large scale risks our planet might face, if no stringent mitigation measures are taken. It aims to protect health, promote health equity and security, and provide healthy environments in a changing climate in the WHO European Region. It is designed to support action by Member States of the WHO European Region and other partners (WHO, 2010). The revised WHO global work plan (2014-2019) on climate change and health will provide support to Member States to respond to the health risks presented by climate change, by strengthening the resilience of health systems to climate risks and improving their capacity to adapt to long-term climate changes; and to identify, assess and promote actions that reduce the burden of diseases associated with air pollution, heat and other health consequences of policies that also cause climate change. The updated work plan is focus to:

- (i) establishment of a partnership “platform” to respond to the increasing number of activities and actors engaged in this field;
- (ii) greater emphasis on actions that can improve health while also mitigating the extent of climate change; and
- (iii) promoting the need and providing tools for more systematic provision of country-specific information and monitoring of progress (WHO, 2014).

Advocating for further improvement, development and implementation of heat-wave preparedness, planning and response in European countries would lead to a reduction in heat-related mortality . A focus should be placed on developing strong intersectoral coordination, effective early warning and health system response mechanisms as well as surveillance and evaluation measures (Bittner, Matthies, Dalbokova, & Menne, 2014)). Long-term planning, including urban planning and housing, becomes even more relevant than before.

Key messages

Climate change will exacerbates existing health problems even in 2°C world - such as deaths during the heat events for instance.

Improving links between health and climate policy. It is important that actions in protecting health and the environment are coherent and mutually reinforcing, from individual, to community, national and international levels.

Strengthening of health programmes to address climate risks. Even in 2°C world we will require a comprehensive approach to strengthen the core health system functions, and to identify and prioritize the specific interventions that are most protective against climate risks.

Gaining health benefits of mitigating climate change. Many policies and individual choices have the potential to reduce greenhouse gas emissions and produce major health co-benefits.

Valuation of heat related mortality

Following the analysis for air pollution, it is also possible to value the heat related mortality impacts above, though there are some differences in the exact approach. As noted earlier, the impacts on human health are difficult to value, because there are no observed market prices. However, it is possible to derive monetary values for this non-market sector, by considering the total effect on society's welfare. This requires analysis of three components which each capture different parts of the total effect. These are the resource costs i.e. medical treatment costs; the opportunity costs, in terms of lost productivity; and dis-utility i.e. pain or suffering, concern and inconvenience to family and others.

The first two components can be captured relatively easily. Techniques are also available to capture the third component, by assessing the 'willingness to pay' or the 'willingness to accept compensation' for a particular health outcome. These are derived using survey-based "stated" preference methods and/or "revealed" preferences methods that are based on observed expenditures such as on consumer safety.

However, there is substantial debate concerning the correct approach to valuation of mortality risks in the context of air pollution. As outlined above, these can be valued using a long-established metric, the value of statistical life (VSL) - also known as the value of a prevented fatality, VPF - but changes in life expectancy can also be valued using the value of a life year (VOLY), which provides a way of accounting for differing lengths of remaining life expectancy. Both approaches are used in the literature and both have strengths and weaknesses. Impact2C has used both.

The main results reported below use a VOLY of €63,000. A key issue relates to the period of life lost, and in this analysis a value of €315,000 (equivalent to seven life-years) is used, consistent with earlier studies (e.g. Watkiss and Hunt, 2012). These values are taken from Hurley et al (2005), for which an extensive review of the valuation literature was carried out, and updated to 2010 price levels. They have also been updated to take account of subsequent literature, for example by Alberini et. al (2006) and Desaiques et al (2011). The values shown are interpreted as being average values for the EU region, and hence are applied without adjustment by country. The VSL is also applied, using values of €1.16 million⁵. Consistent with all sector-based analysis in IMPACT2C, the economic valuation results below are presented in terms of constant 2010 prices in Euros over future years, without any adjustments or discounting to facilitate direct comparison, over time, and between sectors. However, subsequent policy analysis that looks at the costs and benefits of adaptation or mitigation policy would need to work with present values (i.e. values that are adjusted and discounted as with standard economic appraisal).

These values can be applied to the values in Table 15 above.

⁵ This value is towards the lower end of the range suggested by a recent OECD review, which indicates values of low 1.85million, central 3.75million and high 5.55million.

	Numbers	Bill Euro	Bill Euro		Bill Euro	Bill Euro
EU28*	2 ⁰ C World	VOLY	VSL	3 ⁰ C World	VOLY	VSL
AD.SMHI model	25592	8.1	29.7	66995	23.4	77.7
AD.CSC model	15297	4.8	17.7	60157	21.1	69.8
AD.KMNI model	13884	4.4	16.1	54203	19.0	62.9
AD.MOHC model	25433	8.0	29.5	95747	33.5	111.1
AD.MOHC (RCP4.5)	35468	11.2	41.1	37799	13.2	43.8
Average	23135	7.3	26.8	62980	22.0	73.1

Table 16: Valuation of heat attributable deaths for 2⁰ C and 3⁰C Worlds in EU countries. Climate change signal

These values include the effects of climate change alone. The effects of climate and socio-economic change is shown below.

	Numbers	Bill Euro	Bill Euro		Bill Euro	Bill Euro
EU28*	2 ⁰ C World	VOLY	VSL	3 ⁰ C World	VOLY	VSL
AD.SMHI model	37473	11.8	43.5	78394	27.4	90.9
AD.CSC model	27178	8.6	31.5	71556	25.0	83.0
AD.KMNI model	25765	8.1	29.9	65602	23.0	76.1
AD.MOHC model	37314	11.8	43.3	107146	37.5	124.3
AD.MOHC (RCP4.5)	47349	14.9	54.9	49198	17.2	57.1
Average	35016	11.0	40.6	74379	26.0	86.3

Table 17: Valuation of heat attributable deaths for 2⁰ C and 3⁰C Worlds in EU countries. Combined climate and socio-economic signal.

5. References

- Alberini A, Hunt A, and A. Markandya (2006). Willingness to Pay to Reduce Mortality Risks: Evidence from a Three-country Contingent Valuation Study. *Environmental and Resource Economics*. 33 (2). 251-264.
- Amann, M., Bertok, I., Borken-Kleefeld, J., Cofala, J., Heyes, C., Höglund-Isaksson, L., Klimont, Z., Nguyen, B., Posch, M., Rafaj, P., Sandler, R., Schöpp, W., Wagner, F., Winiwarter, W. (2011), Cost-effective control of air quality and greenhouse gases in Europe: Modeling and policy applications. *Environmental Modelling and Software* 26, 1489-1501.
- Amatulli G, Camia A, San-Miguel-Ayaz J. Estimating future burned areas under changing climate in the EU-Mediterranean countries. *Science of the Total Environment*, 2013; 450-451:209–222.
- Andersson, C. and Engardt, M. (2010), European ozone in a future climate: Importance of changes in dry deposition and isoprene emissions. *J. Geophys. Res.*, 115, D02303. doi:10.1029/2008JD011690
- Andersson, C., Langner, J. and Bergström, R. (2007), Interannual variation and trends in air pollution over Europe due to climate variability during 1958-2001 simulated with a regional CTM coupled to the ERA40 reanalysis. *Tellus* 59B, 77-98. doi: 10.1111/j.1600-0889.2006.00196.x
- Andersson-Sköld, Y. and Simpson, D. (1999), Comparison of the chemical schemes of the EMEP MSC-W and IVL photochemical trajectory models, *Atmos. Environ.*, 33, 1111–1129, doi:10.1016/s1352-2310(98)00296-9.
- Aström C et al. Heat-related respiratory hospital admissions in Europe in a changing climate: a health impact assessment. *BMJ open*, 2013; 3(1).
- Baccini M, Biggeri A, Accetta G, Kosatsky T, Katsouyanni K, Analitis A, et al. Heat Effects on Mortality in 15 European Cities. *Epidemiology*. 2008;19(5):[Epub ahead of print].
- Ballester, J., J. Robine, F.R. Herrmann, and X. Rodo, 2011: Long-term projections and acclimatization scenarios of temperature-related mortality in Europe. *Nature Communications*, 2(1), 358, doi:10.1038/ncomms1360.
- Benali A et al. (2014). Satellite-derived estimation of environmental suitability for malaria vector development in Portugal. *Remote Sensing of Environment*, 145(0):116–130.
- Bennett, C.M., McMichael, A.J., Non-heat related impacts of climate change on working populations. *Global health Action* 2010; 3. doi:10.3402/gha.v3i0.5640
- Berge, E. and Jakobsen, H. A. (1998), A regional scale multi-layer model for the calculation of long-term transport and deposition of air pollution in Europe, *Tellus B*, 50, 205–223, doi:10.1034/j.1600-0889.1998.t01-2-00001.x.
- Bessagnet, B., A. Hodzic, R. Vautard, M. Beekmann, S. Cheinet, C. Honore, C. Liousse, and L. Rouil (2004), Aerosol modeling with CHIMERE— Preliminary evaluation at the continental scale, *Atmos. Environ.*, 38, 2803 – 2817.
- Bittner MI, et al. (2014) Are European countries prepared for the next big heat-wave? *Eur J Public Health*. 24(4):615-9.

Bousserez, N., Attié, J.-L., Peuch, V.-H., Michou, M., Pfister, G., Edwards, D., Emmons, L., Mari, C., Barret, B., Arnold, S. R., Heckel, A., Richter, A., Schlager, H., Lewis, A., Avery, M., Sachse, G., Browell, E. V., and Hair, J. W. (2007), Evaluation of the MOCAGE chemistry transport model during the ICARTT/ITOP experiment, *J. Geophys. Res.*, 112, D10S42, doi:10.1029/2006JD007595.

Boylan, J.W., Russell, A.G., (2006). PM and light extinction model performance metrics, goals, and criteria for three-dimensional air quality models. *Atmospheric Environment* 40, 4946-4959.

Bouزيد M et al. (2014). Climate change and the emergence of vector-borne diseases in Europe: case study of dengue fever. *BMC Public Health*, 14:781.

CEC (2005). Thematic Strategy on Air Pollution (COM(2005) 446). Directive on Ambient Air Quality and Cleaner Air for Europe (the “CAFE” Directive) (COM(2005) 447), Published by the Commission of the European Communities, Brussels.

CEC (2005). Commission Staff Working Paper. Impact Assessment accompanying The Communication on Thematic Strategy on Air Pollution and The Directive on “Ambient Air Quality and Cleaner Air for Europe” Brussels, 21 9.2005. SEC (2005) 1133. Published by the Commission of the European Communities, Brussels.

CEC (2013). A Clean Air Programme for Europe. Communication From The Commission To The European Parliament, The Council, The European Economic And Social Committee And The Committee Of The Regions. COM/2013/0918 final.

Cecchi L et al. (2010). Projections of the effects of climate change on allergic asthma: the contribution of aerobiology. *Allergy*, 65(9):1073–1081.

Ciscar J-C, editor. Climate change impacts in Europe. Final report of the PESETA research project: European Commission, 2009.

Ciscar, J.-C., A. Iglesias, L. Feyen, L. Szabó, D. Van Regemorter, B. Amelung, R. Nicholls, P. Watkiss, O.B. Christensen, R. Dankers, L. Garrote, C.M. Goodess, A. Hunt, A. Moreno, J. Richards, and A. Soria, 2011: Physical and economic consequences of climate change in Europe. *Proceedings of the National Academy of Sciences of the United States of America*, 108(7), 2678-2683.

Colette, A., Granier, C., Hodnebrog, Ø., Jakobs, H., Maurizi, A., Nyiri, A., Bessagnet, B., D’Angiola, A., D’Isidoro, M., Gauss, M., Meleux, F., Memmesheimer, M., Mieville, A., Rouil, L., Russo, F., Solberg, S., Stordal, F., and Tampieri, F. (2011), Air quality trends in Europe over the past decade: a first multi-model assessment, *Atmos. Chem. Phys.*, 11, 11657–11678, doi:10.5194/acp-11-11657-2011.

Colette, A., Granier, C., Hodnebrog, O., Jakobs, H., Maurizi, A., Nyiri, A., Rao, S., Amann, M., Bessagnet, B., D’Angiola, A., Gauss, M., Heyes, C., Klimont, Z., Meleux, F., Memmesheimer, M., Mieville, A., Rouil, L., Russo, F., Schucht, S., Simpson, D., Stordal, F., Tampieri, F., Vrac, M. (2012), Future air quality in Europe: a multi-model assessment of projected exposure to ozone. *Atmos. Chem. Phys.* 12, 10613-10630.

Derognat, C., Beekmann, M., Baeumle, M., Martin, D., Schmidt, H. (2003), Effect of biogenic volatile organic compound emissions on tropospheric chemistry during the atmospheric pollution over the Paris area (ESQUIF) campaign in the Ile de France region. *J. Geophys. Res.* 108, 8560-8575.

Dogan HM, Cetin I, Egri M (2010). Spatiotemporal change and ecological modelling of malaria in Turkey by means of geographic information systems. *Trans R Soc Trop Med Hyg*, 104(11):726–732.

Dufour, A., Amodei, M., Ancellet, G., and V.-H. Peuch. (2004), Observed and modelled “chemical weather” during ESCOMPTE, *Atmos. Res.*, 74, 161–189, doi:10.1016/atmosres.2004.04.013.

Dunne, J.P., Stouffer, R.J., John, J.G., Reductions in labour capacity from heat stress under climate warming. *Nature Climate Change*. 2013; 563–566. doi:10.1038/nclimate1827

EC (2013). Proposal for a Directive of the European Parliament and of the Council on the reduction of national emissions of certain atmospheric pollutants and amending Directive 2003/35/EC./^{*} COM/2013/0920 final - 2013/0443 (COD) ^{*/}.

ECDC (2012). *Assessing the potential impacts of climate change on food- and waterborne diseases in Europe*. Stockholm, Sweden, ECDC,:19

EU CORDIS (2014) at http://cordis.europa.eu/projects/home_en.html

Engardt, M. (2008), Modelling of near-surface ozone over South Asia. *J. Atmos. Chem.* 59, 61-80. DOI:10.1007/s10874-008-9096-z.

Engardt, M., Bergström, R. and Andersson, C. (2009), Climate and emission changes contributing to changes in near-surface ozone in Europe over the coming decades: Results from model studies. *Ambio* 38, 452–458. DOI: 10.1579/0044-7447-38.8.452

ExterneE (1995). European Commission, DGXII, Science, Research and Development, JOULE. Externalities of Energy, ‘ExterneE’ Project. Volume 2. Methodology. (EUR 16521 EN). http://www.externe.info/externe_d7/?q=node/37. Accessed 20/6/2012.

ExterneE (1999). European Commission Directorate-General XII Science, Research and Development. ExterneE Externalities of Energy. Volume 7: Methodology 1998 Update. http://www.externe.info/externe_d7/?q=node/39. Accessed 20/6/2012.

Guenther, A., Hewitt, C., Erickson, D., Fall, R., Geron, C., Graedel, T., Harley, P., Klinger, L., Lerdau, M., McKay, W., Pierce, T., Scholes, B., Steinbrecher, R., Tallamraju, R., Taylor, J., and Zimmerman, P. (1995), A global-model of natural volatile organiccompound emissions, *J. Geophys. Res.*, 100, 8873–8892

Guenther, A., Karl, T., Harley, P., Wiedinmyer, C., Palmer, P. I., and Geron, C. (2006), Estimates of global terrestrial isoprene emissions using MEGAN (Model of Emissions of Gases and Aerosols from Nature), *Atmos. Chem. Phys.*, 6, 3181–3210, doi:10.5194/acp-6-3181-2006.

Holland, M., Hunt, A., Hurley, F., Navrud, S. and Watkiss, P. (2005a) Methodology for the Cost-Benefit analysis for CAFE: Volume 1: Overview of Methodology. http://www.cafe-cba.org/assets/volume_1_methodology_overview_02-05.pdf. Accessed 20/6/2012.

Holland, M., Hurley, F., Hunt, A. and Watkiss, P. (2005b) Methodology for the Cost-Benefit Analysis for CAFE: Volume 3: Uncertainty in the CAFE CBA: Methods and First Analysis. Report for European Commission DG Environment. http://www.cafe-cba.org/assets/volume_3_methodology_05-05.pdf. Accessed 20/6/2012.

Holland, M., Amann, M., Heyes, C., Rafaj, P., Schöpp, W. Hunt, A., and Watkiss, P. (2011). The Reduction in Air Quality Impacts and Associated Economic Benefits of Mitigation Policy. Summary of Results from the EC RTD ClimateCost Project. In Watkiss, P (Editor), 2011. The ClimateCost Project. Final Report. Volume 1: Europe. Published by the Stockholm Environment Institute, Sweden, 2011. ISBN 978-91-86125-35-6.

Hurley, F., Hunt, A., Cowie, H., Holland, M., Miller, B., Pye, S. and Watkiss, P. (2005) Methodology for the Cost-Benefit analysis for CAFE: Volume 2: Health Impact Assessment. http://www.cafe-cba.org/assets/volume_2_methodology_overview_02-05.pdf. Accessed 20/6/2012.

Honoré, C., Rouïl, L., Vautard, R., Beekmann, M., Bessagne, B., Dufour, A., Elichegaray, C., Flaud, J.-M., Malherbe, L., Meleux, F., Menut, L., Martin, D., Peuch, A., Peuch, V.-H., and Poisson, N. (2008), Predictability of European air quality: assessment of 3 years of operational forecasts and analyses by the PREV'AIR system, J. Geophys. Res., 113, D04301, doi:10.1029/2007JD008761.

HPA, 2012: Health Effects of Climate Change in the UK 2012 – Current Evidence, Recommendations and Research Gaps [Vardoulakis, S. and C. Heaviside, (eds.)]. Health Protection Agency (HPA), Didcot, UK, 242 pp.

HRAPIE (2013) Health risks of air pollution in Europe-HRAPIE project. Recommendations for concentration response functions for cost benefit analysis of particulate matter, ozone and nitrogen dioxide. <http://www.euro.who.int/en/health-topics/environment-and-health/air-quality/activities/health-aspects-of-air-pollution-and-review-of-eu-policies-the-revihaap-and-hrapie-projects> (accessed 12 Apr 2014). World Health Organization

IPCC, 2014a. Summary for Policymakers, in: Field, C.B., Barros, V.R., Dokken, D.J., Mach, K.J., Mastrandrea, M.D., Bilir, T.E., Chatterjee, M., Ebi, K.L., Estrada, Y.O., Genova, R.C., Girma, B., Kissel, E.S., Levy, A.N., MacCracken, S., Mastrandrea, P.R., White, L.L. (Eds.), Climate Change 2014: Impacts, Adaptation, and Vulnerability. Part A: Global and Sectoral Aspects. Contribution of Working Group II to the Fifth Assessment Report of the Intergovernmental Panel on Climate Change. Cambridge University Press, Cambridge, United Kingdom and New York, NY, USA.

IPCC, 2014b. Summary for Policymakers, in: Climate Change 2014: Mitigation of Climate Change. Contribution of Working Group III to the Fifth Assessment Report of the Intergovernmental Panel on Climate Change [Edenhofer, O., R. Pichs-Madruga, Y. Sokona, E. Farahani, S. Kadner, K. Seyboth, A. Adler, I. Baum, S. Brunner, P. Eickemeier, B. Kriemann, J. Savolainen, S. Schlömer, C. von Stechow, T. Zwickel and J.C. Minx (eds.)]. Cambridge University Press, Cambridge, United Kingdom and New York, NY, USA.

Jaenson TGTT, Lindgren E (2011). The range of Ixodes ricinus and the risk of contracting Lyme borreliosis will increase northwards when the vegetation period becomes longer. *Ticks and tick-borne diseases*, 2(1):44–49.

Joly, M., Peuch, V.-H. (2012), Objective classification of air quality monitoring sites over Europe. *Atmos.-Environ.* 47, 111–123.

Jonson, J. E., D. Simpson, H. Fagerli, and S. Solberg (2005), Can we explain the trends in European ozone levels, *Atmos. Chem. Phys.*, 6, 51 – 66.

Jonson, J. E., Stohl, A., Fiore, A. M., Hess, P., Szopa, S., Wild, O., Zeng, G., Dentener, F. J., Lupu, A., Schultz, M. G., Duncan, B. N., Sudo, K., Wind, P., Schulz, M., Marmer, E., Cuvelier, C., Keating, T.,

Zuber, A., Valdebenito, A., Dorokhov, V., De Backer, H., Davies, J., Chen, G. H., Johnson, B., Tarasick, D. W., Stübi, R., Newchurch, M. J., von der Gathen, P., Steinbrecht, W., and Claude, H. (2010), A multi-model analysis of vertical ozone profiles, *Atmos. Chem. Phys.*, 10, 5759–5783, doi:10.5194/acp-10-5759-2010.

Josse B., P. Simon and V.-H. Peuch. (2004), Rn-222 global simulations with the multiscale CTM MOCAGE, *Tellus*, 56B, 339-356.

Kjellstrom, T., Holmer, I. & Lemke, B. Workplace heat stress, health and productivity—an increasing challenge for low and middle-income countries during climate change. *Glob. Health Action* 2009; 2 (Special volume), 46–51.

Kjellstrom, T.B., Lemke, T.B.. Increased workplace heat exposure due to climate change. *Asian-Pac. Newsl.* 2011; 18, 6–20.

Köble, R. and Seufert, G. (2001), Novel Maps for Forest Tree Species in Europe, A Changing Atmosphere, 8th European Symposium on the Physico-Chemical Behaviour of Atmospheric Pollutants, Torino, Italy, 17–20 September, 2001.

Kovats, R.S., Valentini, R., Bouwer, L.M., Georgopoulou, E., Jacob, D., Martin, E., Rounsevell, M., Soussana, J.-F., 2014. Europe, in: Barros, V.R., Field, C.B., Dokken, D.J., Mastrandrea, M.D., Mach, K.J., Bilir, T.E., Chatterjee, M., Ebi, K.L., Estrada, Y.O., Genova, R.C., Girma, B., Kissel, E.S., Levy, A.N., MacCracken, S., Mastrandrea, P.R., White, L.L. (Eds.), *Climate Change 2014: Impacts, Adaptation, and Vulnerability. Part B: Regional Aspects. Contribution of Working Group II to the Fifth Assessment Report of the Intergovernmental Panel of Climate Change*. Cambridge University Press, Cambridge, United Kingdom and New York, NY, USA, pp. 1267–1326

Krupnick, A., Ostro, B and Bull, K (2004). Peer Review Of The Methodology Of Cost-Benefit Analysis Of The Clean Air For Europe Programme. Alan Krupnick, Editor, Bart Ostro and Keith Bull. Paper prepared for European Commission Environment Directorate General October 12, 2004. <http://ec.europa.eu/environment/archives/cafe/activities/pdf/krupnick.pdf>. Accessed 20/6/2012.

Kukkonen, J., T. Olsson, D. M. Schultz, A. Baklanov, T. Klein, A. I. Miranda, A. Monteiro, M. Hirtl, V. Tarvainen, M. Boy, V.-H. Peuch, A. Poupkou, I. Kioutsoukis, S. Finardi, M. Sofiev, R. Sokhi, K. E. J. Lehtinen, K. Karatzas, R. San José, M. Astitha, G. Kallos, M. Schaap, E. Reimer, H. Jakobs, and K. Eben (2012), A review of operational, regional-scale, chemical weather forecasting models in Europe, *Atmos. Chem. Phys.*, 11, 1-87.

Lacressonnière, G., Peuch, V. H., Arteta, J., Josse, B., Joly, M., Maécal, V., Saint Martin, D., Déqué, M., Watson, L., 2012. How realistic are air quality hindcasts driven by forcings from climate model simulations ? *GMD* 5, 1565–1587.

Lacressonnière G, Watson L, Engardt M, Gauss M, Andersson C, Beekmann M, Colette A, Foret G, Josse J, Marécal V, Nyiri A, Siour G, Sobolowski S, Szopa S, Vautard R (2015) Impact of climate drivers on air quality, focus on European aerosol concentrations, in review. *AE*

Langner, J., Bergström, R. and Pleijel, K. (1998), European scale modeling of sulfur, oxidised nitrogen and photochemical oxidants. Model development and evaluation for the 1994 growing season. Swedish Meteorological and Hydrological Institute, RMK No. 82, 71 pp. (with errata).

Langner, J., Engardt, M. and Andersson, C. (2012a), European summer surface ozone 1990–2100. *Atmos. Chem. Phys.*, 12, 10097–10105. doi:10.5194/acp-12-10097-2012

Langner, J., Engardt, M., Baklanov, A., Christensen, J.H., Gauss, M., Geels, C., Hedegaard, G.B., Nuterman, R., Simpson, D., Soares, J., Sofiev, M., Wind, P. and Zakey, A. (2012b), A multi-model study of impacts of climate change on surface ozone in Europe. *Atmos. Chem. Phys.*, 12, 10423–10440. doi:10.5194/acp-12-10423-2012

Lattuati, M. (1997), Contribution à l'étude du bilan de l'ozone troposphérique à l'interface de l'europe et de l'atlantique nord: modélisation lagrangienne et mesures en altitude. Thèse de sciences, Université Paris 6, France.

Lefèvre, F., Brasseur, G. P., Folkins, I., Smith, A. K., and Simon, P. (1994), Chemistry of the 1991–1992 stratospheric winter: three dimensional model simulations, *J. Geophys. Res.*, 99, 8183–8195.

Liberati A et al. (2009). *The PRISMA statement for reporting systematic reviews and meta-analyses of studies that evaluate health care interventions: explanation and elaboration.*, e1–34.

Lowe D., Ebi K., Forsberg B. (2011) Heatwave Early Warning Systems and Adaptation Advice to Reduce Human Health Consequences of Heatwaves. *Int J Environ Res Public Health*; 8(12):4623–4648.

Lung T et al. (2013). A multi-hazard regional level impact assessment for Europe combining indicators of climatic and non-climatic change. *Global Environmental Change*, 23(2):522–536.

McMichael A. Climate change. In: Ezzati M, Lopez A, Rodgers A, Murray C, editors. *Comparative Quantification of Health Risks: Global and Regional Burden of Disease due to Selected Major Risk Factors*. Geneva: World Health Organization; 2004. p. 1543–649.

Meleux, F., Solmon, F., and Giorgi, F. (2007), Increase in summer European ozone amounts due to climate change, *Atmos. Environ.*, 41, 7577–7587.

Menut L., B. Bessagnet, D. Khvorostyanov, M. Beekmann, A. Colotte, I. Coll, G. Curci, G. Foret, A. Hodzic, S. Mailler, F. Meleux, J.L. Monge, I. Pison, G. Siour, S. Turquety, M. Valari, R. Vautard and M.G. Vivanco: CHIMERE: a model for regionalatmospheric composition modelling, *Geoscientific Model Development*, 6, 981–1028, 2013

Miraglia, M., H.J.P. Marvin, G.A. Kleter, P. Battilani, C. Brera, E. Coni, F. Cubadda, L. Croci, B. De Santis, S. Dekkers, L. Filippi, R.W.A. Hutjes, M.Y. Noordam, M. Pisante, G. Piva, A. Prandini, L. Toti, G.J. van den Born, and A. Vespermann, 2009: Climate change and food safety: an emerging issue with special focus on Europe. *Food and Chemical Toxicology*, 47(5), 1009–1021.

Morabito M et al. (2012). Air temperature-related human health outcomes: Current impact and estimations of future risks in Central Italy. *Science of The Total Environment*, 441:28–40

Paterson, R.R.M. and N. Lima, 2010: How will climate change affect mycotoxins in food? *Food Research International*, 43(7), 1902–1914.

Peuch et al., 1999, , V.-H., Amodei, M., Barthet, T., Cathala, M.-L., Michou, M., and Simon, P. (1999), MOCAGE, MOdèle de Chimie Atmosphérique à Grande Echelle, in: *Proceedings of Météo France: Workshop on atmospheric modelling*, Toulouse, France, 33–36.

Ready, P.D., 2010: Leishmaniasis emergence in Europe. *Eurosurveillance*, 15(10), 29- 39.

Paci D., 2014: Human Health Impacts of Climate change in Europe. Report for the PESETA II project. JRC Technical Reports, Report EUR 26494EN

Pope CA, Thun MJ, Namboodiri MM, Dockery DW, Evans JS, Speizer FE, Heath CW (1995) Particulate air pollution as a predictor of mortality in a prospective study of US adults. *American Journal of Respiratory and Critical Care Medicine* 151, 669-74.

Pope, CA III, Burnett RT, Thun MJ, Calle EE, Krewski D, Ito K, Thurston GD (2002). Lung cancer, cardiopulmonary mortality, and long-term exposure to fine particulate air pollution. *Journal of the American Medical Association*, 287: 1132 - 1141.

Pope, C.A. III, Burnett, R.T., Krewski, D., Jerrett, M., Shi, Y., Calle, E.E. and Thun, M.J. (2009a) Cardiovascular mortality and exposure to airborne fine particulate matter and cigarette smoke: Shape of the exposure response relationship. *Circulation*, 120, 941-948.

Pope, C.A. III, Ezzati, M. and Dockery, D.W. (2009b) Fine particulate air pollution and life expectancy in the United States. *New England Journal of Medicine*. 360, 376-386.

Sainz-Elise S et al. (2010). Malaria resurgence risk in southern Europe: climate assessment in an historically endemic area of rice fields at the Mediterranean shore of Spain. *Malaria journal*, 9:221.

Robertson, L., Langner, J. and Engardt, M. (1999), An Eulerian limited-area atmospheric transport model. *J. Appl. Meteor.* 38, 190-210.

Simpson, D., Benedictow, A., Berge, H., Bergström, R., Emberson, L. D., Fagerli, H., Flechard, C. R., Hayman, G. D., Gauss, M., Jonson, J. E., Jenkin, M. E., Nyíri, A., Richter, C., Semeena, V. S., Tsyro, S., Tuovinen, J.-P., Valdebenito, Á., and Wind, P.: The EMEP MSC-W chemical transport model – technical description, *Atmos. Chem. Phys.*, 12, 7825–7865, 2012, <http://www.atmos-chem-phys.net/12/7825/2012/>.

Sahu, S., Sett, M., Kjellstrom, T., 2013. Heat exposure, cardiovascular stress and work productivity in rice harvesters in India: implications for a climate change future. *Ind. Health* 51, 424–431.

Schröder W, Schmidt G (2008). Mapping the potential temperature-dependent tertian malaria transmission within the ecoregions of Lower Saxony (Germany). *International Journal of Medical Microbiology*, 298, Suppl:38–49.

Semenza JC, Menne B (2009). Climate change and infectious diseases in Europe. *The Lancet Infectious Diseases*, 9(6):365–375.

Shaposhnikov D et al. (2014). Mortality related to air pollution with the moscow heat wave and wildfire of 2010. *Epidemiology (Cambridge, Mass.)*, 25(3):359–64.

Shea K et al. (2008). Climate change and allergic disease. *Clinical reviews in allergy and immunology*, 122(3):443–453.

Simpson, D., Winiwarter, W., Borjesson, G., Cinderby, S., Ferreiro, A., Guenther, A., Hewitt, C. N., Janson, R., Khalil, M. A. K., Owen, S., Pierce, T. E., Puxbaum, H., Shearer, M., Skiba, U., Steinbrecher, R., Tarrason, L., and Oquist, M. G. (1999), Inventorying emissions from nature in Europe, *J. Geophys. Res.*, 104, 8113– 8152.

Simpson, D., Fagerli, H., Jonson, J. E., Tsyro, S., Wind, P., and Tuovinen, J. P. (2003), The EMEP United Eulerian Model. Model Description, EMEP MSC-W Report 1/2003, Norwegian Meteorological Institute, Oslo.

Simpson, D., Benedictow, A., Berge, H., Bergström, R., Emberson, L. D., Fagerli, H., Flechard, C. R., Hayman, G. D., Gauss, M., Jonson, J. E., Jenkin, M. E., Nyíri, A., Richter, C., Semeena, V. S., Tsyro, S., Tuovinen, J.-P., Valdebenito, A., and Wind, P. (2012), The EMEP MSC-W chemical transport model – technical description, *Atmos. Chem. Phys.*, 12, 7825–7865, doi:10.5194/acp-12-7825-2012.

Smith, K.R., Woodward, A., Campbell-Lendrum, D., Chadee, D.D., Honda, Y., Liu, Q., Olwoch, J.M., Revich, B., Sauerborn, R., 2014. Human health: impacts, adaptation, and co-benefits, in: Field, C.B., Barros, V.R., Dokken, D.J., Mach, K.J., Mastrandrea, M.D., Bilir, T.E., Chatterjee, M., Ebi, K.L., Estrada, Y.O., Genova, R.C., Girma, B., Kissel, E.S., Levy, A.N., MacCracken, S., Mastrandrea, P.R., White, L.L. (Eds.), *Climate Change 2014: Impacts, Adaptation, and Vulnerability. Part A: Global and Sectoral Aspects. Contribution of Working Group II to the Fifth Assessment Report of the Intergovernmental Panel of Climate Change*. Cambridge University Press, Cambridge, United Kingdom and New York, NY, USA, pp. 709–754.

Solazzo, E., Bianconi, R., Pirovano, G., Matthias, V., Vautard, R., Moran, M.D., Wyatt Appel, K., Bessagnet, B., Brandt, J., Christensen, J.H., Chemel, C., Coll, I., Ferreira, J., Forkel, R., Francis, X.V., Grell, G., Grossi, P., Hansen, A.B., Miranda, A.I., Nopmongkol, U., Prank, M., Sartelet, K.N., Schaap, M., Silver, J.D., Sokhi, R.S., Vira, J., Werhahn, J., Wolke, R., Yarwood, G., Zhang, J., Rao, S.T., Galmarini, S. (2012a), Operational model evaluation for particulate matter in Europe and North America in the context of AQMEII. *Atmospheric Environment* 53, 75-92.

Solazzo, E., Bianconi, R., Vautard, R., Appel, K.W., Moran, M.D., Hogrefe, C., Bessagnet, B., Brandt, J., Christensen, J.H., Chemel, C., Coll, I., Denier van der Gon, H., Ferreira, J., Forkel, R., Francis, X.V., Grell, G., Grossi, P., Hansen, A.B., Jericevic, A., Kraljevic, L., Miranda, A.I., Nopmongkol, U., Pirovano, G., Prank, M., Riccio, A., Sartelet, K.N., Schaap, M., Silver, J.D., Sokhi, R.S., Vira, J., Werhahn, J., Wolke, R., Yarwood, G., Zhang, J., Rao, S.T., Galmarini, S. (2012b), Model evaluation and ensemble modelling of surface-level ozone in Europe and North America in the context of AQMEII. *Atmospheric Environment* 53, 60-74.

Stockwell, W. R., Kirchner, F., Khun, M., and Seinfeld, S. (1997), A new mechanism for regional atmospheric chemistry modelling, *J. Geophys. Res.*, 102, 25847–25879.

D.S.Stevenson, P.J. Young, V. Naik, J.-F. Lamarque, D.T. Shindell, A. Voulgarakis, R.B. Skeie, S.B. Dalsoren, G. Myhre, T.K. Berntsen, G.A. Folberth, S.T. Rumbold, W.J Collins, I.A. MacKenzie, R.M. Doherty, G. Zeng, T.P.C. Van Noije, A. Strunk, D. Bergmann, P. Cameron-Smith, D. A. Plummer, S.A. Strode, L. Horowitz, Y.H. Lee, S. Szopa, K. Sudo, T. Nagashima, B. Josse, I. Cionni, M. Righi, V. Eyring, A. Conley, K.W. Bowman, and O. Wild. (2012), Tropospheric ozone changes, radiative forcing and attribution to emissions in the Atmospheric Chemistry and Climate Model Inter-comparison Project (ACCMIP), *Atmos. Chem. Phys. Discuss.*, 12, 26047-26097.

Szopa, S., Balkanski, Y., Schulz, M., Bekki, S., Cugnet, D., Fortems-Cheiney, A., Turquety, S., Cozic, A., Deandreis, C., Hauglustaine, D., Idelkadi, A., Lathiere, J., Lefevre, F., Marchand, M., Vuolo, R., Yan, N., Dufresne, J.-L. (2012), Aerosol and ozone changes as forcing for climate evolution between 1850 and 2100. *Climate Dynamics*, doi:10.1007/s00382-012-1408-y

Takahashi K, Honda Y, Emori S. Assessing mortality risk from heat stress due to global warming. *J Risk Res.* 2007; 10:339–54.

Tuovinen, J.-P., Ashmore, M., Emberson, L., and Simpson, D. (2004), Testing and improving the EMEP ozone deposition module, *Atmos. Environ.*, 38, 2373–2385.

US-EPA (2005), “Guidance on the use of models and other analyses in attainment demonstrations for the 8-hour ozone NAAQS,” US EPA Report EPA-454/R-05-002, Office of Air Quality Planning and Standards, Research Triangle Park, NC, USA.

van Loon, M., Vautard, R., Schaap, M., Bergstrom, R., Bessagnet, B., Brandt, J., Builtjes, P., Christensen, J., Cuvelier, C., Graff, A., Jonson, J. E., Krol, M., Langner, J., Roberts, P., Rouil, L., Stern, R., Tarrasón, L., Thunis, P., Vignati, E., White, L., Wind, P. (2007), Evaluation of long-term ozone simulations from seven regional air quality models and their ensemble. *Atmos.-Environ.* 41, 2083–2097.

Van Vuuren, D.P., Riahi, K., Moss, R., Edmonds, J., Thompson, A., Nakicenovic, N., Kram, T., Berkhout, F., Swart, R., Janetos, A., Rose, S.K., Arnell, A. (2012), A proposal for a new scenario framework to support research and assessment in different climate research communities. *Global Environmental Change* 22 (1), 21-35.

Vautard, R., M. Beekmann, J. Roux, and D. Gombert (2001), Validation of a deterministic forecasting system for the ozone concentrations over the Paris area, *Atmos. Environ.*, 35, 2449 – 2461.

Vautard, R., Szopa, S., Beekmann, M., Menut, L., Hauglustaine, D.A., Rouil, L and Roemer, M. (2006), Are decadal anthropogenic emission reductions in europe consistent with surface ozone observations ? *Geophysical research Letters*, 33(13).

Vautard, R., Builtjes, P.H.J., Thunis, P., Cuvelier, C., Bedogni, M., Bessagnet, B., Honore, C., Moussiopoulos, N., Pirovano, G., Schaap, M., Stern, R., Tarrason, L., Wind, P. (2007), Evaluation and intercomparison of Ozone and PM10 simulations by several chemistry transport models over four European cities within the CityDelta project. *Atmospheric Environment* 41, 173-188.

Vieno, M., Dore, A.J., Stevenson, D.S., Doherty, R., Heal, M.R., Reis, S., Hallsworth, S., Tarrason, L., Wind, P., Fowler, D., Simpson, D., and Sutton, M.A. (2010), Modelling surface ozone during the 2003 heat-wave in the UK, *Atmos. Chem. Phys.*, 10, 7963-7978, doi:10.5194/acp-10-7963-2010.

Watkiss P, ed al. *The ClimateCost Project. Final Report. Volume 1: Europe*. Stockholm, Sweden, Stockholm Environment Institute, 2011:1–31.

Watkiss P et al. (2013). *IMPACT2C Policy Update on 2°C Warming*. Germany, Climate Service Center.

Weber R (2012). Impact of climate change on aeroallergens. *Annals of Allergy, Asthma & Immunology*, 108(5):294–299.

WHO, Parma Declaration on Environment and Health, 2010. Commitment to act EUR/55934/5.1.

WHO. Quantitative risk assessment of the effects of climate change on selected causes of death, 2030s and 2050s. Geneva, 2014

WHO. The WHO Work Plan on Climate Change And Health. EB136/16, Dec. 2014

WHO, Review of evidence on health aspects of air pollution – REVIHAAP Project, Technical Report, 2013.



WHO-Europe (2004) Health aspects of air pollution – answers to follow-up questions from CAFE.

Report on a WHO Working Group Meeting, Bonn, Germany, 15-16 January 2004.

http://www.euro.who.int/_data/assets/pdf_file/0019/165007/E82790.pdf. Accessed 20/6/2012.